INTERCEPTION TECHNIQUES FOR DIRECT SEQUENCE SPREAD SPECTRUM SIGNALS

A THESIS SUBMITTED TO

THE GRADUATE SCHOOL OF NATURAL AND APPLIED SCIENCES

OF

MIDDLE EAST TECHNICAL UNIVERSITY

BY

UYGAR KARADENİZ

IN PARTIAL FULFILLMENT OF THE REQUIREMENTS
FOR
THE DEGREE OF MASTER OF SCIENCE
IN
ELECTRICAL AND ELECTRONICS ENGINEERING

DECEMBER 2005

Approval of the Graduate School of Natural and Applied Sciences

Prof. Dr. Canan Özgen

Director

I certify that this thesis satisfies all the requirements as a thesis for the degree of Master of Science

Prof. Dr. İsmet Erkmen

Head of Department

This is to certify that we have read this thesis and that in our opinion it is fully adequate, in scope and quality, as a thesis for the degree of Master of Science.

Prof . Dr. Buyurman Baykal

Supervisor

Examining Committee Members

Assoc. Prof. Dr. Temel Engin Tuncer	(METU,EEE)	
Prof. Dr. Buyurman Baykal	(METU,EEE)	
Assoc. Prof. Dr. Tolga Çiloğlu	(METU,EEE)	
Dr. Özgür Yılmaz	(METU,EEE)	
Dicle Sönmez	(S.T M. A.Ş.)	

I hereby declare that all information in this document has been obtained and presented in accordance with academic rules and ethical conduct. I also declare that, as required by these rules and conduct, I have fully cited and referenced all material and results that are not original to this work.

Uygar Karadeniz :

Signature :

ABSTRACT

INTERCEPTION TECHNIQUES FOR DIRECT SEQUENCE SPREAD SPECTRUM SIGNALS

Karadeniz, Uygar

M.Sc. in Department of Electrical and Electronics Engineering

Supervisor: Prof. Dr. Buyurman Baykal

November 2005, 152 Pages

In this work interception and spreading sequence estimation of Direct Sequence Spread Spectrum (DSSS) signals, in low signal to noise power ratios is discussed. For interception an approach based on autocorrelation fluctuations is employed and also symbol period is estimated from this interception process. Spreading sequence estimation is performed by using eigenanalysis of the correlation matrix and estimated symbol period.

These approaches are applied on different kinds of DSSS signals including 3rd generation UMTS signal and LPI radar signals. In order to examine the channel effects such as; multipath, interference and colored noise, on the performance of applied techniques, detailed analysis results are obtained. The results are compared with the performances of alternative interception techniques.

Keywords: DSSS, interception, Spreading Sequence

ÖZ

DSSS SİNYALLER İÇİN TESPİT TEKNİKLERİ

Karadeniz, Uygar

Yüksek Lisans, Elektrik ve Elektronik Mühendisliği Bölümü

Tez Yöneticisi : Prof. Dr. Buyurman Baykal

Kasım 2005, 152 Sayfa

Bu çalışmada doğrudan dizi yayılı spektrum sinyallerinin düşük işaret güç oranlarında tespiti ve bu sinyallerde kullanılan yayan dizilerin kestirimi ele alınmıştır. Tespit işlemi temel olarak özilinti fonksiyonundaki dalgalanmalara dayanır . Ayrıca tespit işlemi sonucunda sembol periyodu kestirimi de yapılmaktadır. Yayan dizilerin kestirimi için ise ortak değişinti matrisinin öz analizi ve kestirimi yapılan sembol periyodu kullanılmıştır.

Bu yaklaşımlar (3. nesil) UMTS ve kestirim olasılığı düşük radar sinyallerini de içeren değişik doğrudan dizi yayılı spektrum sinyalleri üzerinde uygulanmıştır. Çok yolluluk, kanal karışması ve renkli gürültü gibi kanal etkilerinin bu metotların performansları üzerinde yarattığı değişimler detaylı analizler ile incelenmiştir. Bulunan sonuçlar alternatif tekniklerin performansları ile karşılaştırılmıştır.

Anahtar Kelimeler: doğrudan dizi yayılı spektrum sezim, tespit, yayılı dizi

ACKNOWLEDGEMENTS

I would like to express my gratitude to Prof. Dr. Buyurman BAYKAL. I have been fortunate to receive his valuable assistance, suggestions, guidance and endless support. Without his guidance this thesis would not be possible.

I am particularly indebted to my dear family, my wife and friends for their continuous and important support and with deep faith and patience.

I would also like to thank STM Inc. For providing me significant support for this thesis and my colleagues from whose insights and valuable perspectives I have benefited.

TABLE OF CONTENTS

LIST OF TABLES

LIST OF FIGURES

LIST OF ABBREVIATIONS

ADC: Analog to Digital Converter

AF: Ambiguity Function

BER: Bit Error Rate

BPSK: Binary Phase Shift Keying

CDMA: Code Division Multiple Access

CCF: Cross-Correlation Function

COMINT: Communication Intelligence

CSD: Cross-Spectral Density

CWD: Choi-Williams Distribution

DDC: Digital Down Converter

DPCCH: Dedicated Physical Control Channel

DPDCH: Dedicated Physical Data Channel

DSP: Digital Signal Processor

DSSS: Direct Sequence spread spectrum

ELINT: Electronic Intelligence

ESM: Electronic Support Measures

FFHSS: Fast Frequency Hopping Spread Spectrum

FFT: Fast Fourier Transform

FHSS: Frequency Hopping Spread Spectrum

FIR: Finite Impulse Response

FISINT: Foreign Instrumentation Signals Intelligence

FPGA: Field Programmable Gate Array

FrFT: Fractional Fourier Transform

FSK: Frequency Shift Keying

IF: Intermediate Frequency

IFM: Instantaneous Frequency Measurement

LFHSS: Low Frequency Hopping Spread Spectrum

LPI: Low probability of Detection

LOS: Line Of Sight

OVSF: Orthogonal Variable Spreading Factor

PA: Power Amplifier

PRI: Pulse Repetition Interval

PRN: Pseudo-Random Code

PSK: Phase Shift Keying

S-ATFR: Short Adaptive Time Frequency Representation

SIGINT: Signals intelligence

SNR: Signal to Noise Ratio

STFT: Short-Time Fourier Transform

TFDS: Time-Frequency Distribution Series

THSS: Time Hopping Spread Spectrum

UMTS: Universal Mobile Telecommunications System

WVD: Wigner-Ville Distribution

CHAPTER 1

INTRODUCTION

The principle aim of this study is to examine the performance of a new approach based on autocorrelation fluctuations for interception and spreading code estimation of DSSS signals at low SNR's. It is also aimed to investigate the robustness of DSSS signals to interception by applying this approach and obtaining detailed performance analysis results. The analysis is diversified in order to determine the effects of channel characteristics and different DSSS signal types on the success of applied techniques. Furthermore necessary comparisons with performances of alternative interception techniques are accomplished.

The main target of interception technique applied in this study is DSSS signals. The DSSS signals are of interest because; the improvements in military communications and electronic warfare systems technology give rise to the development of DSSS transmissions in order to be able to cope with new challenges for spectrum surveillance. Coming out from military technology; DSSS also becomes a fundamental block in next generation wireless communications. One of the important properties of DSSS transmissions is low probability of interception (LPI). So it is a new challenge from the aspect of interception. The low probability of interception property of DSSS signals is obtained due to their statistics which is similar to noise statistics. Furthermore military DSSS signals usually transmitted below the noise level.

The interception idea uses profit of the fact that the DSSS signal's statistical properties are not the same as the noise statistical properties. This approach mainly depends on the fluctuations of autocorrelation estimators Also the symbol period is estimated from the output of interception process. The method for the estimation of the pseudo random sequence is based on eigenanalysis of the correlation matrix, obtained from the temporal windows of the received signal [5]. Symbol period which is estimated from the detector output is also used. For both methods there is no need to apply any Fourier Analysis and this can be considered as the main difference of this interception approach from time frequency based analysis. Time frequency analysis is also discussed in the following chapters.

The interception approach is applied on a basic intercept receiver model and tested with different type of DSSS signals by using different channel effects. The performance analysis are obtained for typical DSSS signals, Universal Mobile Telecommunications System (UMTS) waveform created depending on technical specification of European Telecommunications Standards Institute (ETSI) and typical LPI radar signals. Also channel effects such as; multipath, interference and colored noise is included in performance analysis.

Once the spreading sequence has been estimated, a classical spread-spectrum receiver can demodulate the signal. After demodulation process the DSSS signal becomes narrow-band, time frequency approach can be used for further analysis. [2]

The experimental results in the later sections show that spread spectrum signals can be detected and spreading sequence can be estimated in a non cooperative context at very low SNR's and application of different channel effects does not result with major interception performance decreases.

In the following chapters first the Signals intelligence (SIGINT) concept is discussed in order to understand the problem of interception from a practical point of view. Then the main interception approaches are explained for placing the applied method somewhere among other approaches, considering the main trends of interception systems. Then the spread spectrum concept is explained in order to examine the main characteristics of DSSS transmissions.

After background studies the applied interception technique is discussed in detail in two main parts; the detection of DSSS signals and estimation of spreading sequence. The simulation models used for each process are introduced in these chapters. In the following part the performance analysis and evaluation of the results and also comparisons with alternative interception methods is given. Finally in the last chapter, conclusions obtained from the overall study are given. The detailed derivation of the interception technique is also given in Appendix A.

CHAPTER 2

SIGNAL INTELLIGENCE AND INTERCEPTION

2.1 SIGNAL INTELLIGENCE

Signal intelligence (SIGINT) concept is very important in order to understand the problem of interception in practical point of view. SIGINT systems gather intelligence derived from the searching and analysis of electromagnetic signals. Basically SIGINT systems detect, locate and analyze enemy signals.

Considering the modern military trend, communication is critically important. Every individual unit requires a steady flow of information between headquarters and other units in order to become a part in the organization and serve the overall strategy. Communications surveillance is critical to achieving information superiority. Today having control over enemy communications while maintaining the capability of own data transmissions is an important part of over all military strategy. Control over enemy communications is achieved by the ability to collect information from enemy communications when necessary and by the ability to deny the communications.

As the radars are electromagnetic eyes of the armed forces and security organizations, intelligence about radars are also essential to success. Gathering information about radars is defined in electronic warfare concept which is also composes an important role in military domain. In Russian sources Electronic warfare is named “Electromagnetic Warfare” and deals with radars and electro-optic sensors. The definition of Electronic warfare is the use of electromagnetic and directed energy to control the electromagnetic spectrum or attack the enemy. Electronic warfare and SIGINT overlaps when the aim is gathering information by using electromagnetic spectrum. Also SIGINT can be considered as a part of EW. These classifications and separation of concepts may vary from source to source.

It is important to mention, these considerations are not limited to the military domain. The development of wireless transmissions (wireless indoor networks, cellular telephones) points out the need of mastering interception techniques to protect transmissions. Mostly security agencies and police organizations deals with non-military signal intelligence against crime organizations and terrorism.

Signal Intelligence concept is comprised of the following main disciplines, according to the source of information carried by the electromagnetic wave.

- Communication Intelligence (COMINT)
- Electronic Intelligence and Electronic Support Measure (ELINT & ESM)
- Foreign instrumentation signals intelligence (FISINT)

COMINT deals with the information carried by communication systems. Mainly military communications are of interest of COMINT. As said before communication intelligence is very important.

In both ELINT and ESM, the source of information is radar systems. ELINT systems are less time depended than ESM systems and consist of detailed offline analysis. ESM systems use the gathered information about radars to inform the personnel and related attack systems to react immediately. So, response time is critical and important in these systems. ELINT and ESM can be considered as the information obtaining parts of electronic warfare.

In FISINT electromagnetic waves associated with the testing and operational deployment of foreign aerospace, surface, and subsurface systems are the sources of information.

No matter what the source of information is the first and extremely important step of signal intelligence is finding the interested signal. This concept is defined under the interception title.

2.2 BACKGROUND ON INTERCEPTION

It is important to clarify the concept of interception before clarifying the idea for interception of DSSS signals. This section describes meaning of the interception from the overall system point of view. By using this approach after the definition of interception, architecture of receivers used for interception and common interception techniques are explained. The aim of this section is to help clarifying the overall system approaches and architectures before concentration on interception of DSSS signals.

Interception is act of searching signals of interest in the spectrum for analyzing and extracting the information carried by the signal. Interception is considered to be the basic first step in SIGINT systems. Because if you want to analyze the signal first thing you must do is finding the signal. This concept is also known as "spectrum surveillance".

Due to the nature of human being; if some one wants to steal some thing, the owner will try to hide it. In our concern the information carried by the signal is valuable and the modern transmitters try to hide signal. From the theoretical point of view best way to hide the signal is making no transmissions at all. Making no transmissions means that using no power in the spectrum and this approach is a guide which leads to using lower peak powers and wide frequency bands in the spectrum by the transmitters. These kinds of techniques are mainly used by military communications in which the information carried is so valuable that it becomes matter of life in battle field.

The techniques used for interception is related to the architecture of the receiver and the target signal source. If the target frequency is known by the receiver then that means; the frequency band will be analyzed is fixed. In that case only a channel activation search will be enough in the frequency of interest. But that is a very simple case and today it is not valid for most digital transmissions.

In the following sections the basic interception receiver architectures and interception techniques are described.

2.2.1 INTERCEPTION BASED ON RECEIVER ARCHITECTURE

In this section, some of the basic interception receiver types are defined for clarifying the devices that are used for implementation of the different interception approaches. With the exception of digital receivers, the interception capability and technique is based on the architecture of receiver so every receiver architecture defined here is also indicates a different technique of interception. At this point digital receivers are totally different from the others because of their capability of high speed digital signal processing and mostly software defined capabilities.

The special interception techniques for special signal types like DSSS signals and digital transmissions need digital signal processing for interception, demodulation and decoding so digital receiver architecture is the most important type among others because of the proliferation of digital communication systems. Considering interception of DSSS signals, the other receiver types are only examples for alternatives of digital receivers.

We must clear that this receiver types are not only for interception. They are also used as the receiver module of the total signal intercepting and analyzing system. Most of these receiver types try to measure the frequency of the signal by using different techniques. This measurement also indicates that the interception is done in frequency domain.

Another important point is; there are also receivers which have the advantages of one or more different kind of receivers by using hybrid architectures. These kinds of receivers mostly apply digitizing on narrowband IF stages and form analog-digital mixed receiver architecture.

Some of the receiver types that are being used for interception are summarized below;

- Crystal Video Receivers
- Superheterodyne Receivers
- Instantaneous Frequency Measurement Receivers
- Digital Receivers

2.2.1.1 Crystal Video Receivers

Crystal video receivers are old, small and cheap. They have a simple architecture. The envelope detector diode removes carrier frequency from the signal and produces the envelope of the signal. The signal is amplified by video amplifier and then compared with a threshold for signal interception.

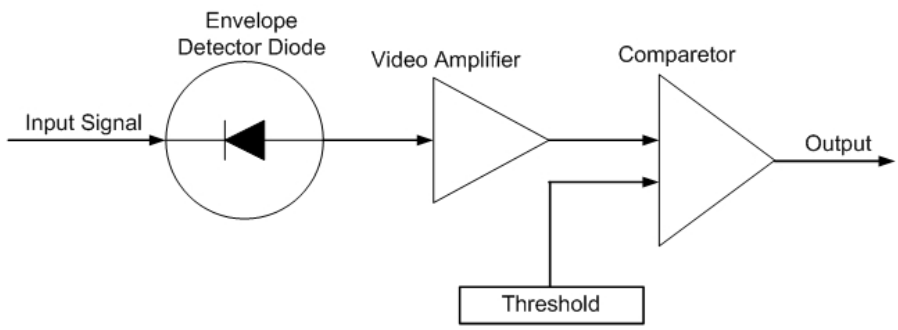

Figure 2.1 Crystal Video Receiver

Crystal video receivers have relatively low sensitivity and are unable to determine the frequency of the received signals and so cannot differentiate between simultaneous signals. They can only determine if there is energy in the input band of the receiver.

2.2.1.2 Superheterodyne Receivers

This receiver type is also old but it is still being used. The popularity of these receivers is because of their simple architecture and accepted technology with many manufacturers in the world. Simply the input signal is mixed to an IF frequency and passed through an IF filter at the beginning. Then the output of the IF filter is amplified and the simple threshold detection operation is done by using this signal.

The key point of this receiver is the mixer and IF filter at the beginning. The mixer chooses the frequency band that is to be interested from the antenna and IF filter bandwidth and shape defines the resolution of the detection process. With narrow bandwidths and sharp cut-off characteristics, superheterodyne receivers have high sensitivity and good selectivity. But a trade-off is exists with these properties. These receivers usually have low instantaneous frequency bandwidth.

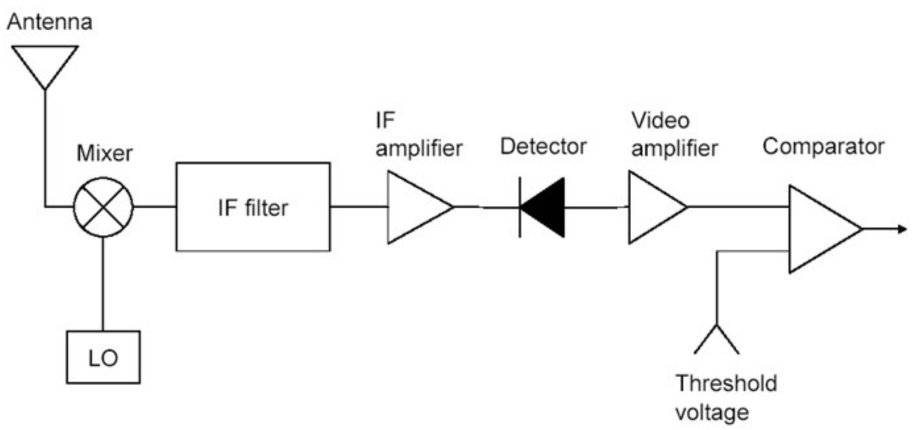

Figure 2.2 Superheterodyne Receiver

2.2.1.3 Instantaneous Frequency Measurement (IFM) Receivers

These kinds of receivers are named after their capability of measuring instantaneous frequency on wide bands. Simply the input signal is split into two paths. One path is time delayed and the other is preserved. Original and delayed signals are used in phase correlators in order to produce cos(wt) and sin(wt) components.

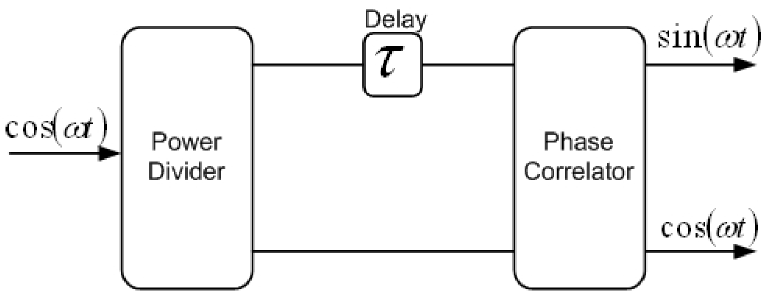

Figure 2.3 Superheterodyne Receiver [13]

After the output of the phase correlators is obtained, carrier frequency can be determined. This is done by using the relation between time delay and phase. The equations are given below;

$$\theta = \omega\tau = 2\pi f_c \tau \qquad \text{E- 2.1}$$

$$\theta = \tan^{-1}\left(\frac{\sin(\omega\tau)}{\cos(\omega\tau)}\right) \qquad \text{E- 2.2}$$

and carrier frequency is obtained from;

$$f_c = \frac{1}{2\pi\tau}\tan^{-1}\left(\frac{\sin(\omega\tau)}{\cos(\omega\tau)}\right) \qquad \text{E- 2.3}$$

IFM receivers have wide instantaneous bandwidth but they are unable to distinguish between simultaneous signals. The signal interception is done with these kind receivers by using measuring the input signal frequency as a searching mechanism; if the input exists than the measurement will give a result.

2.2.1.4 Digital Receivers

In this kind of receivers; after a RF translation stage the signal is transferred into digital domain by using Analog to Digital Converter (ADC). A digital signal can be defined as quantized samples of a continuous time signal. A digital signal is discrete both in time and in magnitude. Applying some mathematical operations on this signal is called digital signal processing. Today digitally modulated signals are very important for communication systems. Such signals are utilized in many civilian and military applications.

After digitizing every operation is done with digital equipments like Digital Down Converters (DDC), Digital Signal Processors (DSP) and Field Programmable Gate Arrays (FPGA). The operational disadvantages of analog processing like distortion harmonics are eliminated by digital processing.

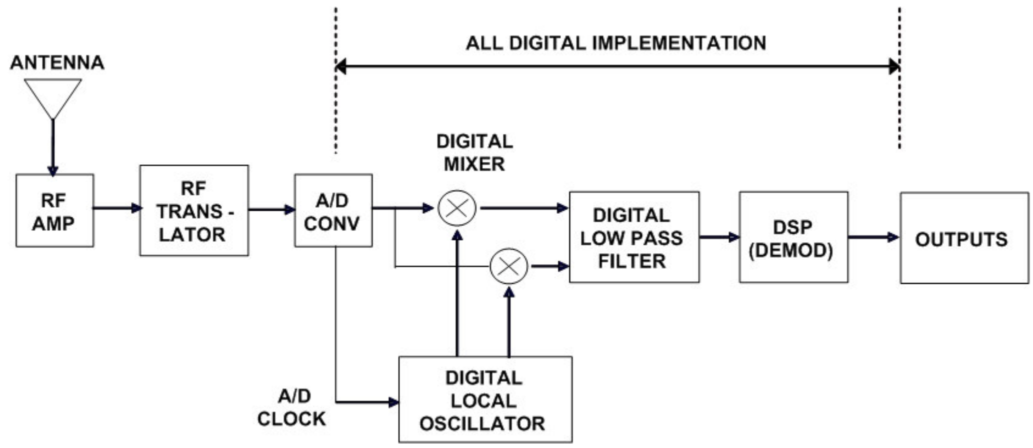

Figure 2.4 Digital Receiver

As a result of examining today's receivers which are named "digital receiver", the digital receiver definition becomes more and more confusing. Because it is tended to name a receiver digital if it is more "digital" than another one. Actually there is a level of being digital and it is indicated by the place of ADC in the receiver. This is come out by the improvements in ADC technology. As the speed (sampling frequency) and resolution (sampling resolution) of the ADC increase, the place of the ADC becomes closer to the antenna because they start to digitize wider frequency bands and analog mixing process starts to leave the job to digital mixing modules and DDC's. Today the entire HF band can be digitized without using any analog mixers

Interception techniques being used in digital receivers implemented by software's running on DSP's and by hardware description languages defining FPGA configurations. Also the overall architecture must be compatible with the target signal sources.

As a conclusion; interception of DSSS signals needs digital signal processing so this approach can be implemented by using only digital receivers. In the following section interception techniques that are being used in digital receivers are defined.

2.2.2 INTERCEPTION TECHNIQUES

As the high performance digital transmission devices become common, different techniques for interception of these signals began to implement on digital receivers. In this section interception techniques being used on digital receivers are introduced. Also analog signal can be intercepted with these receivers.

Interception is mainly based on frequency analysis in digital domain. When the direction of the antenna beam is fixed the next job is to search the signal energy in frequency domain. When the data flow in digital interception receivers is examined it is seen that the input of digital signal processors are band limited signals. The limited band is formed by either the tuners or DDC's according to the target signal bandwidth and target frequency band. In the digital signal processor's input bandwidth, a frequency analysis is made in order to intercept the energy on frequency components. At this point modern mathematical tools such as time-frequency analysis are used. Time-frequency analysis is also a fundamental tool for analyzing frequency agile signals. These techniques and basic properties are summarized below [18];

- Wigner-Ville Distribution (WVD)
    - Good Time-Frequency resolution
    - Cross-term interference (for multiple signals)
- Ambiguity Function (AF)
    - AF is the 2D Fourier Transform of the WVD
    - A correlative Time-Frequency distribution
- Choi-Williams Distribution (CWD)
    - Used to suppress WVD cross-term interference (for multiple signals), though preserves horizontal/vertical cross-terms in T-F plane
    - Basically a low-pass filter
- Time-Frequency Distribution Series (Gabor Spectrogram) (TFDS)
    - Used to suppress WVD cross-term interference (for multiple signals) by:
        - Decomposing WVD into Gabor expansion
        - Selecting only lower order harmonics (which filters cross-term interference)

- Short-Time Fourier Transform (STFT)
    - STFT is a sliding windowed Fourier Transform
    - Cannot accommodate both time and frequency resolution simultaneously
    - Square of STFT is Spectrogram (which is the convolution of the WVD of the signal and analysis function)
    - Not well suited for analyzing signals whose spectral content varies rapidly with time
- Short Adaptive Time Frequency Representation (S-ATFR)
    - Adaptive determination of kernel function for increasing performance
    - Time-frequency interference suppression
- Fractional Fourier Transform (FrFT)
    - The FrFT is the operation which corresponds to the rotation of the WVD
    - The Radon Wigner Transform is the squared magnitude of the FrFT
    - Main application may be a fast computation of the AF and WVD

These approaches mostly have better performances for not spreaded transmissions. All of these techniques use Fourier analysis at different levels in order to obtain time-frequency behavior of the signal.

The technique discussed in this thesis which is based on autocorrelation fluctuations and eigen analysis is specialized on DSSS signals and different form the time frequency based approaches [3] . First of all there is no need to make any frequency analysis in order to detect the signal. The alternative techniques proposed for interception of DSSS signals which are also used for comparisons in this work can be summarized as below;

- Amplitude Moment Function
- The cross-correlation function (CCF) and the cross-spectral density (CSD)
- Cyclostationary spectral analysis

These techniques are discussed in more detail at the last part of performance analysis chapter. Also performance analysis for these techniques is investigated in order to make necessary comparisons.

In the following section spread spectrum signals including DSSS is discussed.

2.3 SPREAD SPECTRUM

Spread-spectrum communications technology was first described on paper by an actress and a musician. In 1941, Hollywood actress Hedy Lamarr and pianist George Antheil described a secure radio link to control torpedoes and received U.S. patent #2.292.387. [14]

It was not taken seriously and was forgotten until the 1980s. After 1980s this approach came alive, and has become increasingly popular for applications that involve radio links in hostile environments.

Typical applications for the resulting short-range data transceivers include satellite-positioning systems (GPS), 3G mobile telecommunications which also used in simulations in later sections, W-LAN (IEEE802.11a, IEEE802.11b, IEE802.11g), and Bluetooth.[14]

Spread spectrum approach is apparent in Shannon and Hartley theorem of channel capacity.

$$C = B \times Log_2(1 + S/N) \quad \text{E- 2.4}$$

"C" in the equation is channel capacity defined in bit per second (bps). This is the maximum data rate for a theoretical bit error rate (BER). B is the channel bandwidth in Hz and S/N is signal to noise power ratio.

In other words C defines the amount of information allowed by the channel and represents the desired performance. Bandwidth is the amount of limited source that is used for communication and S/N represents the environmental conditions.

Modifying the equation by changing the log base from 2 to e (Napierian number);

$$C/B = (1/\ln 2) \times \ln(1 + S/N) \quad \text{E- 2.5}$$

Applying MacLaurin series;

$$\ln(1 + x) = x - x^2/2 + x^3/3 - x^4/4 + ... + (-1)^{k+1} x^k/k + ... \quad \text{E- 2.6}$$

$$C/B = 1.443 \times \left(S/N - 1/2(S/N)^2 + 1/3(S/N)^3 - ...\right) \quad \text{E- 2.7}$$

S/N is usually low for spread-spectrum applications. (As mentioned before, the signal can be even below the noise level.) Assuming S/N<<1 Shannon's expression becomes;

$$C/B = 1.443 \times S/N \quad \text{E- 2.8}$$

To send error-free information for a given noise-to-signal ratio in the channel, therefore, we need only perform the fundamental signal-spreading operation: increase the transmitted bandwidth. In conventional communication systems the efficiency is obtained by utilizing signal energy and bandwidth. But to increase robustness of the system to external interferences, jamming, multipath and also interception, it is appropriate to make concessions on efficiency.

By using the explanations above we can make the definition of spread spectrum as; an RF communications system in which the baseband signal bandwidth is intentionally spread over a larger bandwidth by injecting a higher frequency signal. As a direct consequence, energy used in transmitting the signal is spread over a wider bandwidth, and appears as noise. [14]

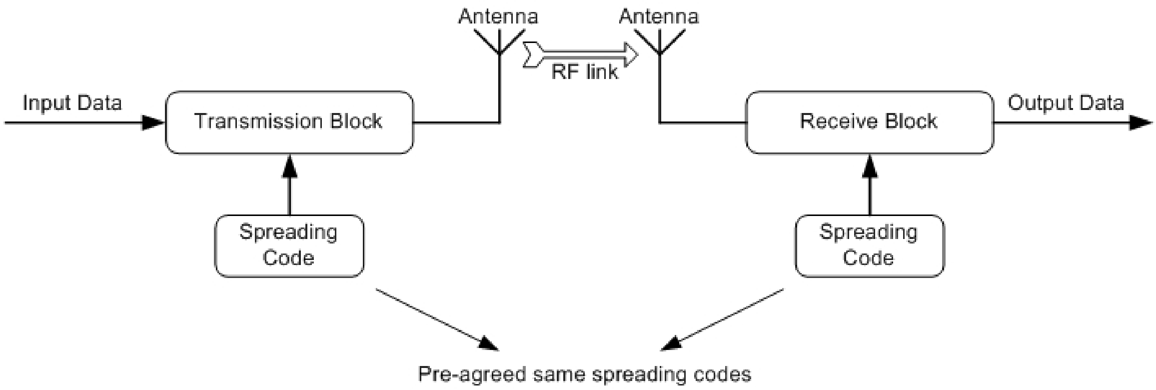

Figure 2.5 Spread Spectrum Communications

All the spread spectrum techniques have one approach in common; the key (also called spreading code or sequence) inserted to the communication channel. The point of inserting this code defines the spreading technique. The simple block diagram of the spread spectrum communications system is given in Figure 2.5.

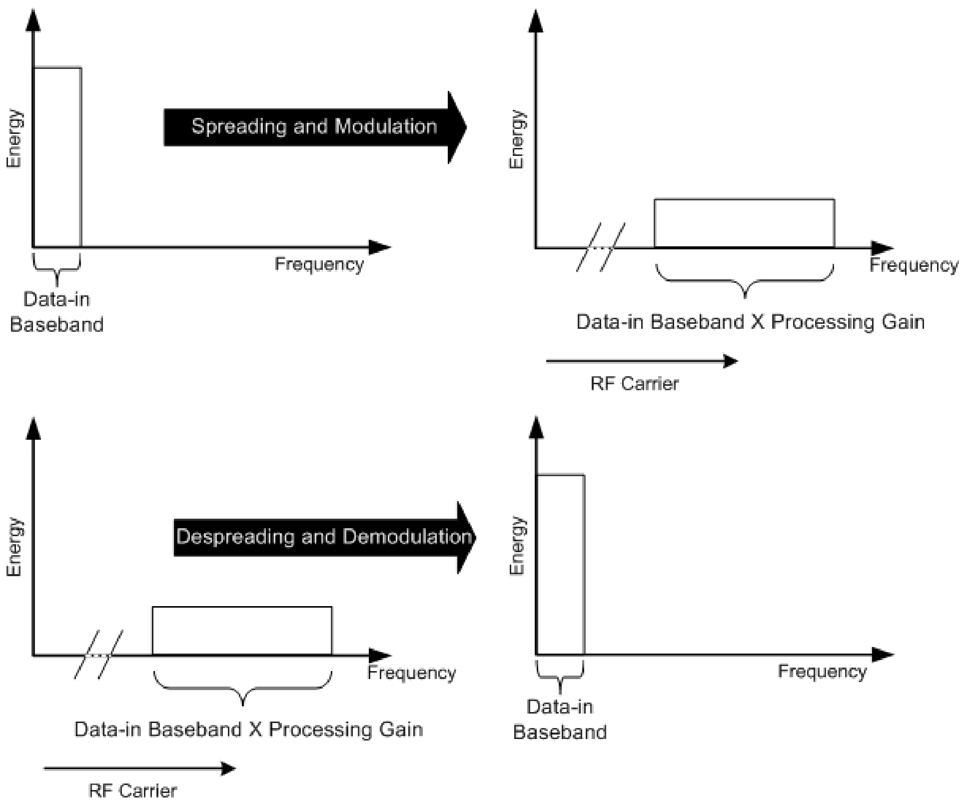

Figure 2.6 Effects of spreading on bandwidth

The ratio (in dB) between the spread baseband (BW_{SB}) and the original signal (BW_{OS}) is called 'processing gain' (G_P). The effect of spreading operation on frequency bandwidth is shown in Figure 2.6.

$$G_p = \frac{BW_{SB}}{BW_{OS}} \qquad \text{E- 2.9}$$

Spreading results directly in the use of a wider frequency band (by the factor "processing gain"), so it doesn't spare the limited frequency resource. That inefficient use is well compensated by also sharing enlarged frequency band by many users as used in Code Division Multiple Access (CDMA) communications.

We know that in spread spectrum systems there exists a code or key, which must be known in advance by the transmitter and receiver. In modern communications, the codes are digital sequences that must be as long and as random as possible to appear as "noise-like". But in any case, they must remain reproducible. Otherwise, the receiver will be unable to extract the message that has been sent. Thus, the sequence is "nearly random." Such a code is called a pseudo-random number (PRN) or sequence. (Also interception idea uses profit of this fact that the DSSS signal’s statistical properties are “noise like” but not the same as the noise statistical properties.) The method most frequently used to generate pseudo-random codes is based on a feedback shift registers.

There are three kinds of spread spectrum techniques, distinguished according to the point in the system at which the pseudo-random code is inserted to the communication channel. ;

- Frequency Hopping Spread Spectrum (FHSS)
- Time Hopping Spread Spectrum (THSS)
- Direct Sequence Spread Spectrum (DSSS)

2.3.1 Frequency Hopping Spread Spectrum (FHSS) Systems

In this method, as the name indicates; the carrier hopes from frequency to frequency over a wide band according to a sequence defined by the PRN. The speed at which the hops are executed depends on the data rate of the original information. According to this speed there are two kinds of hopping systems; Fast Frequency Hopping (FFHSS) and Low Frequency Hopping (LFHSS). LFHSS is the most common method. It allows several consecutive data bits to modulate the same frequency. FFHSS, on the other hand, is characterized by several hops within each data bit.[14]

The frequency hopper's output is flat over the band of frequencies used. The bandwidth of a frequency-hopping signal is simply N times the number of frequency slots available, where N is the bandwidth of each hop channel. [14] The basic block diagram of a FHSS system is given in Figure 2.7. (PA→ Power Amplifier, LO → Local Oscillator)

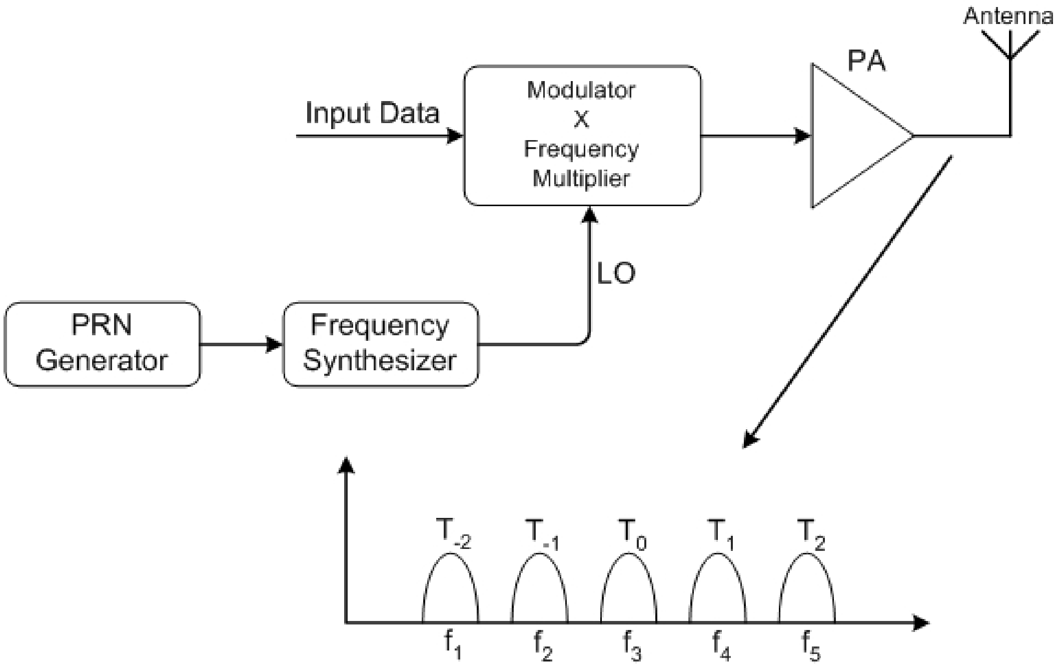

Figure 2.7 Block diagram of a FHSS system

2.3.2 Time Hopping Spread Spectrum (THSS) Systems

This method is not well developed today. The basic principle is applying on and off sequences to the Power Amplifier which are adjusted by using PRN sequence. [14]

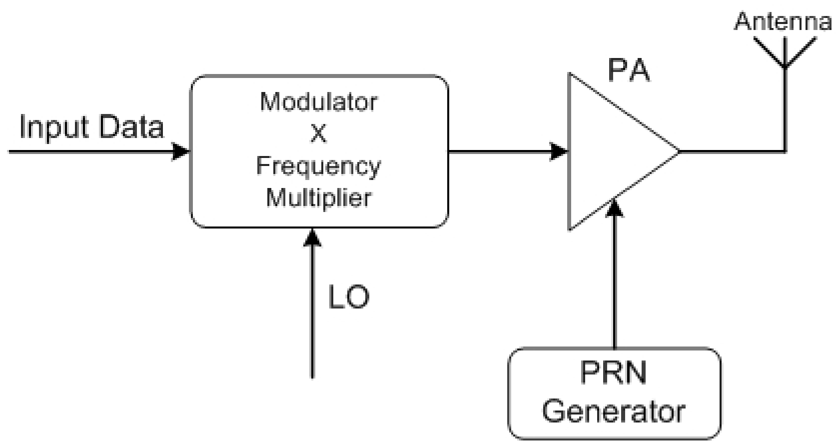

Figure 2.8 Block diagram of a THSS system

2.3.3 Direct Sequence Spread Spectrum (DSSS) Systems

In this thesis this technique is in interest. In DSSS systems, the PRN is applied directly to data entering the carrier modulator. PRN code sequence is named chip sequence and the data rate of this sequence is named chip rate. The modulator therefore sees a much larger bit rate, which corresponds to the chip rate of the PRN sequence.

The result of modulating an RF carrier with such a code sequence is to produce a direct-sequence-modulated spread spectrum.

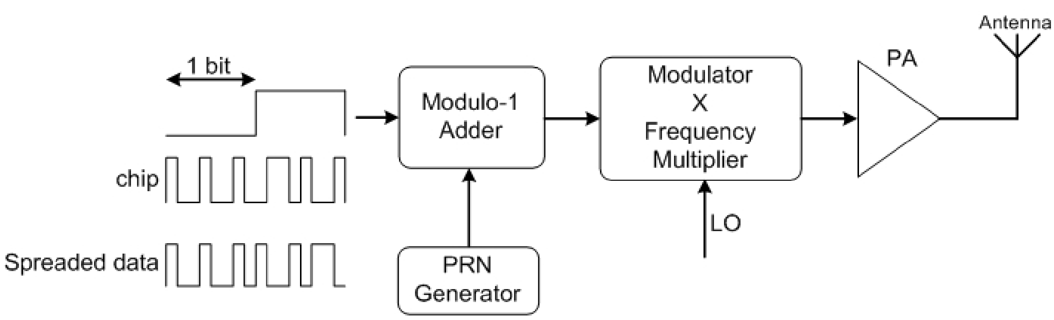

Figure 2.9 Block diagram of a DSSS system

CHAPTER 3

DETECTION OF DSSS SIGNALS

3.1 Introduction

In this chapter and following chapters instead of "interception" the word "detection" is used. Because the approach given here is a more concentrated subject that deals with DSSS signals, besides detection with no a priori knowledge can be considered as interception [3] .

This chapter consists of detailed explanations and analysis of the detection idea that uses profit of the fact that the signal statistical properties are not the same as the noise statistical properties. This approach depends on calculation of fluctuations of autocorrelation estimators. The more detailed derivation of the approach is given in Appendix A.

3.2 Assumptions and Signal Model

This section mainly describes the assumptions which identify the receiver filter, DSSS signal and noise characteristics. Besides the assumptions explained in this section, we consider that no a priori information is available. As the spreading sequence, symbol period and other information used in DSSS receivers are not known, we use the statistical properties of the signal which is the basic principle of detection methods [3].

The detection receiver, receives y(t) as the input of its receiver filter (Figure 3.1) which is assumed as a simple band pass filter. Filter passes the band in which we look for a DSSS signal hidden under noise level.

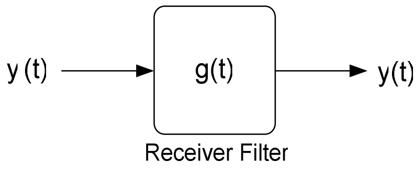

Figure 3.1 Receiver Filter

The received signal is;

$$y'(t) = s'(t) + n'(t) \qquad \text{E- 3.1}$$

The output of the receiver filter is;

$$y(t) = s(t) + n(t) \qquad \text{E- 3.2}$$

Output of the receiver filter consists of, noise n(t) and filtered noise-free DSSS signal s(t);

$$\begin{aligned} s(t) &= g(t) * s'(t) \\ n(t) &= g(t) * n'(t) \end{aligned} \qquad \text{E- 3.3}$$

The structure of noise free, received DSSS signal which is given in E- 3.3. The signal is consisted of symbols a_k that are multiplied by pseudo-random sequence which spreads the bandwidth. The spreading sequence is symbolized as h(t) and it is represented by the pseudo random sequence c_k and p(t) which is the convolution of the transmission filter and the channel filter.

$$\begin{aligned} s'(t) &= \sum_{k=-\infty}^{+\infty} a_k h(t - kT_s) \\ h(t) &= \sum_{k=0}^{P-1} c_k p(t - kT_c) \end{aligned} \qquad \text{E- 3.4}$$

where T_c is chip period and T_s is symbol period,

$$c_k = k = 0, \ldots, P-1 \qquad \text{E- 3.5}$$

so;

$$T_s = T_c P \qquad \text{E- 3.6}$$

As a conclusion, the assumptions about transmission are summarized below [3];

- Symbols are centered and uncorrelated
- The received noise is white, Gaussian, centered and uncorrelated with the signal. Its power spectral density is $N_0/2$
- The time extension of g(t)*h(t) is only a little more than Ts
- The signal is hidden in noise (the signal to noise ration at the output of the receiver filter is negative)

3.3 Idea of Autocorrelation Fluctuations

The main idea of spread spectrum signals is to be similar to noise in order to have low probability of intercept ability. So the autocorrelation function of spread spectrum signals are close to diract function as well as autocorrelation of white noise. This property is gained by using pseudo random sequence for spreading.

Although the autocorrelation of DSSS signal is similar to autocorrelation of noise, the fluctuations of autocorrelation estimator function is different at all [1]. The fluctuations of autocorrelation function are computed by dividing the received signal into M temporal windows. In each window an autocorrelation estimator is applied and second order moment of these estimators gives the fluctuations. This approach is shown in Figure 3.2

As the window number is denoted by n and the window duration is denoted by T the estimation of autocorrelation is defined by;

$$\hat{R}_{yy}^{n}(\tau) = \frac{1}{T}\int_{0}^{T} y(t)\, y^{*}(t-\tau)\,dt \qquad \text{E- 3.7}$$

Fluctuations of autocorrelation estimations (p(τ)) are defined by the second order moment of estimated correlation and total number of windows is M [3] so;

$$\rho(\tau) = E\left\{\left|\hat{R}_{yy}(\tau)\right|^{2}\right\} = \frac{1}{M}\sum_{n=0}^{M-1}\left|\hat{R}_{yy}^{n}(\tau)\right|^{2} \qquad \text{E- 3.8}$$

Simply we use p(τ) as a tool to detect the DSSS signal hidden in noise and the fluctuations at the multiples of symbol period is the evidence of presence of the DSSS signal. This idea can be found in [3], [2] and [1].

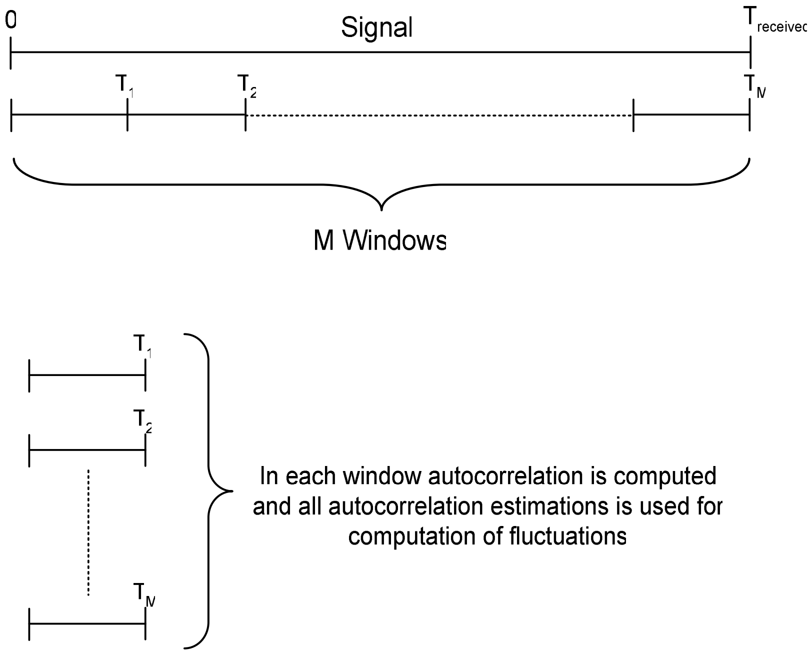

Figure 3.2 Idea of autocorrelation fluctuations

3.4 Output SNR and Performance

SNR definition at the output of the detector explains the parameters that has an effect on the performance of the detection and it also gives an idea about the SNR level that the detection can be accomplished. By using the context; fluctuations at the multiples of symbol period is the evidence of presence of the DSSS signal, SNR at the output of detector is defined as [3];

$$SNR_{out} = 20\log\left(\frac{m_p^s}{\sigma_p^n}\right) \qquad \text{E- 3.9}$$

It is significant to determine the peaks caused by signal among the peaks caused by noise. So instead of comparing m_p^s with m_p^n it is better to compare m_p^s with σ_p^n.

By using the equations for m_p^s and σ_p^n;

$$\frac{m_p^s}{\sigma_p^n} = \frac{T_s/_T\, \sigma_s{}^4}{\sqrt{\frac{2}{M} m_p^n}} \qquad \text{E- 3.10}$$

we write m_p^n equation

$$\frac{m_p^s}{\sigma_p^n} = \frac{T_s/_T\, \sigma_s{}^4}{\sqrt{\frac{2}{M}\left(\frac{1}{TW}\sigma_n{}^4\right)}} \qquad \text{E- 3.11}$$

$$\frac{m_p^s}{\sigma_p^n} = WT_s \sqrt{\frac{M}{2}}\left(\frac{\sigma_s 2}{\sigma_n{}^2}\right)^2 \qquad \text{E- 3.12}$$

when we use this equation at SNR_{out} we get;

$$SNR_{out} = 4SNR_{in} + 20\log(WT_s) + 10\log(M) - 10\log(2) \qquad \text{E- 3.13}$$

We must note that ‘W’ does not always increase output SNR. The optimum case is W equal to the signal bandwidth. However the tolerance is large enough. For example if W is twice the signal bandwidth the input SNR decreases 3dB but from the 20log(WT_s) expression we gain 6dB and over all 6dB lost in output SNR [3].

Also increasing window number ‘M’ is not always possible. Because more windows you use, more computational power you need and also there is a limited time for detection.

3.5 Simulation Model

In this section simulation model is described. MATLAB running on AMD Athlon 2500 with 1GB RAM is used for simulations. The modularity criterion is applied on over all design. The functional block diagram is defined in Figure 3.3. The simulation starts with the signal generation. Different types of DSSS signals are generated in order to test the detection system on different types of signals. After signal generation channel effects are applied on transmitted signal to obtain received signal. Finally detection process starts with autocorrelation fluctuation calculation and detection of peaks caused by the signal among the peaks generated by noise.

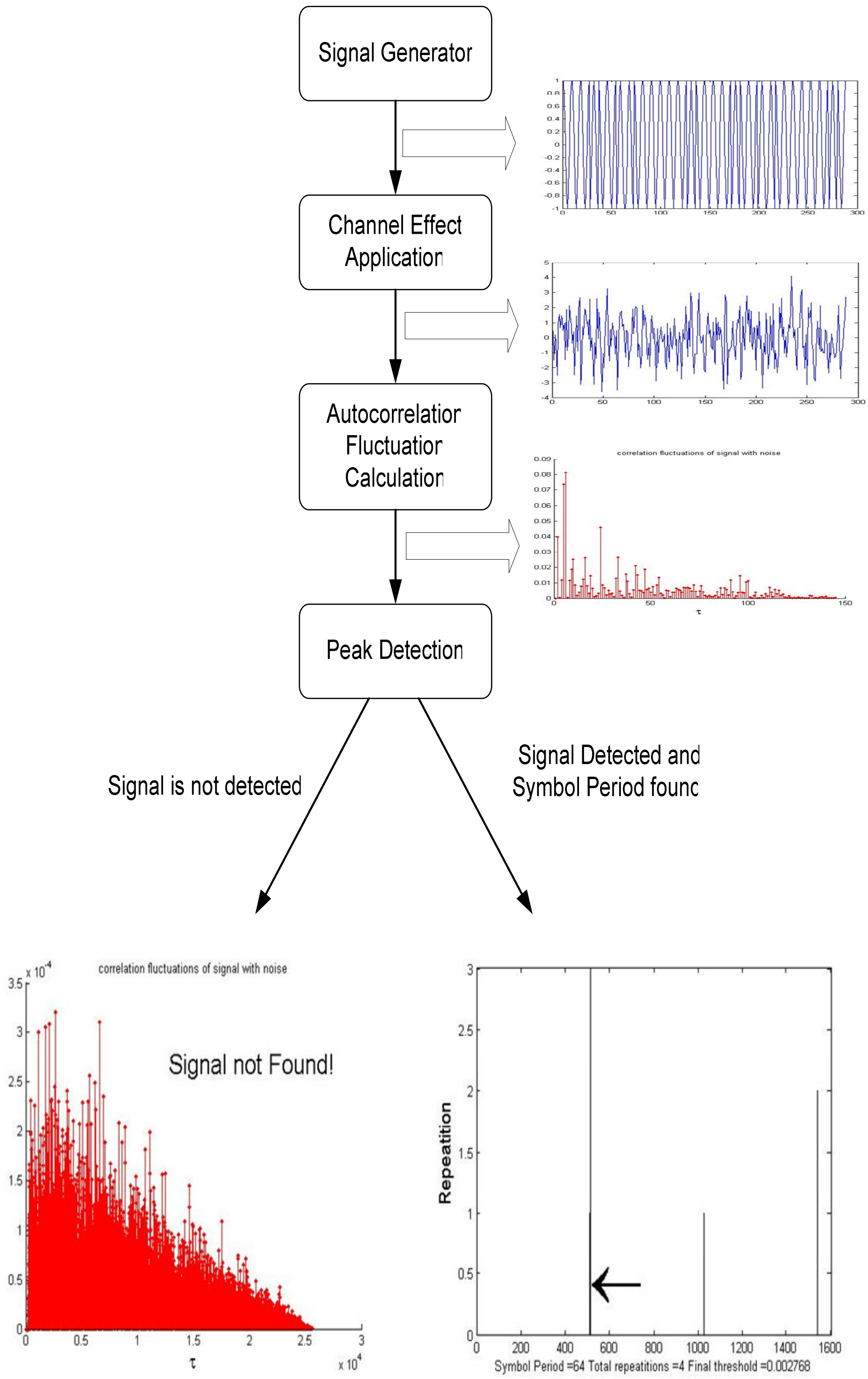

Figure 3.3 Simulation Functional Block Diagram.

In the following parts these functional blocks are described in more detail.

3.5.1 Signal Generation

This is the start of simulation process. Different kinds of DSSS signals with different utilization areas are generated. The types of input signals can be summarized as below;

- Typical DSSS Signals
- Third Generation CDMA Signals (UMTS)
- Typical LPI Radar Signals

In the following sections the properties of generated input DSSS signals are described. The parametric values (spreading size, number of symbols etc.) are given with each simulation result in order to ensure integrity.

3.5.1.1 Typical DSSS Signals

The first input signal is typical DSSS signals. By using typical DSSS signals for simulation the performance of the algorithm on basic characteristics of DSSS signals is tested. It is chosen to generate baseband (Pulse Amplitude Modulated) signals and Square-Root Raised Cosine filter with roll-off factor of 0.1 is applied on generated signal before transmission. The specific parameters are given in following with each simulation result.

3.5.1.2 Third Generation CDMA Signals (UMTS)

The second input is Universal Mobile Telecommunications System (UMTS) waveform created based on technical specification of ETSI TS 125 213 v6.2.0 (2005-3) [7] and detection algorithm is tested by using this waveform.

The signal generated here is simple uplink channel with DPDCH (Dedicated Physical Data Channel) and DPCCH (Dedicated Physical Control Channel) included. The data modulation of both the DPDCH and the DPCCH is Binary Phase Shift Keying (BPSK). Spreading modulation is applied after data modulation. The spreading modulation used in the uplink is dual channel QPSK This modulation structure is based on mapping DPDCH and DPCCH to I and Q channels (Figure 3.4). Spreading modulation is consists of two type of operations.

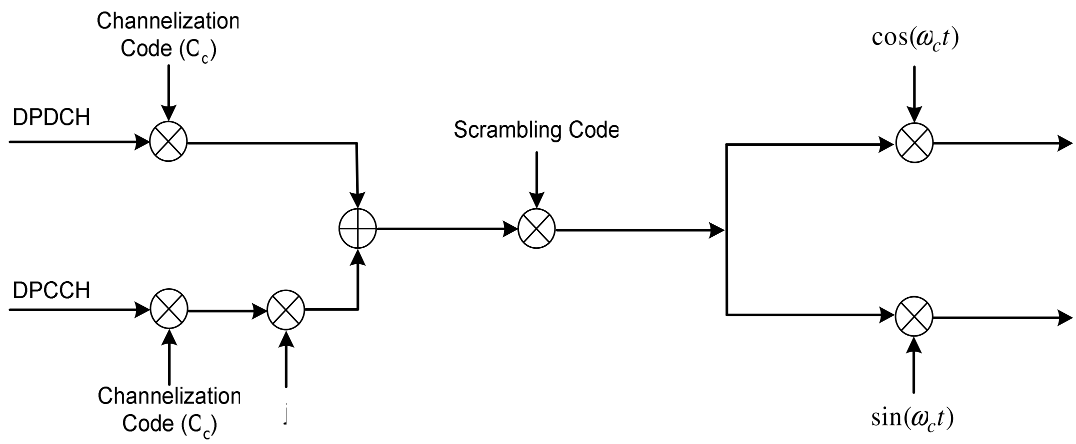

Figure 3.4 Spreading Modulation of UMTS Uplink [7]

The first one is spreading where each data symbol is spread to a number of chips given by the spreading factor. This increases the bandwidth of the signal. UMTS standard defined Orthogonal Variable Spreading Factor (OVSF) codes are created and used in this operation.

The most important purpose of the spreading codes is to help preserve orthogonality among different physical channels. The code structure is based on the tree architecture shown in Figure 3.5. Here each level of the tree corresponds to a different spreading factor. All the codes of the same level constitute a set and they are orthogonal to each other. Any two codes of different levels are orthogonal to each other as long as one of them is not the mother of the other code [8].

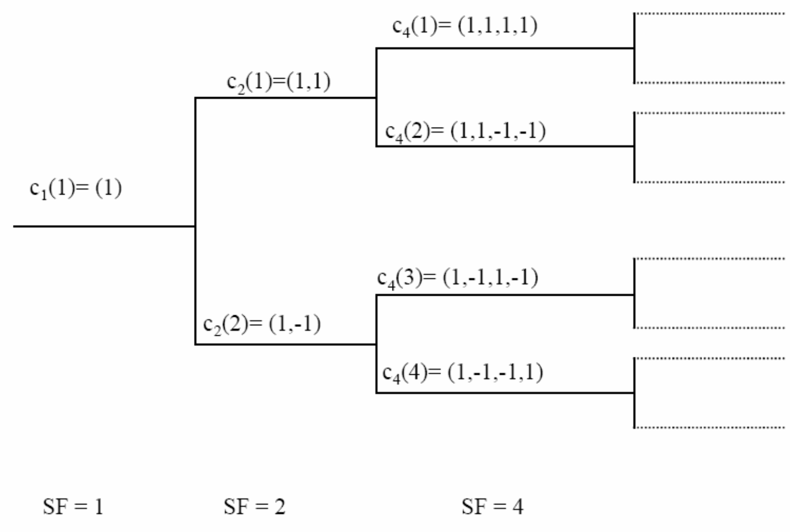

Figure 3.5 Orthogonal Variable Spreading Factor (OVSF) codes [7]

The second operation is scrambling where a complex valued scrambling code is applied to spreaded signal. These scrambling codes defined by the upper levels and used to help maintain separation between different mobile stations. There are two kinds of scrambling code as; short scrambling codes and long scrambling codes. Short scrambling codes are recommended for base stations equipped with advanced receivers employing multi-user detection or interference cancellation. Long scrambling codes are simpler but considering limited time and computational power aspect the short code is preferred for simulation.

Also Square-Root Raised Cosine filter with roll-off factor of 0.22 is applied on generated signal before transmission as defined in the standard.

3.5.1.3 Typical LPI Radar Signals

The second, generated input is typical LPI radar signals. Many users of radar today are specifying a Low Probability of Intercept (LPI) concept as an important tactical requirement. Pulse compression is a very common technique that is being used to acquire LPI property. This approach mainly depends on achieving higher range resolutions by using higher bandwidths while decreasing emitted average power levels.

The bandwidth can be increased by applying modulation on pulses. Usually different types of frequency phase and hybrid modulation techniques can be used. In pulse compression approach a code that defines the modulation is used. This is evidently needed because there is not any information to be transmitted and so there is not any data to be used is modulation operation. Here instead of information transmission, the main goal is to obtain a waveform that is efficient for radar. At this point ambiguity function is used to determine the performance characteristics of the code used.

A common code the is used in FSK modulation is Costas frequency codes. [9] These codes are used to determine the order of the frequencies that is to be used for transmission. (Normally in communication systems this is done according to symbols.)

For the PSK modulation on pulse technique, usually Barker and Frank codes are used. An efficient alternative to these codes is pseudo-random codes which lead to the concept of DSSS.

3.5.2 Channel Effects

In the simulation three kind of channel effects are tested;

- (Colored) Noise
- Interference
- Multipath

By using these effects detailed performance analysis is obtained. The results of these analyses are given in the preceding sections. The noise is generated in the pass band of the receiver filter so noise is colored in over all frequencies but it is white in the receiver pass band. The shape of the filter and detailed analysis are given in the preceding sections. For interference effect, different signals are added to input bandwidth of the receiver filter. These interference signals are also considered to be colored noise. Finally for the multipath effect, lower amplitude echoes of the original transmitted signal are generated and applied to channel.

3.5.3 Autocorrelation Fluctuation Calculation

The autocorrelation estimation is done by using the equations defined in previous sections. In calculation the window size is arranged according to the number of symbols generated. There is a restriction about the computational power so a limited number of symbols can be generated.

In Figure 3.6 there is an example of output of the autocorrelation fluctuation calculation.

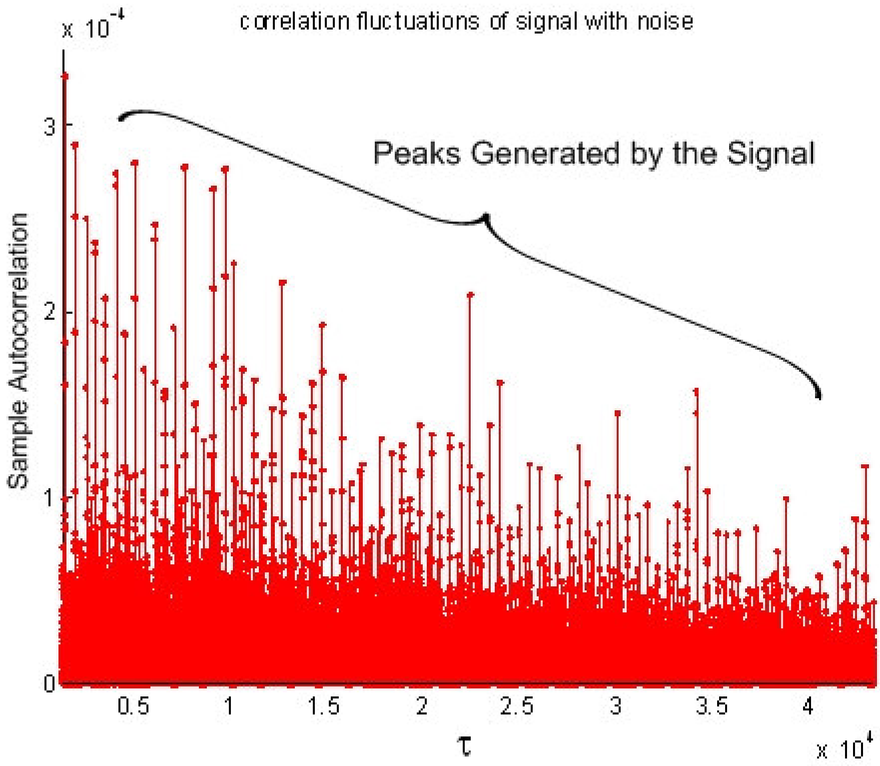

Figure 3.6 Example output of the autocorrelation fluctuations

3.5.4 Detection of the Peaks

This function is used for distinguishing peaks caused by the signal among the ones caused by the noise. Simply theoretical threshold $m_p^n + 4\sigma_p^n$ can be used for detection. If there are any peaks above that threshold it means that there exists a signal hidden under noise. This approach is true but works well for SNR's higher that -10dB. To improve the detection capability of the algorithm a different method is applied at this point.

The peak detector calculates the threshold level $m_p^n + 4\sigma_p^n$ and the level of the highest peak and divides the area between these amplitudes to 100 search levels. These levels are shown in Figure 3.7. On every level form the top there made a search for periodically repeating peaks. The basic principle is to use the property of the peaks caused by the signal to be periodical by the symbol period to recognize them.

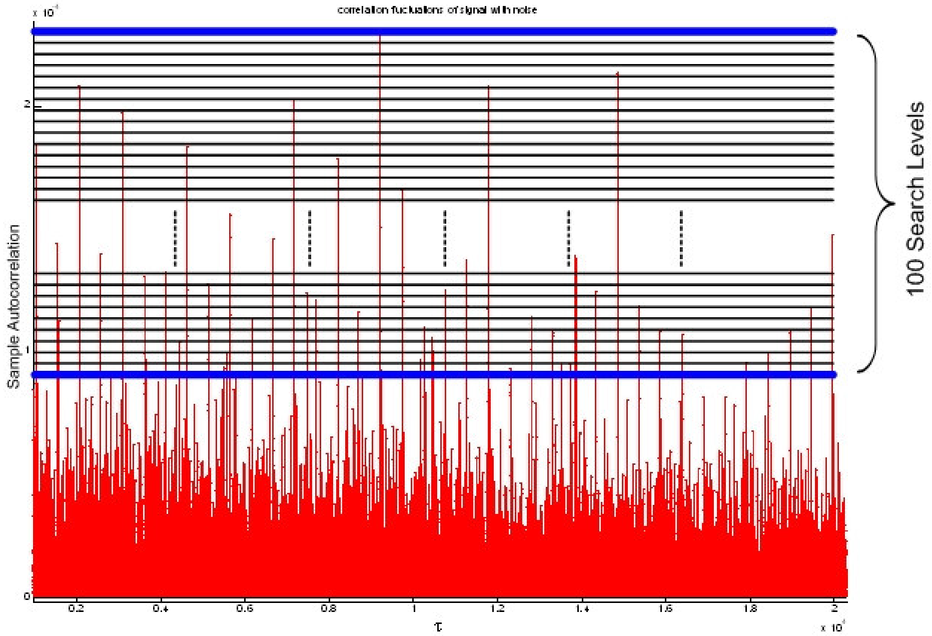

Figure 3.7 Peak Detector’s search levels

The search on every level is done with two steps. First step is measuring the distance between the peaks above the level and second step is to make histogram of the distances to get the periodicity. The minimum accepted limit of number of repetition for ensuring that repetition is caused by signal is 6. So at least 6 peaks must be repeated with the same period above the threshold, to be sure that there is a signal hidden under noise. This number can be arranged due to total number of symbols in the window. In Figure 3.8 example of the detector’s histogram output is shown.

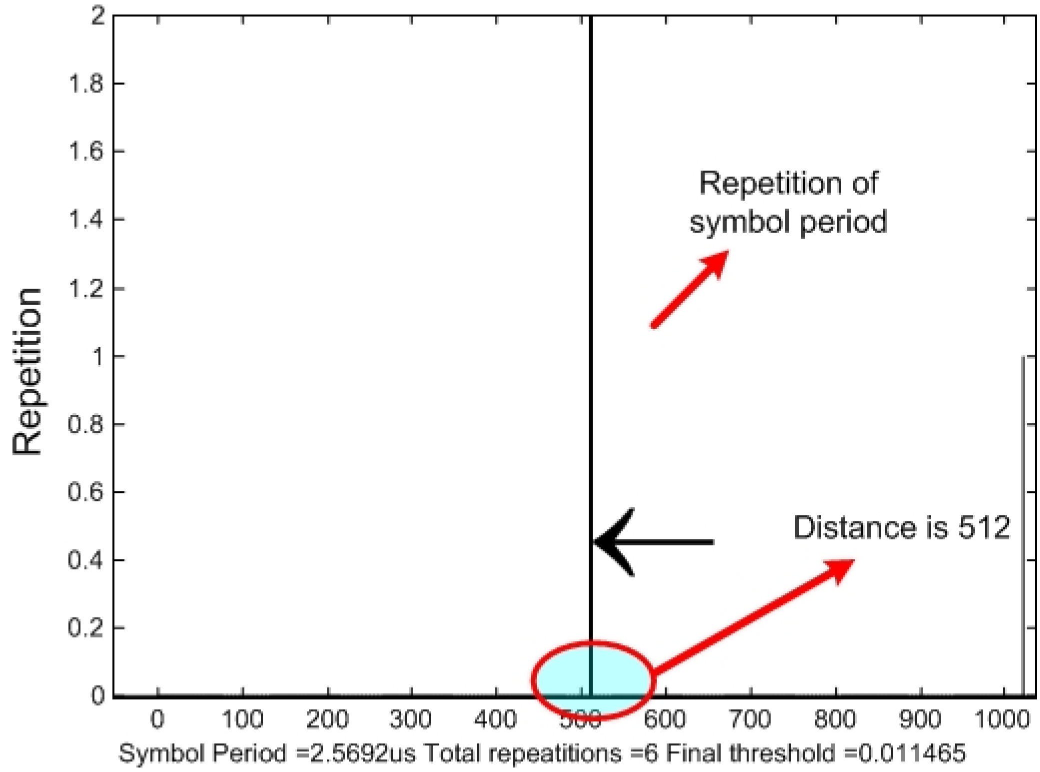

Figure 3.8 Peak Detector's histogram output

In the Figure 3.8 most repeating period is 511 but the near by periods in the histogram (509, 510, 512, 513) is also considered. Here a window of length 10 is used in order to make detect the peaks caused by the signal which are shifted due to low SNR and autocorrelation nature. So here an error of 10/200MHz=0.05µs is acceptable when compared to the possibility of not detected the hidden signal. So this approach increases the possibility of detection and it is similar to the approach used for deinterleaving of the radar pulses according to the PRI values and histograms.

Finally the mean of the periods in the window of length 10 is divided to sampling frequency and the real symbol period is found as 2.5692. The other repeating period is 1022 and it is the multiple of the original one.

Today this kind of algorithms mainly used to help the operator that uses the interception tool. But it is important to mention that using experienced operator who is familiar with different types of input signals always improve the performance. This can be seen in simulation results when signal is not found while the existence of the signal is clearly seen at the output of autocorrelation fluctuation calculation. This fact is so accepted that it being tried to simulate the decisions of an experienced operator for automated systems and this is another area including AI. Also neural network solutions are tend to be used.

3.6 Simulation Results

In this section simulation results are given for the signal type described in the previous chapter in order to clarify the algorithms. The inputs of the MATLAB codes which determine the transmitted signal and channel characteristics are explained for each simulation. Also comments about the results are given. It is important to note that these are the results for specific channel conditions and they are not given for the performance analysis. Performance analysis is given in preceding section.

3.6.1 Typical DSSS Signals

Input parameter values that are used to generate the DSSS signal is summarized in Table 3.1 . The channel parameters are given in Table 3.2. and the receiver parameters are given in Table 3.3.

Table 3.1 Typical DSSS signal parameters (Simulation Results-1)

Parameters	Values
Chip Rate	64chips/symbol
Sampling Freq.	200MHz
Observation time	1024168 samples
Symbol Period	20.48μs
Signal Bandwidth	5MHz

Table 3.2 Channel Parameters (Simulation Results-1)

Channel Type	Values
Gaussian Noise	SNR at Output of Receiver Filter = –11dB

Table 3.3 Receiver parameters (Simulation Results-1)

Parameters	Values
Receiver filter bandwidth	20MHz
Window Number	20

In the figure Figure 3.9 the frequency content of DSSS signal which is pulse shaped and than low pass filtered by transmitter is given without adding any noise.

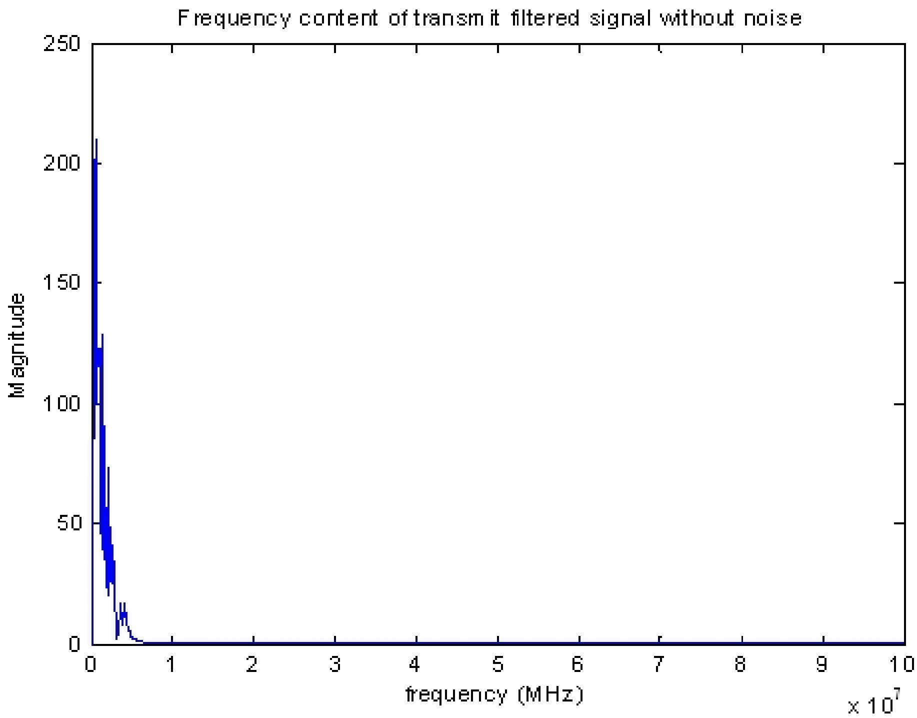

Figure 3.9 Frequency content of transmit filtered DSSS signal without noise

As seen the bandwidth is 5MHz. In the Figure 3.10 the frequency content of output of 20MHz receiver filter is seen. The SNR at he output of receive filter is –11dB and 2048 points FFT is used here. The signal is hidden in the 5MHz of 20MHz receiver bandwidth. This figure indicates that the signal is cannot be detected by using this kind of FFT analysis.

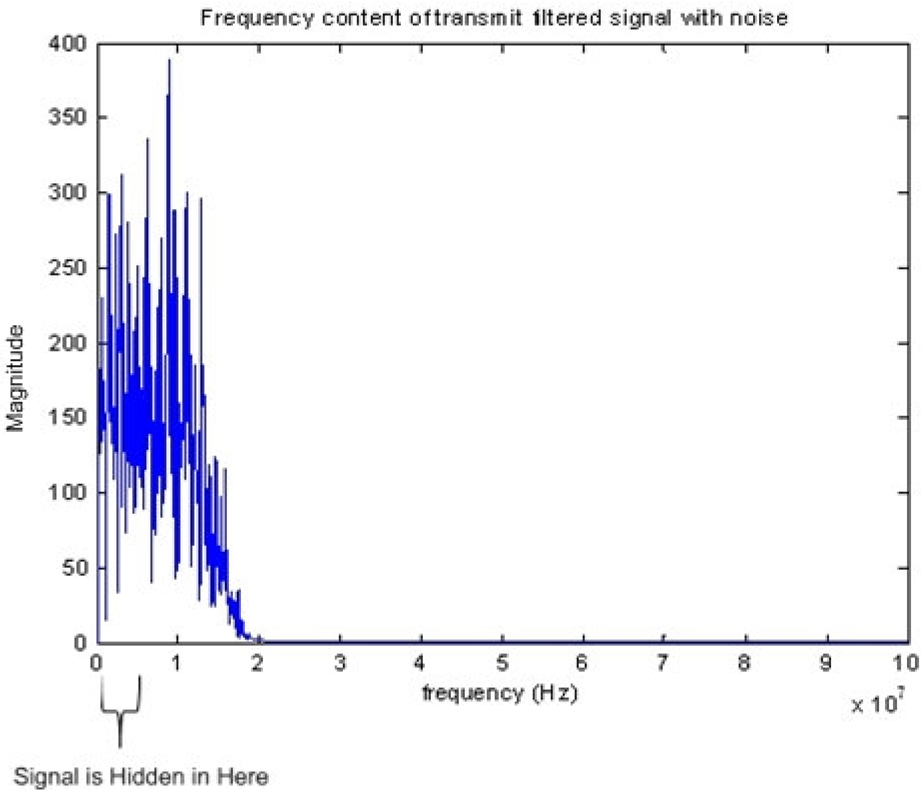

Figure 3.10 Frequency content of output of receiver filter when there is a hidden signal

In the Figure 3.11 an example to the output of autocorrelation fluctuation is given. The fluctuations caused by the signal are seen clearly.

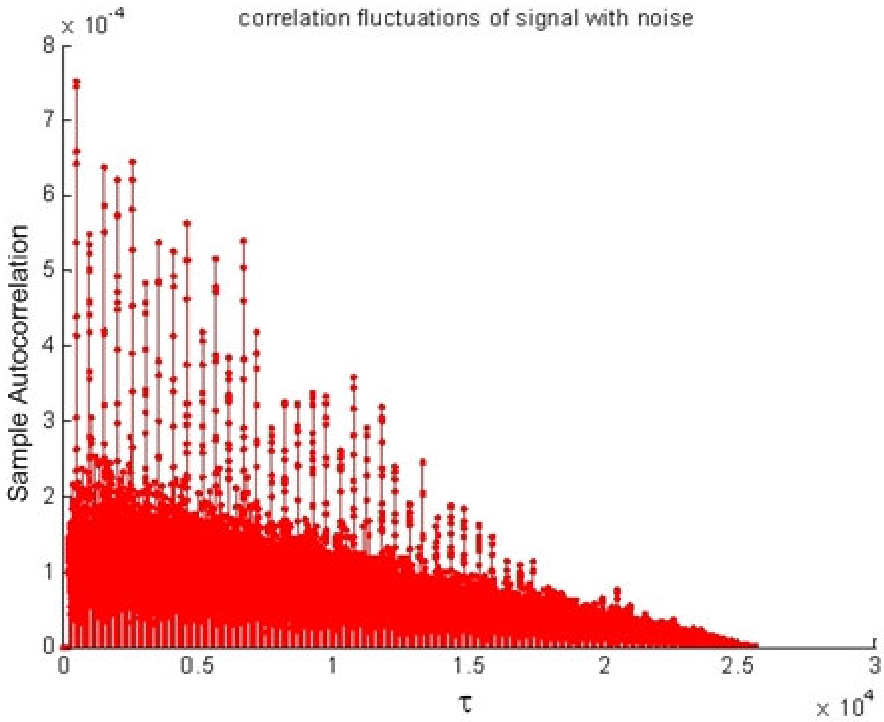

Figure 3.11 Output of autocorrelation fluctuation calculation

In the Figure 3.12 the output of the peak detector is given. The symbol period is detected correctly. By using this approach the peaks that are periodic but not visible due to peaks of the noise are extracted. Today these kinds of applications often used with manual operator help due to unknown characteristic of the input signal. If the operator is available this kind of automatic algorithms are not used alone so an improvement must be expected in the results in practical usage.

This result is only an example for specific conditions and as mentioned before the detailed performance analysis is done in the next section.

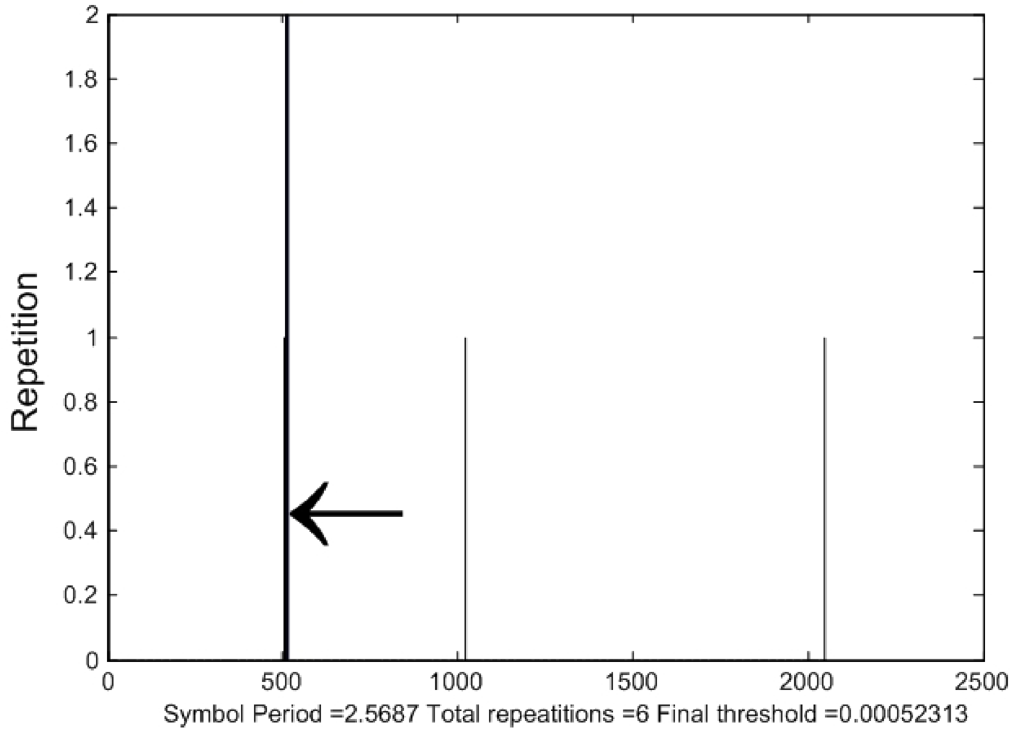

Figure 3.12 Peak Detector's histogram output

In the next simulation a channel with multipath effect is used for the same generated typical DSSS signal. Also same receiver parameters are used. The channel parameters are given in Table 3.4.

Table 3.4 Channel Parameters (Simulation Results-2)

Channel Type	Values
Gaussian Noise	SNR at Output of Receiver Filter = –14.68dB
Multipath Effect	1.Path→ delay: 10μs Attenuation: %70 2.Path→ delay: 100μs Attenuation: %80 3.Path→ delay: 1000μs Attenuation: %90

In the Figure 3.13 output of autocorrelation fluctuation is given. However the SNR is lower than the previous simulation, the fluctuations caused by the signal are seen clearly.

The symbol period is also calculated correctly as seen in Figure 3.14 . This is because delayed version of the signal is also generating the same peaks at the output of autocorrelation fluctuation calculation. These results must be considered as examples. The detailed performance analysis for multipath is given in following sections.

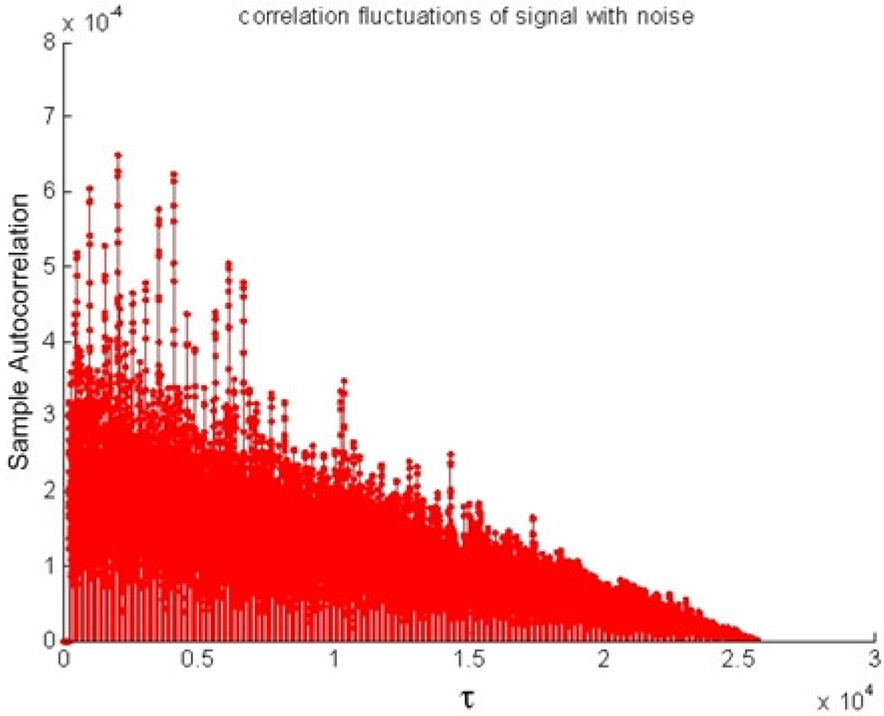

Figure 3.13 Output of autocorrelation fluctuation calculation

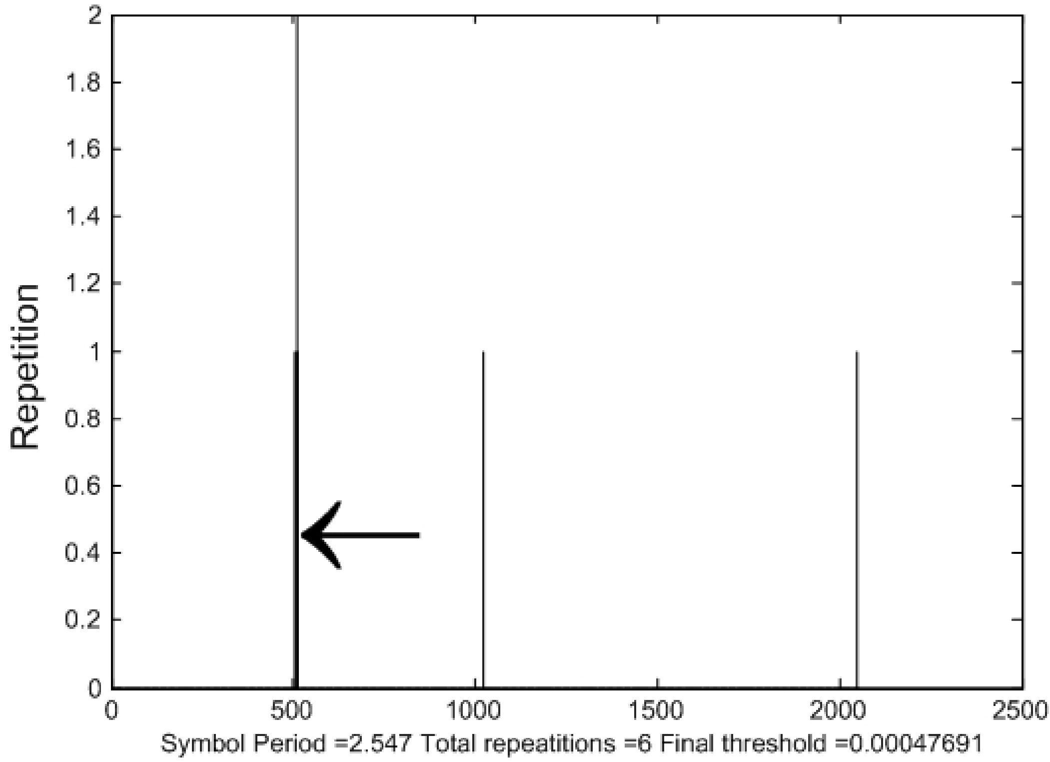

Figure 3.14 Peak Detector's histogram output

In the next simulation a channel with interference is used for the same generated typical DSSS signal. Also same receiver parameters are used. The interference signal is generated by using FIR filter and Gaussian noise. The interference signal can be also considered as colored noise. In this example the bandwidth of the interference signal is 11MHz and it is not in the band of DSSS signal. The condition that the interference is in the band of DSSS signal is also examined in performance analysis.

The interference signal is put in the pass band of receiver filter. The frequency content of the interference signal is given in Figure 3.15. The frequency content of the receiver output is also given in Figure 3.16.

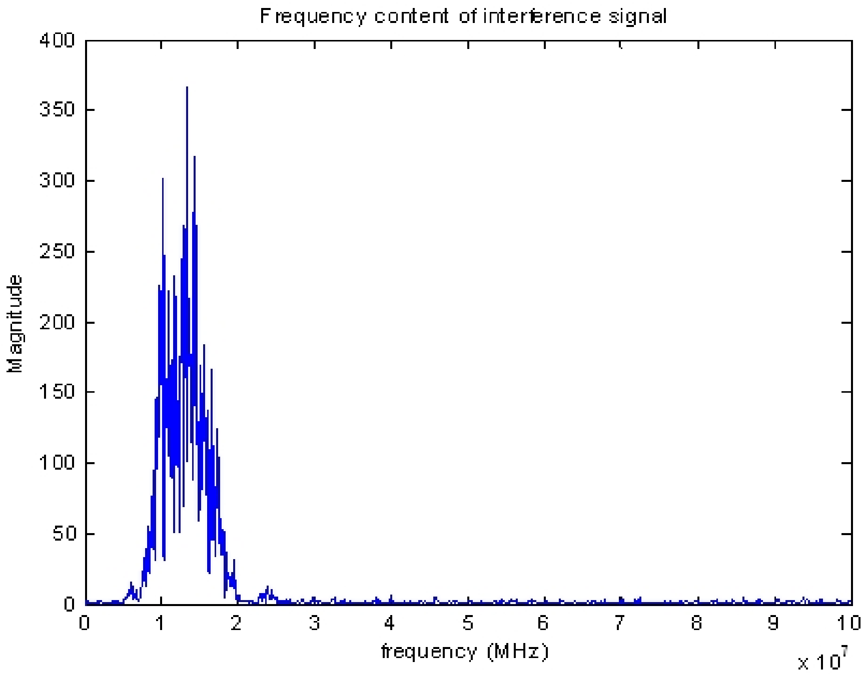

Figure 3.15 The frequency content of the interference signal

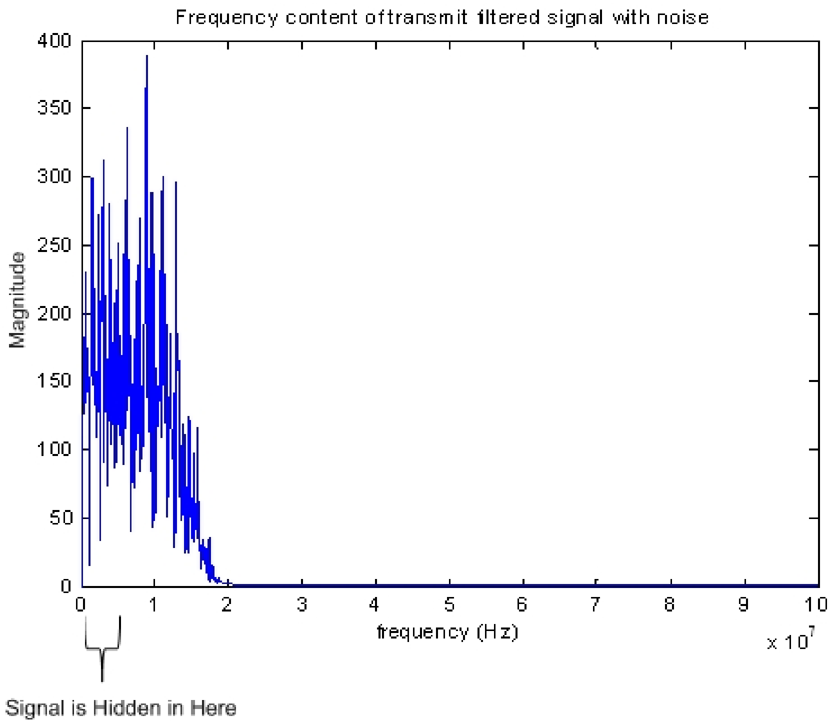

Figure 3.16 Frequency content of output of receiver

The white Gaussian noise added to all receiver pass band generates a SNR of –-9.98dB. The interference can be considered as noise so the actual SNR is -11.84. The channel parameters are summarized in Table 3.4.

Table 3.5 Channel Parameters (3)

Channel Type	Values
Gaussian Noise	(noise only) SNR at Output of Receiver Filter = –9.98dB
Interference signal	(noise + interference) SNR at Output of Receiver Filter = –11.84dB
Interference bandwidth	11MHz

In the Figure 3.17 output of autocorrelation fluctuation for this channel type is given. The symbol period is also calculated correctly as seen in Figure 3.18.

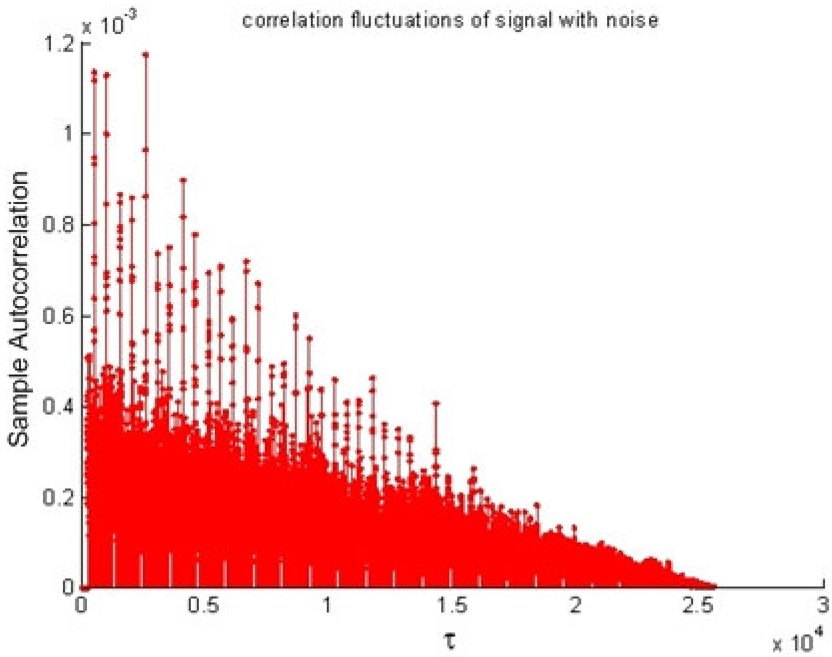

Figure 3.17 Output of autocorrelation fluctuation calculation

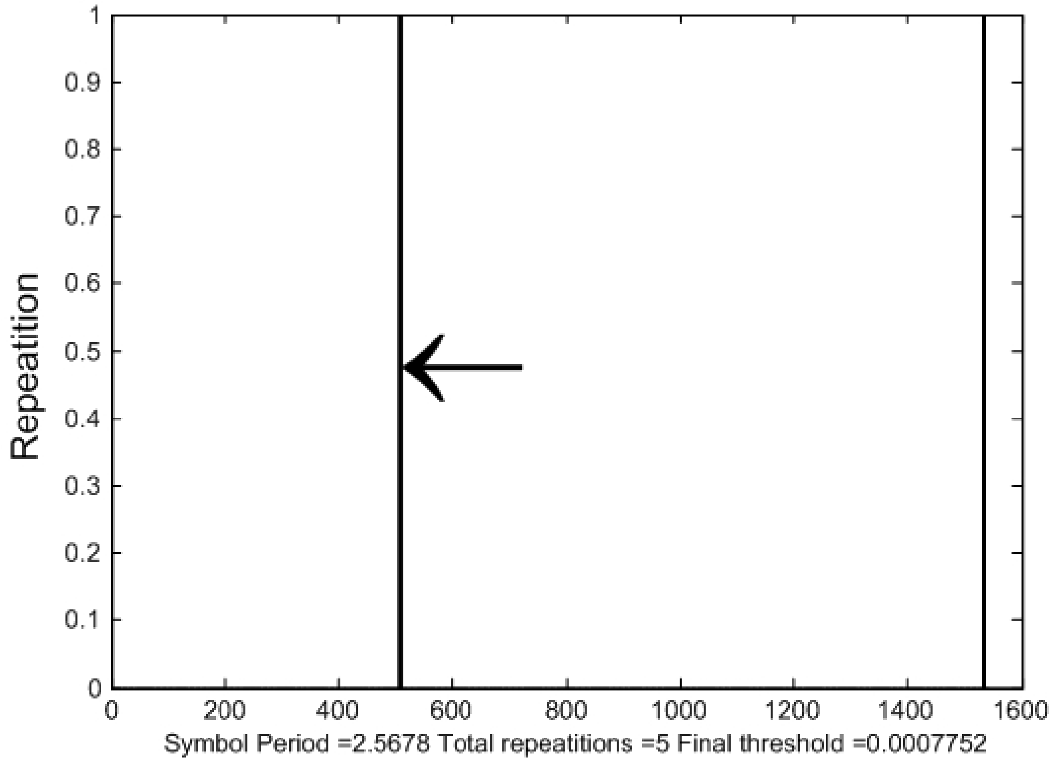

Figure 3.18 Peak Detector’s histogram output

3.6.2 Third Generation CDMA Signals (UMTS)

In this part the basic UMTS signal described in Section 3.5.1.2 is simulated and detector is tried with simple Gaussian noise channel. In Table 3.6 the properties of UMTS signal that is generated are summarized.

Table 3.6 UMTS signal parameters (4)

Parameters	**Values**
Modulation Type	Dual channel QPSK
Scrambler	Short
Channels	DPDCH,DPCCH
Chip Rate	256chips/symbol
Total number of symbols	100
Bandwidth	5MHz

Table 3.7 Channel Parameters (4)

Channel Type	Values
Gaussian Noise	SNR at Output of Receiver Filter = –5dB

Table 3.8 Receiver parameters (5)

Parameters	**Values**
Receiver filter bandwidth	10MHz
Window Number	20
Threshold level	$m_p^n + 4\sigma_p^n$

The output of the detector when signal to noise ration is –5dB is given in Figure 3.19 . Normally UMTS signals are not transferred below noise level but here the possibility of UMTS like hidden signals are considered. This is a considerable possibility because this kind of standards are tend to be modeled in order to secure special (ex: military) communications.

In Figure 3.19 the black line shows the $m_p^n + 4\sigma_p^n$ level and above that threshold it is observed that besides the peaks which define the symbol period, there exists a second peak which do not match with the symbol period. This second peak belongs to DPDCH's spreading code which is also repeating inside. This shows that the periodicity can be used in order to detect peaks caused by signal in order to eliminate the non-periodically appearing peaks. This outcome is simply caused by multichannel and multispreading code architecture.

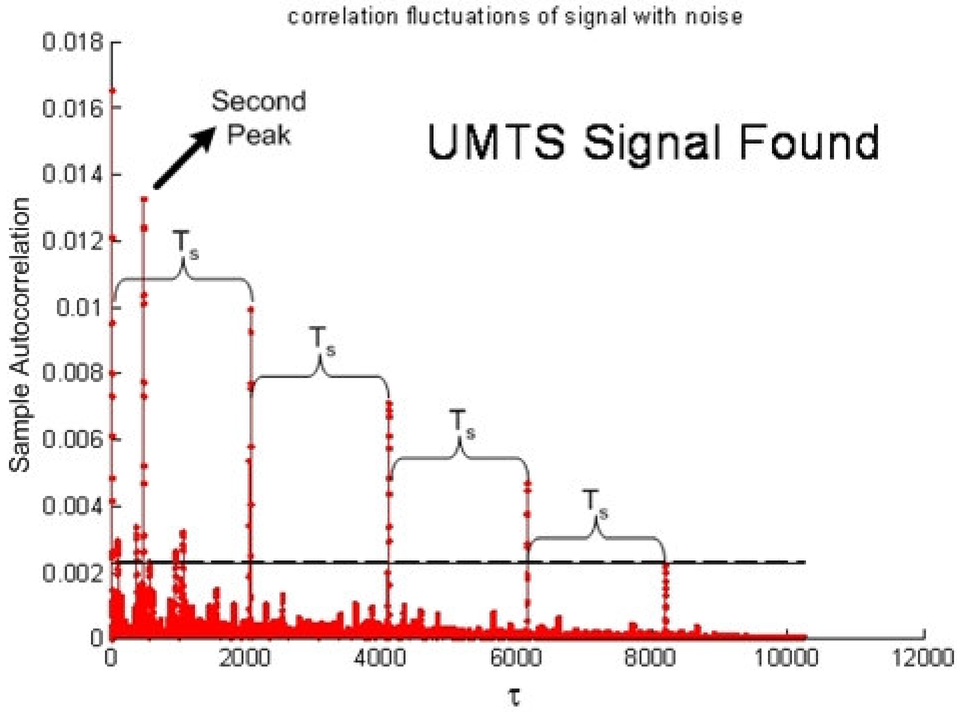

Figure 3.19 Output of autocorrelation fluctuation calculation

3.6.3 Typical LPI Radar Signals

At Table 3.9 the parameters of DSSS radar signal that is generated is given. The receiver parameters are given in Table 3.11 . The peak detector used for LPI radar is different because of the structure of the output of the fluctuation detector; a special approach is used.

First a threshold check is done to be sure that there is a hidden radar signal and than the algorithm simply calculates the time difference between four near max peaks and then uses sampling frequency to calculate the PRI (Pulse Repetition

Interval). This is done by making zero after finding the max peak. The peaks at the output is more Gaussian like than the typical DSSS signals so the making zero process is done in a window of length of the total peak.

Table 3.9 DSSS Radar Signal Parameters

Parameters	Values
Modulation Type	BPSK
Sampling Freq.	200MHz
Number of periods used in each pulse	4
Total sample number	1000000
Bandwidth	40MHz
Total number of pulses	20
PRI	256µs

Table 3.10 Channel Parameters (4)

Channel Type	Values
Gaussian Noise	SNR at Output of Receiver Filter = –5.3dB

Table 3.11 Receiver parameters (5)

Parameters	**Values**
Receiver filter bandwidth	80MHz
Window Number	2
Threshold level	$m_p^n + 4\sigma_p^n$

In Figure 3.20 the generated DSSS radar signal without noise is shown. The illustration is given to help understanding of the signal structure.

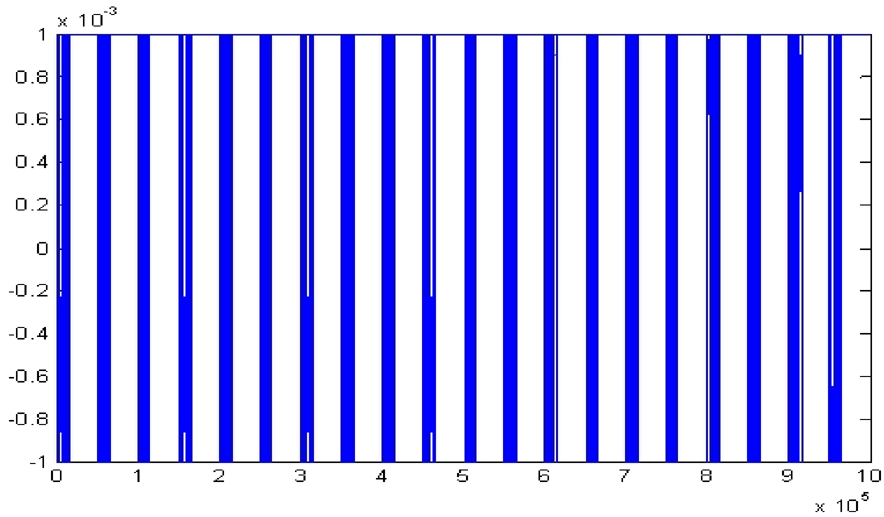

Figure 3.20 DSSS Radar Signal without Noise

The output of the autocorrelation fluctuation when signal to noise ration is -5.3dB is given in Figure 3.21. Here the detection is clear but this time the symbol period corresponds to PRI (Pulse Repetition Interval) value of the radar.

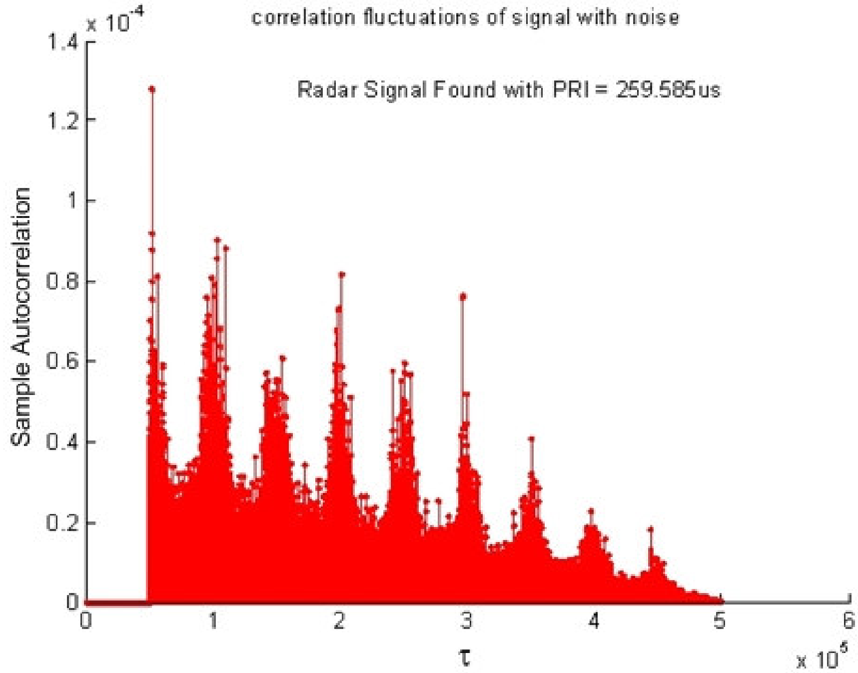

Figure 3.21 Output of autocorrelation fluctuation with -5.3dB SNR

CHAPTER 4

ESTIMATION OF THE SPREADING SEQUENCE

4.1 Introduction

The detection of the DSSS signal is discussed in the previous section. Now the problem is to estimate the spreading sequence. The assumptions that are made in section are valid for this section too. Except, the signal is assumed to be detected and symbol period is calculated a priori. No other information about the signal will be used to estimate the spreading sequence.

4.2 Eigenanalysis Technique

The method of estimating spreading sequence is based on eigenanalysis and the analysis starts with the division of received signal into non-overlapping windows the durations of which are equal to the symbol period, calculated from the detector output. Each window provides a vector which feeds the eigenanalysis module [5]

Then a correlation matrix is estimated from the vectors, which is defined as;

$$R = E\left\{ \vec{y} \cdot \vec{y}^{H} \right\} \qquad \text{E- 14}$$

where ^{H} denotes Hermitian transpose.

Since the window duration is equal the symbol duration; a window always contains the end of a symbol duration followed by the beginning of the next symbol duration [2].This is illustrated in Figure 4.1.

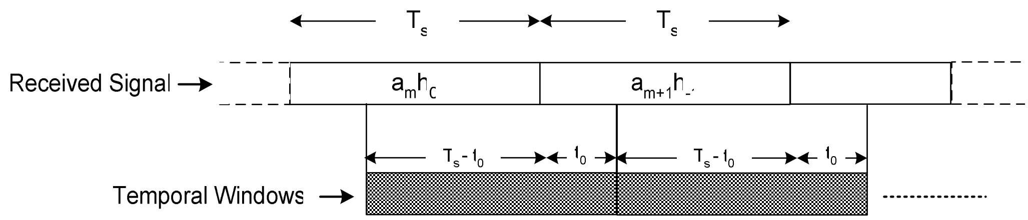

Figure 4.1 Non- over lapping windows

So we can write;

$$y = a_m h_0 + a_{m+1} h_{-1} + n \qquad \text{E- 15}$$

where h_0 is a vector containing the end of the spreading waveform for a duration and followed by zeros and h_{-1} is a vector starts with zeros and followed by the next spreading waveform. The structures of vectors h_0 and h_{-1} are shown below in Figure 4.2.

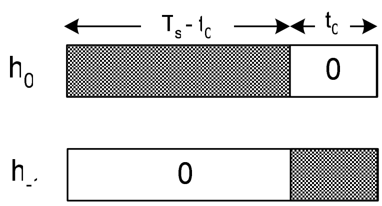

Figure 4.2 Vector Structures

By using the two equations the following expression is obtained for correlation matrix;

$$R = E\{|a_m|^2\} h_0 h_0^H + E\{|a_{m+1}|^2\} h_{-1} h_{-1}^H + \sigma_n^2 I \qquad \text{E- 16}$$

From this expression it is understood that the two eigenvalues must be large than the others. This is because *R* can also be expressed as the linear combination of eigenvectors and eigenvalues. Finally this approach leads us to the useful fact that; from the eigenvectors corresponding to first two eigenvalues, h_0 and h_{-1} can be obtained [5].

4.3 Simulation Results

In this section the method of estimating spreading sequence is simulated on a typical DSSS signal with 64 bit spreading sequence with -5dB SNR. The UMTS signal and LPI radar signals can not be used for this application because of the characteristics. In UMTS complex spreading prevents the spreading code estimation and in LPI radar signals is not continuous so doesn't match with assumptions.

In Figure 4.3 and Figure 4.4 first and second eigenvectors that are estimated from the correlation matrix is shown.

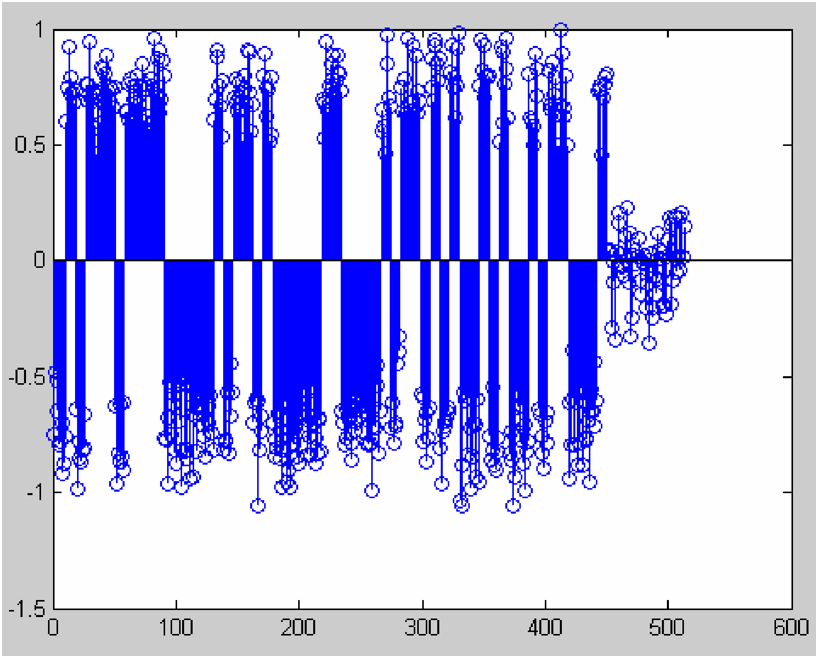

Figure 4.3 First Eigenvector

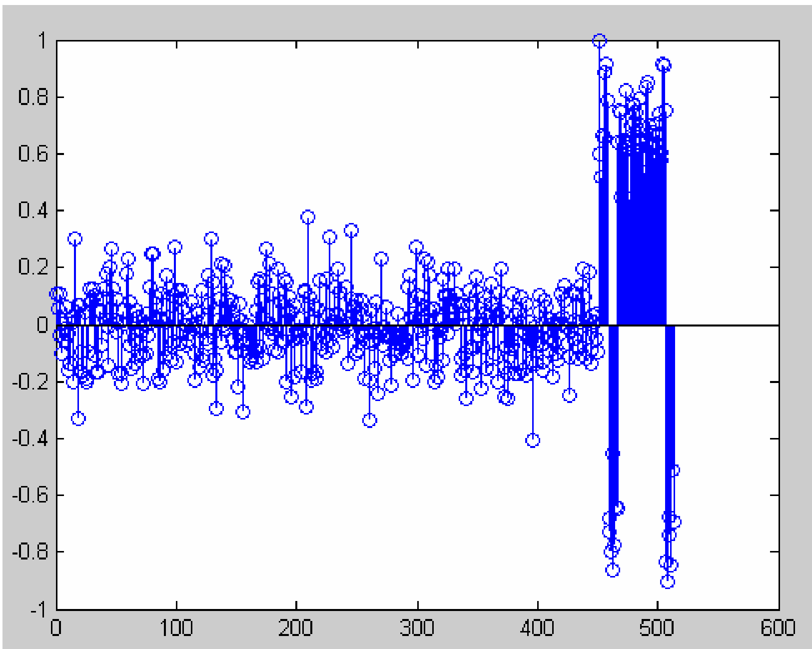

Figure 4.4 Second Eigenvector

By using estimated eigenvectors the spreading sequence estimation is finalized. In Figure 4.5 the estimated spreading sequence is shown and in Figure 4.6 original spreading sequence can be seen. As a result spreading sequence is estimated correctly.

For performing performance analysis and transforming the estimated spreading sequence into bit form firstly the two eigen vectors are added one after other then a threshold is calculated in order to extract the peaks defining the bits of spreading sequence. After using threshold a smoothing algorithm is applied in order to eliminate the peaks caused by noise among the bit defining sequence. The results of detailed performance analysis are given in preceding chapter.

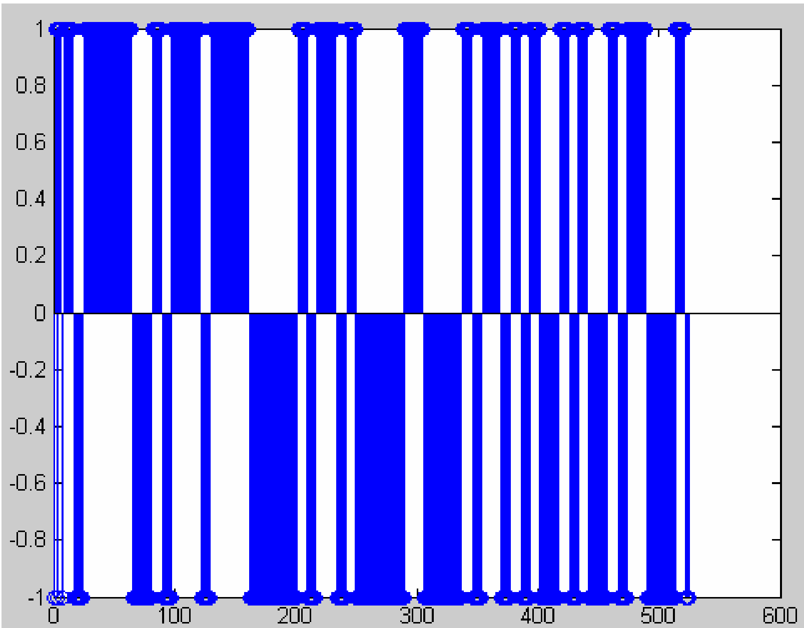

Figure 4.5 Estimated Spreading Sequence

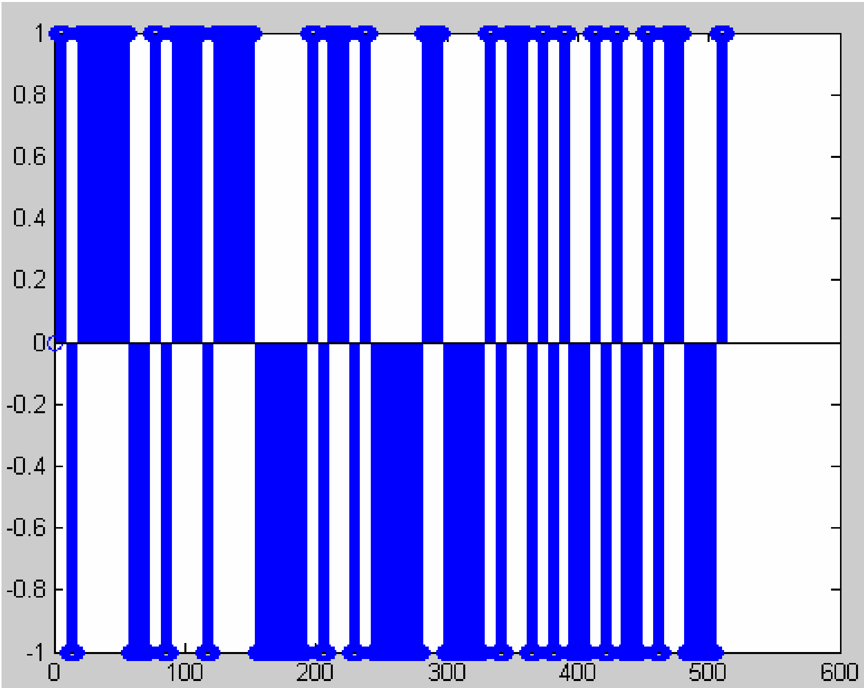

Figure 4.6 Original Spreading Sequence

CHAPTER 5

PERFORMANCE ANALYSIS

5.1 Introduction

In this chapter detailed performance analysis is given for typical DSSS signals, UMTS signal and LPI radar signals. By using the peak detectors output the symbol period found for typical DSSS signals and UMTS signal. For LPI radar signals the performance analysis for PRI calculation is given. Also spreading sequence estimation is performed for typical DSSS signals. Different channel effects are tested during performance analysis. In performance analysis numbers of experiments are chosen to be as large as possible but obviously there is limit due to computational power needs.

5.2 Performance Analysis of Typical DSSS Signals

The first signal type is Typical DSSS signals and the parameters of the signal are summarized in Table 5.1. The receiver parameters are given in Table 5.2. The channel type and necessary channel parameters are given for result of each experimental trial set. The object of this first analysis is to obtain the performance of the detection technique due to low SNR conditions so the channel is implementing simple Gaussian noise. Also the symbol period that is estimated is given for each SNR.

Table 5.1 Typical DSSS signal parameters

Parameters	Values
Chip Rate	64chips/symbol
Sampling Freq.	200MHz
Observation time	1024168 samples
Symbol Period	20.48µs
Signal Bandwidth	5MHz

Table 5.2 Receiver parameters

Parameters	Values
Receiver filter bandwidth	20MHz
Window Number	50

In Figure 5.1 the symbol period estimation performance due to SNR result is given. As seen the deviation of the estimated symbol period is increasing due to low SNR. In

Figure 5.2 detection result the due to SNR result is given. This figure shows the response of receiver to decreasing SNR in a continuous manner. Gaussian Noise Channel is used in these first simulations. The channel effects are discussed in the following parts.

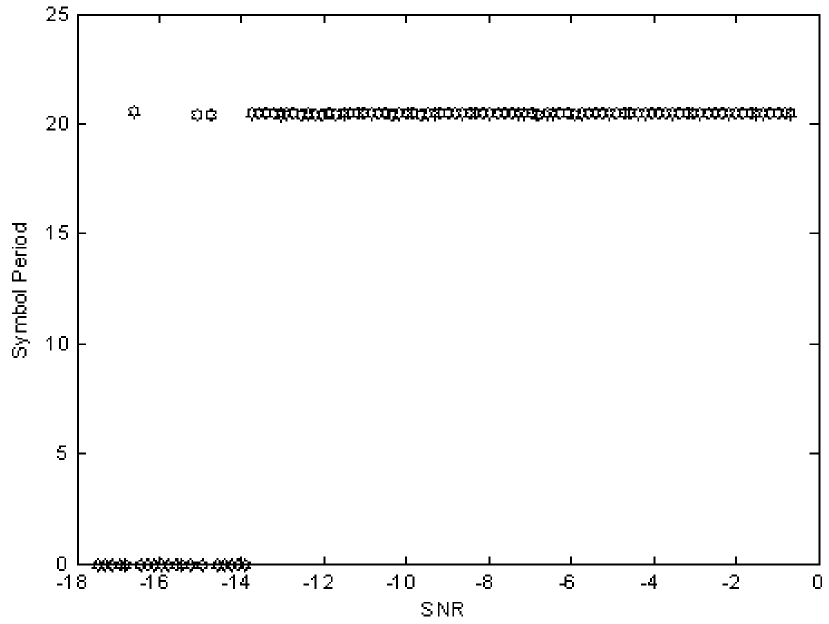

Figure 5.1 Symbol Period Estimation due to SNR (Typical DSSS signal, Gaussian Noise Channel)

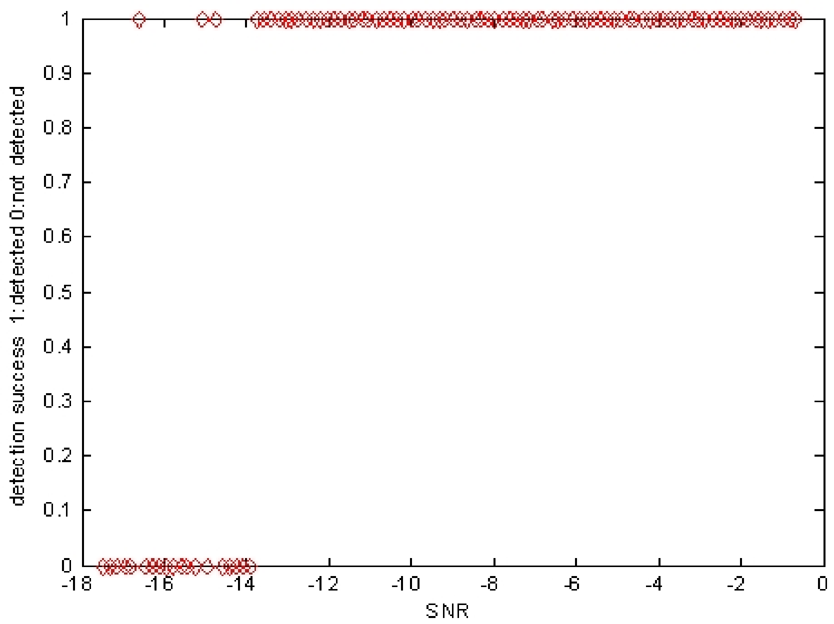

Figure 5.2 Detection Success due to SNR (Typical DSSS signal, Gaussian Noise Channel)

The evaluations of the results are summarized below. Final SNR that the Signal Can be Detected is -16.61dB.

In the following part results are obtained for specific SNR's; -5dB, -10dB, - 13dB and -15dB to clarify the detection performance of the receiver. The performance analysis for SNR = -5dB is given below.

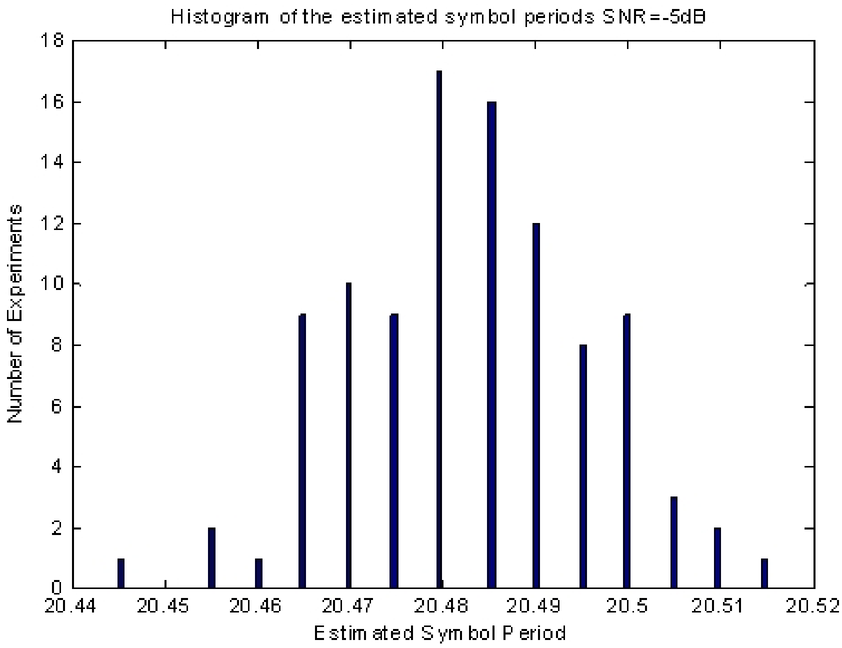

Figure 5.3 Symbol Period Estimation at SNR= -5dB (Typical DSSS signal, Gaussian Noise Channel)

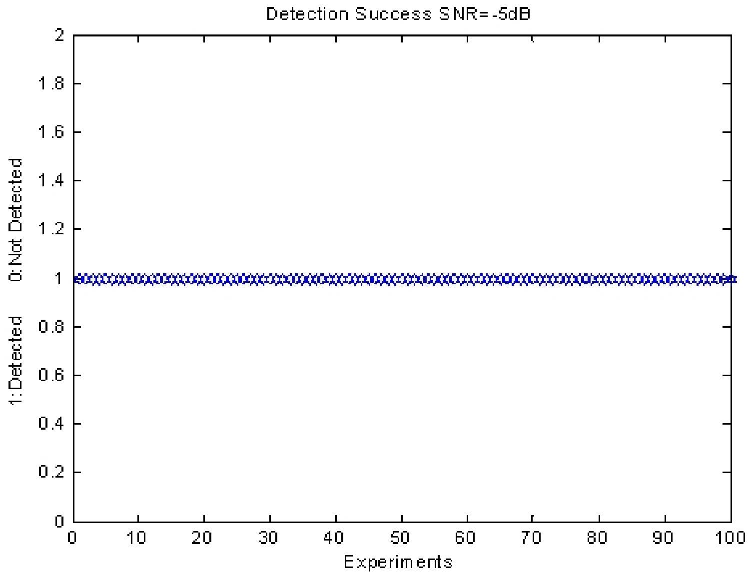

Figure 5.4 Detection Success at SNR=–5dB (Typical DSSS signal, Gaussian Noise Channel)

The evaluations of the results at SNR=-5dB is summarized below.

Table 5.3 The evaluations of the results at SNR=-5dB (Typical DSSS signal, Gaussian Noise Channel)

P(Detected)	1
P(Not Detected)	0
P(Correct Symbol period estimation I Detected)	1
P(Wrong Symbol period estimation I Detected)	0
Mean of Correct Estimated Symbol Periods	20.4828µs
Mean of Wrong Estimated Symbol Periods	-
Standard Deviation of Correct Estimated Symbol Periods	0.0132µs
Max Deviation of Correct Estimated Symbol Periods	0.0378µs

The performance analysis for SNR = -10dB is given below.

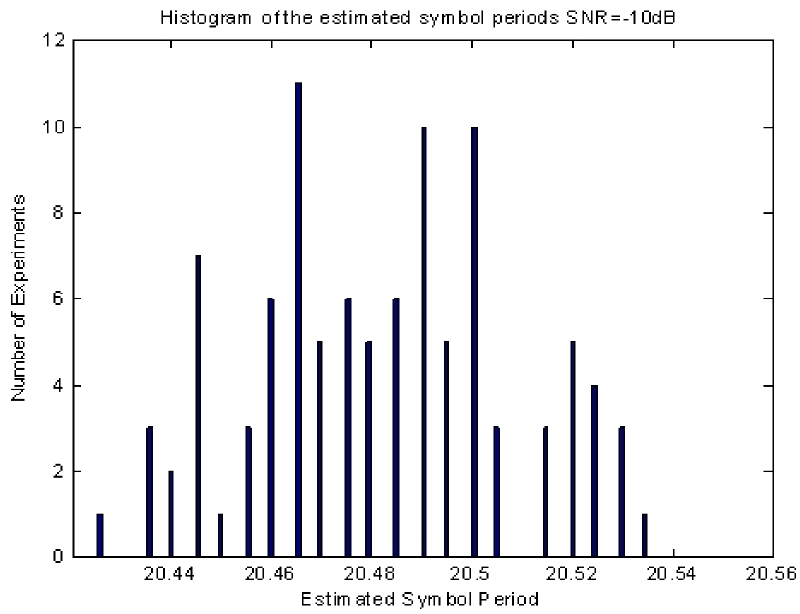

Figure 5.5 Symbol Period Estimation at SNR= -10dB (Typical DSSS signal, Gaussian Noise Channel)

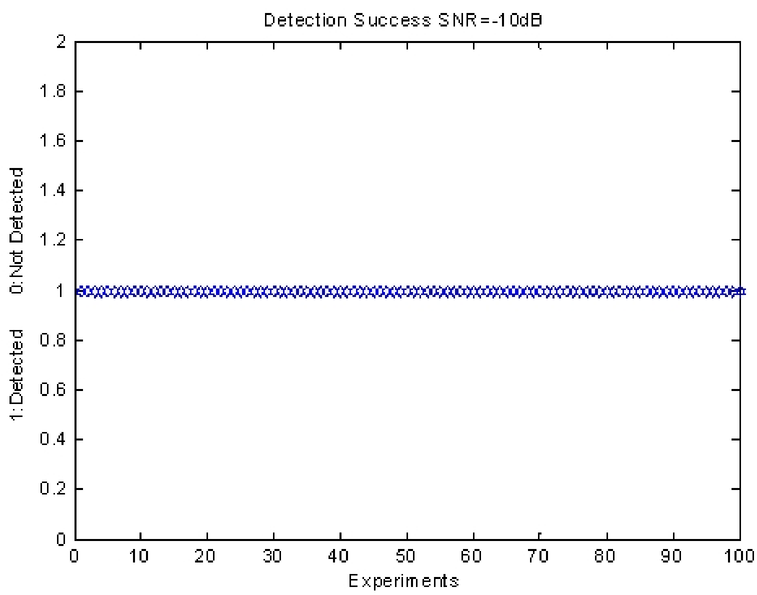

Figure 5.6 Detection Success at SNR = –10dB (Typical DSSS signal, Gaussian Noise Channel)

The evaluations of the results at SNR=-10dB is summarized below.

Table 5.4 The evaluations of the results at SNR=-10dB (Typical DSSS signal, Gaussian Noise Channel)

P(Detected)	1
P(Not Detected)	0
P(Correct Symbol period estimation I Detected)	1
P(Wrong Symbol period estimation I Detected)	0
Mean of Correct Estimated Symbol Periods	20.4818μs
Mean of Wrong Estimated Symbol Periods	-
Standard Deviation of Correct Estimated Symbol Periods	0.0261μs
Max Deviation of Correct Estimated Symbol Periods	0.0368μs

The performance analysis for SNR = -13dB is given below.

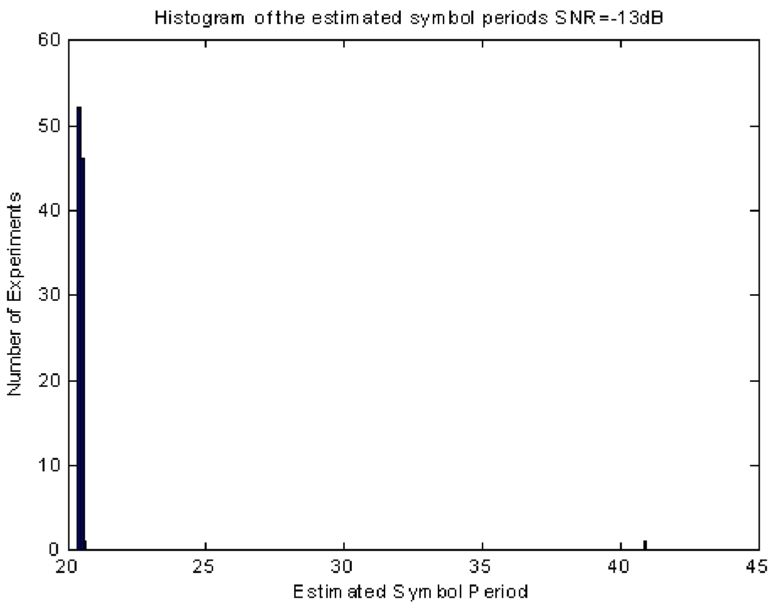

Figure 5.7 Symbol Period Estimation at SNR= -13dB (Typical DSSS signal, Gaussian Noise Channel)

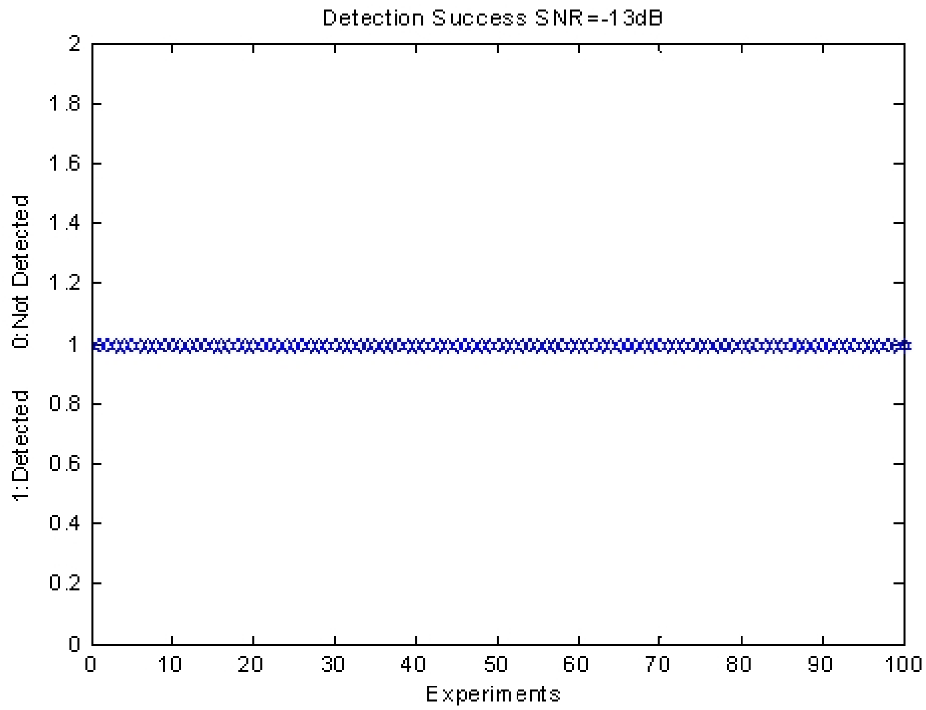

Figure 5.8 Detection Success at SNR = –13dB (Typical DSSS signal, Gaussian Noise Channel)

The evaluations of the results at SNR=-13dB is summarized below.

Table 5.5 The evaluations of the results at SNR=-13dB (Typical DSSS signal, Gaussian Noise Channel)

P(Detected)	1
P(Not Detected)	0
P(Correct Symbol period estimation I Detected)	0.99
P(Wrong Symbol period estimation I Detected)	0.01
Mean of Correct Estimated Symbol Periods	20.4867μs
Mean of Wrong Estimated Symbol Periods	41.287μs
Standard Deviation of Correct Estimated Symbol Periods	0.0414μs
Max Deviation of Correct Estimated Symbol Periods	20.4833μs

The performance analysis for SNR = -15dB is given below.

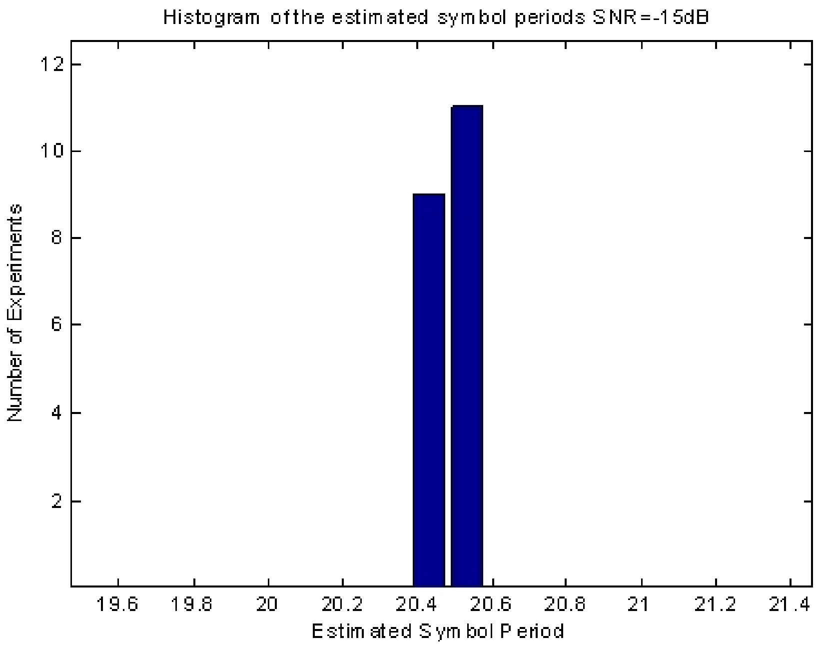

Figure 5.9 Symbol Period Estimation at SNR= -15dB (Typical DSSS signal, Gaussian Noise Channel)

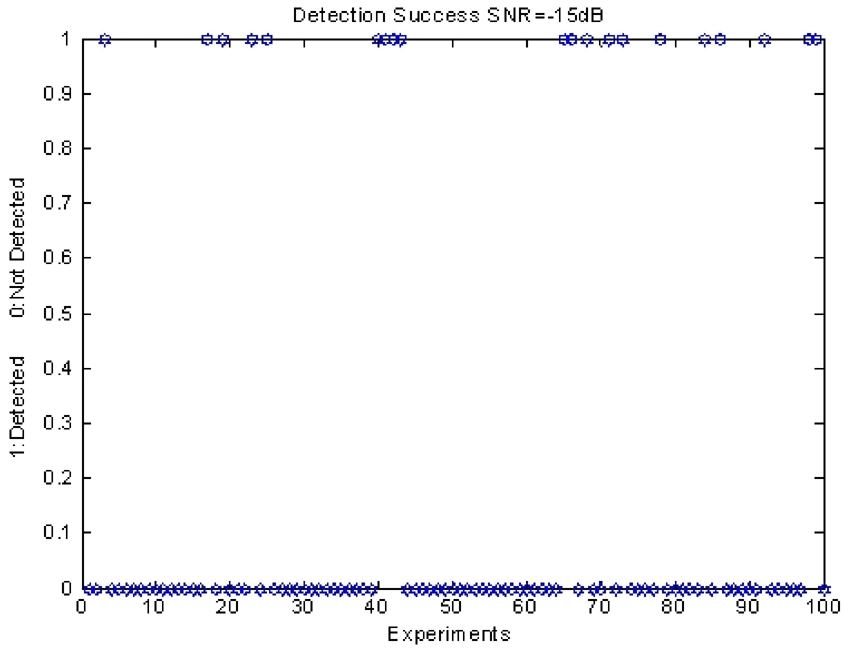

Figure 5.10 Detection Success at SNR = –15dB (Typical DSSS signal, Gaussian Noise Channel)

The evaluations of the results at SNR=-15dB is summarized below.

Table 5.6 The evaluations of the results at SNR=-15dB (Typical DSSS signal, Gaussian Noise Channel)

P(Detected)	0.2
P(Not Detected)	0.8
P(Correct Symbol period estimation | Detected)	1
P(Wrong Symbol period estimation | Detected)	0
Mean of Correct Estimated Symbol Periods	20.4780µs
Mean of Wrong Estimated Symbol Periods	-
Standard Deviation of Correct Estimated Symbol Periods	0.0502µs
Max Deviation of Correct Estimated Symbol Periods	0.1070µs

The false alarm rate for these parameters is obtained as %2 for only threshold detection. The experimental result for false alarm is given in Figure 5.11. The false alarm rate for the same signal is %0 for peak detection uses periodicity histogram.

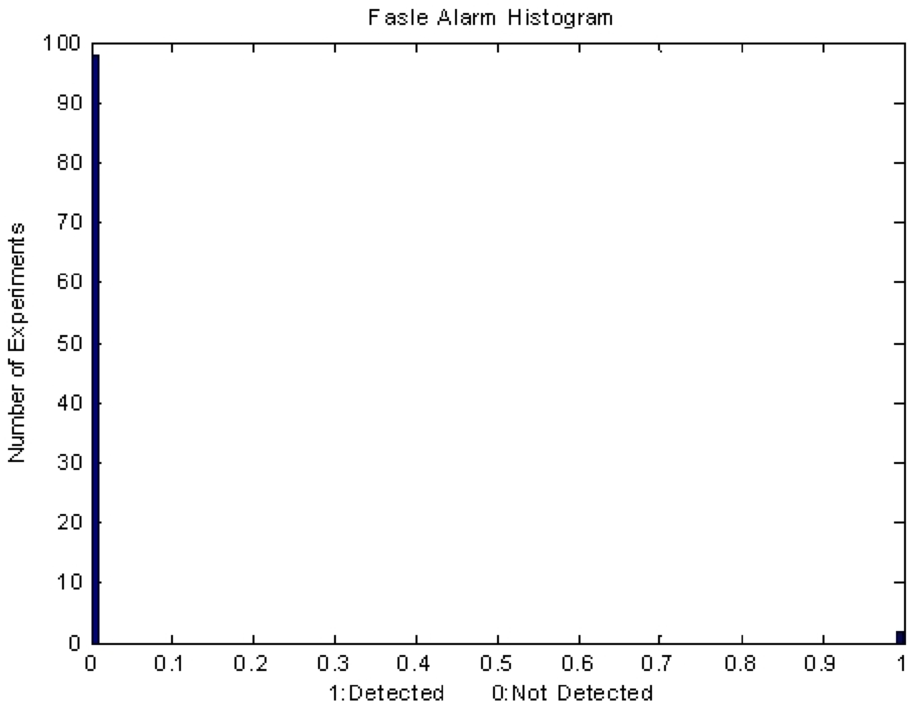

Figure 5.11 False Alarm Rate

In the following part the analysis is done and results are obtained for specific SNR's; -5dB, -10dB, and - 13dB but for channels with two kinds of multipath effect. In the first multipath effect, it is assumed that the interception system does not present in the LOS (Line Of Sight) of the DSSS signal source and receives the same power of signal form the different delayed multipaths. In the second multipath effect signal is received from both LOS and multipaths so the input signal power is increased. The sum of two periodic signals with same periodicity will be again periodic with the same period so multipath effect preserves the symbol period and also the performance of the detection does not change as seen in the following results. Performance analysis of first case is given below. The channel parameters are given in Table 5.7. The same signal and receiver parameters are used in order to make comparisons.

Table 5.7 Channel Parameters (multipath-1)

Channel Type	Values
Multipath Effect	1.Path→ delay: 0.5μs Attenuation: %60 2.Path→ delay: 5μs Attenuation: %70 3.Path→ delay: 25μs Attenuation: %80 4.Path→ delay: 250μs Attenuation: %90

Estimated symbol periods and detection performance due to SNR is given in Figure 5.12 and Figure 5.13.

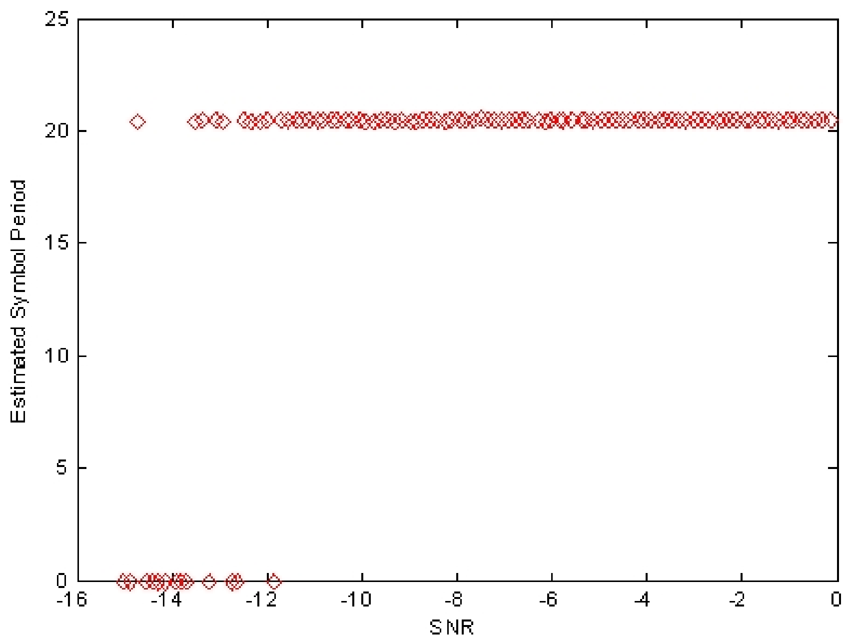

Figure 5.12 Symbol Period Estimation due to SNR (Typical DSSS signal, multipath-1)

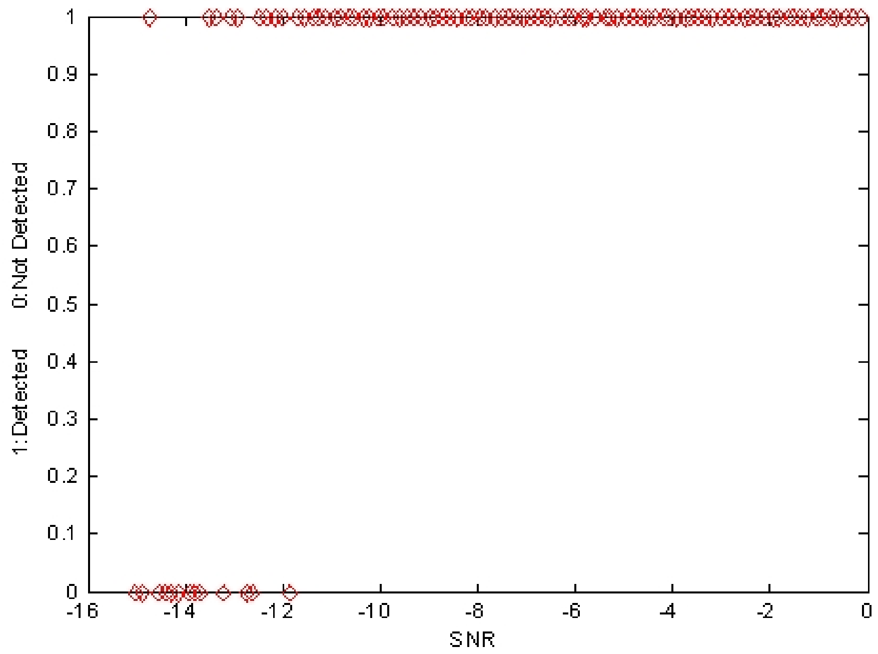

Figure 5.13 Detection Success due to SNR (Typical DSSS signal, multipath-1)

In the following part results are obtained for specific SNR's; -5dB, -10dB, -13dB and -15dB are given. The SNR values of each channel are given before the performance results. The same signal and receiver parameters are used in order to make comparisons. The channel parameters and performance analysis for SNR = -5dB is given below

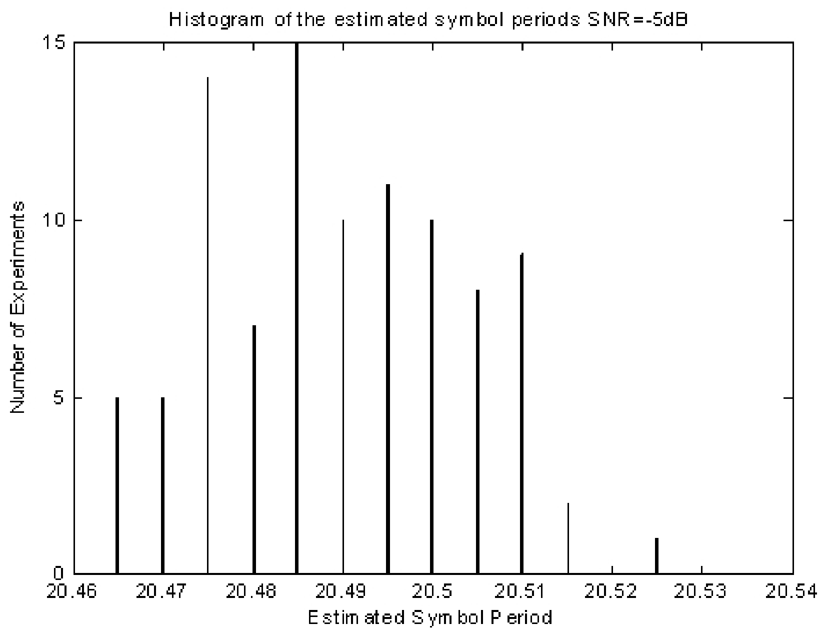

Figure 5.14 Symbol Period Estimation at SNR= -5dB (Typical DSSS signal, multipath-1)

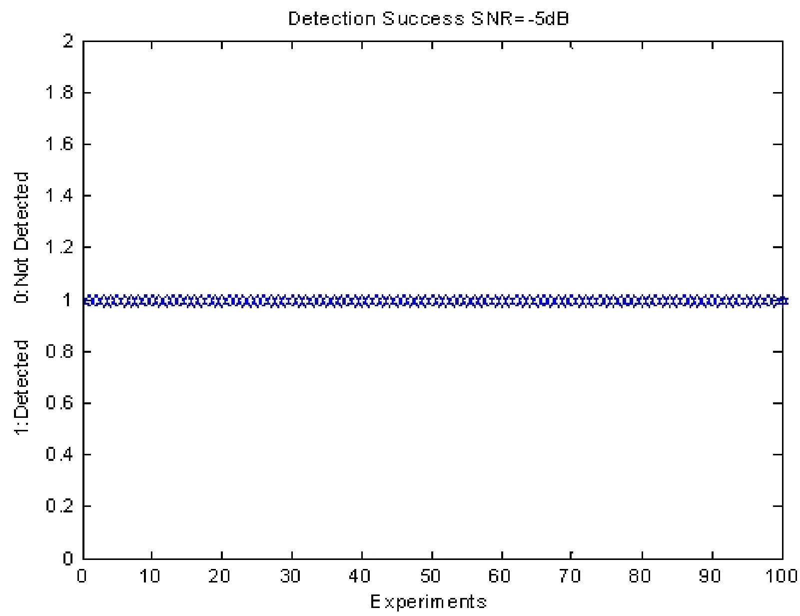

Figure 5.15 Detection Success at SNR = -5dB (Typical DSSS signal, multipath-1)

The evaluations of the results at SNR=-5dB is summarized below.

Table 5.8 The evaluations of the results at SNR=-5dB (Typical DSSS signal, multipath-1)

P(Detected)	1
P(Not Detected)	0
P(Correct Symbol period estimation I Detected)	1
P(Wrong Symbol period estimation I Detected)	0
Mean of Correct Estimated Symbol Periods	20.4887μs
Mean of Wrong Estimated Symbol Periods	-
Standard Deviation of Correct Estimated Symbol Periods	0.0146μs
Max Deviation of Correct Estimated Symbol Periods	0.0363μs

The performance analysis for SNR = -10dB is given below.

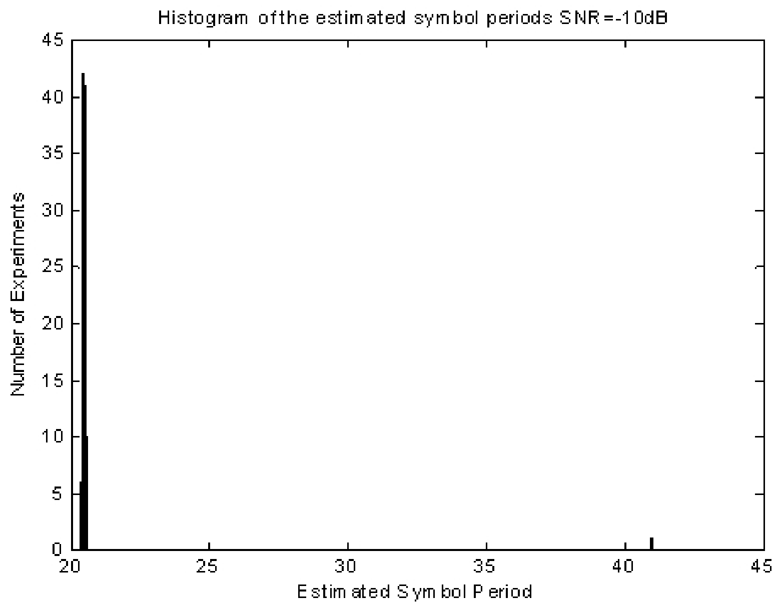

Figure 5.16 Symbol Period Estimation at SNR= -10dB (Typical DSSS signal, multipath-1)

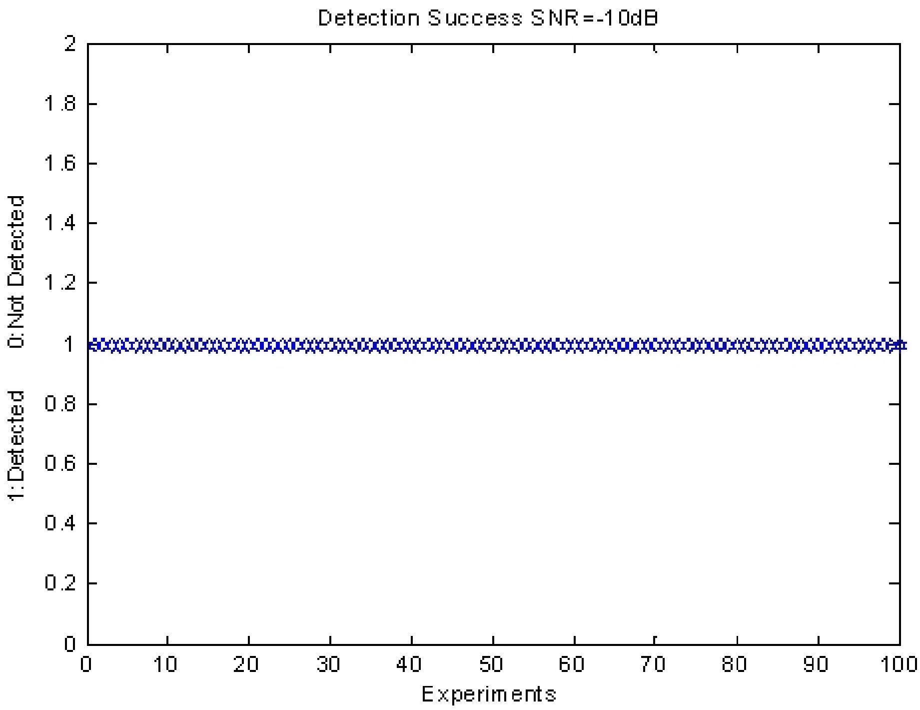

Figure 5.17 Detection Success at SNR =-10dB (Typical DSSS signal, multipath-1)

The evaluations of the results at SNR=-10dB is summarized below.

Table 5.9 The evaluations of the results at SNR=-10dB (Typical DSSS signal, multipath-1)

P(Detected)	1
P(Not Detected)	0
P(Correct Symbol period estimation I Detected)	0.98
P(Wrong Symbol period estimation I Detected)	0.02
Mean of Correct Estimated Symbol Periods	20.4908µs
Mean of Wrong Estimated Symbol Periods	41.197µs
Standard Deviation of Correct Estimated Symbol Periods	0.0342µs
Max Deviation of Correct Estimated Symbol Periods	0.1058µs

The performance analysis for SNR = -13dB is given below.

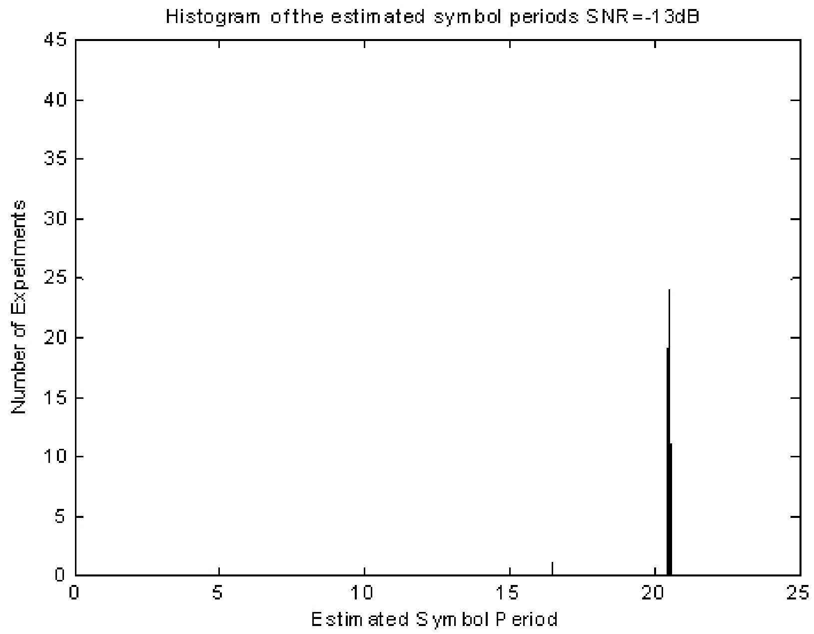

Figure 5.18 Symbol Period Estimation at SNR= -13dB (Typical DSSS signal, multipath-1)

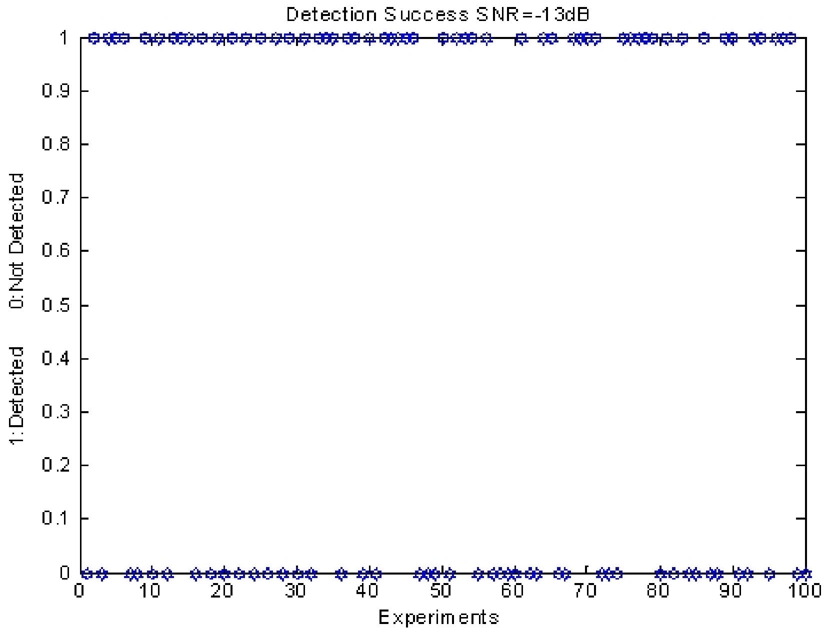

Figure 5.19 Detection Success at SNR = –13dB (Typical DSSS signal, Gaussian noise with interference-1)

The evaluations of the results at SNR= –13dB is summarized below.

Table 5.10 The evaluations of the results at SNR= –13dB (Typical DSSS signal, multipath-1)

P(Detected)	0.55
P(Not Detected)	0.45
P(Correct Symbol period estimation I Detected)	54/55
P(Wrong Symbol period estimation I Detected)	1/55
Mean of Correct Estimated Symbol Periods	20.4221µs
Mean of Wrong Estimated Symbol Periods	16.15
Standard Deviation of Correct Estimated Symbol Periods	0.0369µs
Max Deviation of Correct Estimated Symbol Periods	0.0796µs

The performance analysis for SNR = -15dB is given below.

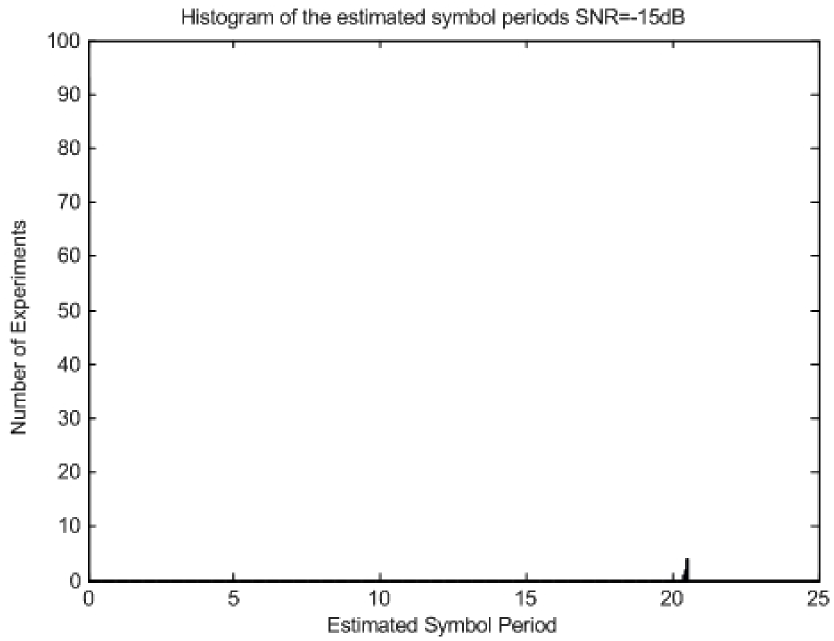

Figure 5.20 Symbol Period Estimation at SNR= -15dB (Typical DSSS signal, multipath-1)

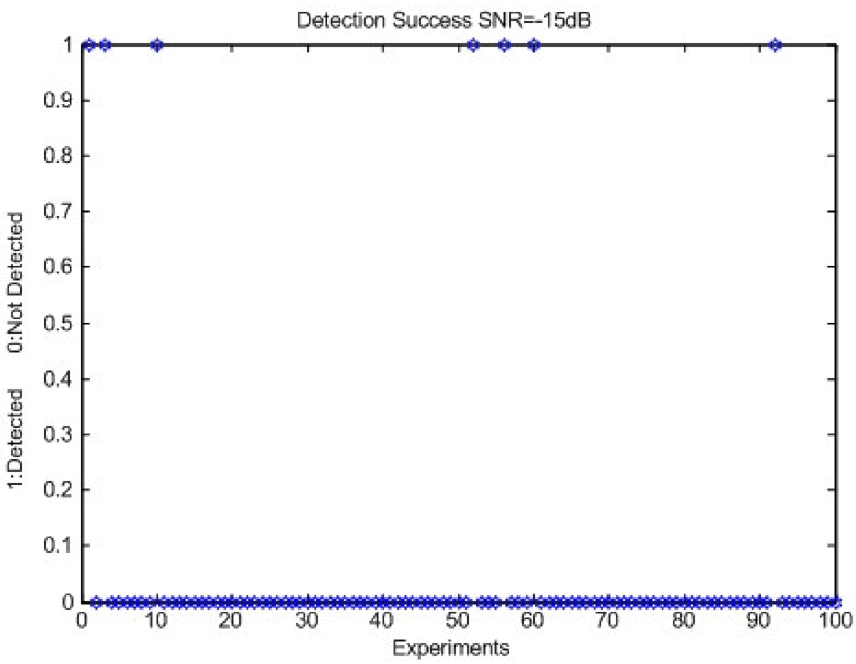

Figure 5.21 Detection Success at SNR=-15dB (Typical DSSS signal, multipath-1)

The evaluations of the results at SNR= –15dB is summarized below.

Table 5.11 The evaluations of the results at SNR= –15dB (Typical DSSS signal, multipath-1)

P(Detected)	0.07
P(Not Detected)	0.93
P(Correct Symbol period estimation | Detected)	1
P(Wrong Symbol period estimation | Detected)	0
Mean of Correct Estimated Symbol Periods	20.4657µs
Mean of Wrong Estimated Symbol Periods	--
Standard Deviation of Correct Estimated Symbol Periods	0.0455µs
Max Deviation of Correct Estimated Symbol Periods	0.0657µs

In the next analysis second type of multipath is examined. The received power is increase because of the multipath effect. Estimated symbol periods and detection performance due to SNR is given in as seen in the figures an increase at the performance is observed as a result of increased input signal power. In the Figure 5.22 the detection performance is given. But more clear performance increase is observed at the detection performance or at SNR=-15dB. Results for SNR=-15dB is given in Figure 5.23 and Figure 5.24. In Table 5.12 it is seen that the probability of detection is increase to 0.22 from 0.07.

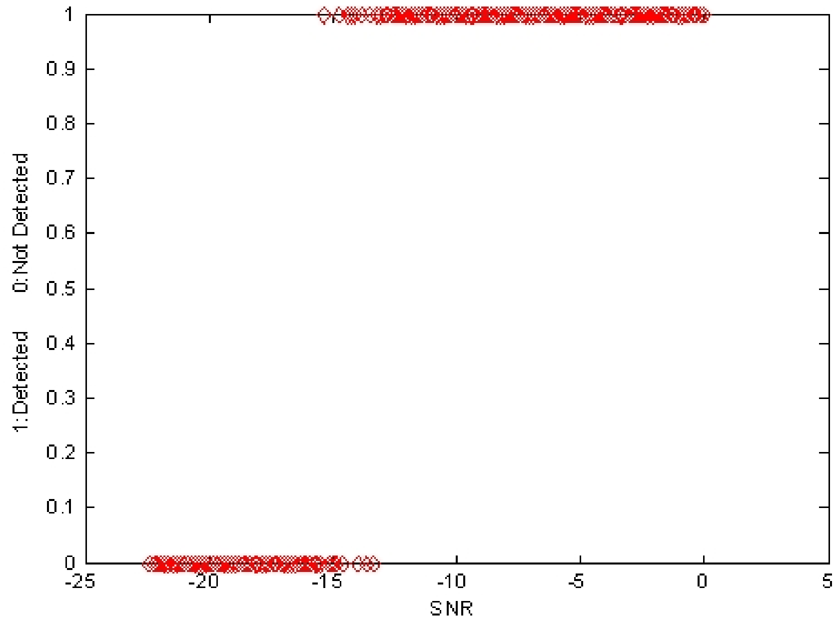

Figure 5.22 Detection Success due to SNR (Typical DSSS signal, multipath-2)

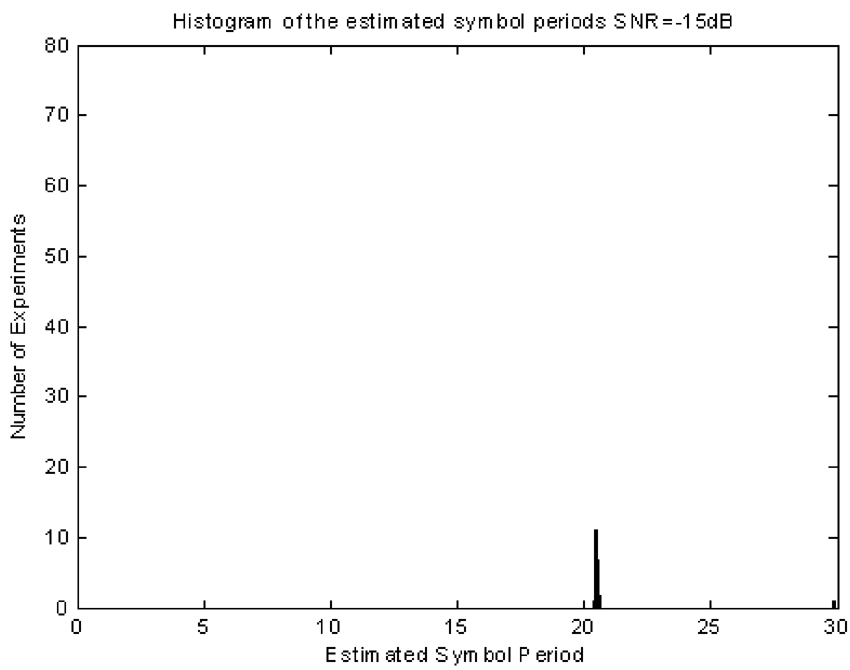

Figure 5.23 Symbol Period Estimation at SNR= -15dB (Typical DSSS signal, multipath-2)

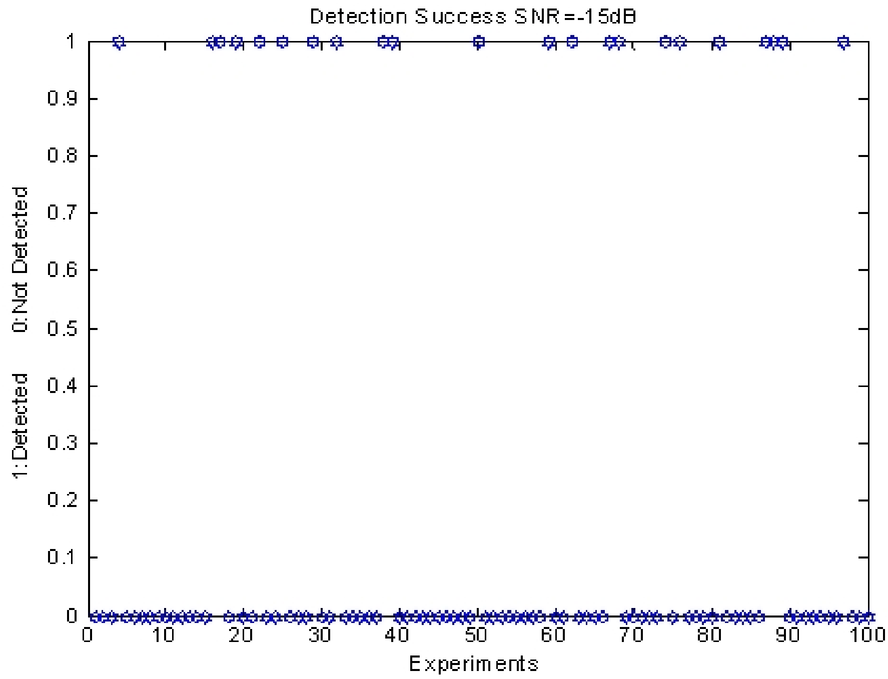

Figure 5.24 Detection Success at SNR=-15dB (Typical DSSS signal, multipath-2)

Table 5.12 The evaluations of the results at SNR= –15dB (Typical DSSS signal, multipath-2)

P(Detected)	0.22
P(Not Detected)	0.78
P(Correct Symbol period estimation I Detected)	21/22
P(Wrong Symbol period estimation I Detected)	1/22
Mean of Correct Estimated Symbol Periods	20.4812μs
Mean of Wrong Estimated Symbol Periods	26.86μs
Standard Deviation of Correct Estimated Symbol Periods	0.0510μs
Max Deviation of Correct Estimated Symbol Periods	0.1188μs

In the following part the analysis is done and results are obtained for channel with interference effect. First detection performance due to SNR is given then results are obtained for specific SNR's; -5dB, -10dB, and -13dB and -15dB. The main point is frequency of interference in not in the band of DSSS signal. The frequency content of the interference signal and signal at the output of receiver filter is given in Figure 5.25 and Figure 5.26.

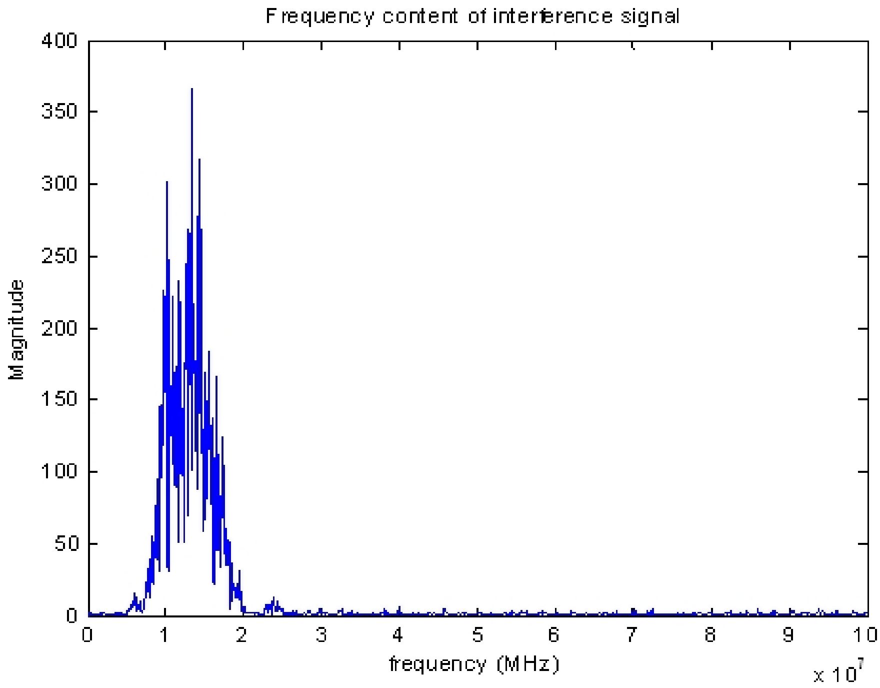

Figure 5.25 The frequency content of the interference signal

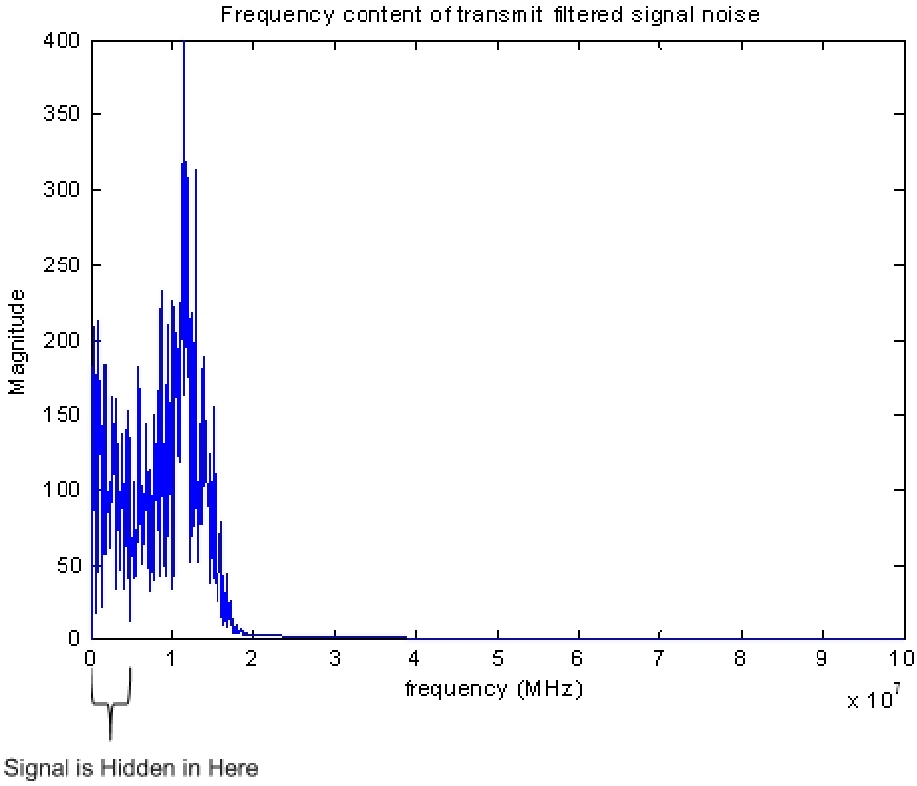

Figure 5.26 Frequency content of output of receiver filter

Estimated symbol periods and detection performance due to SNR is given in Figure 5.27and Figure 5.28.

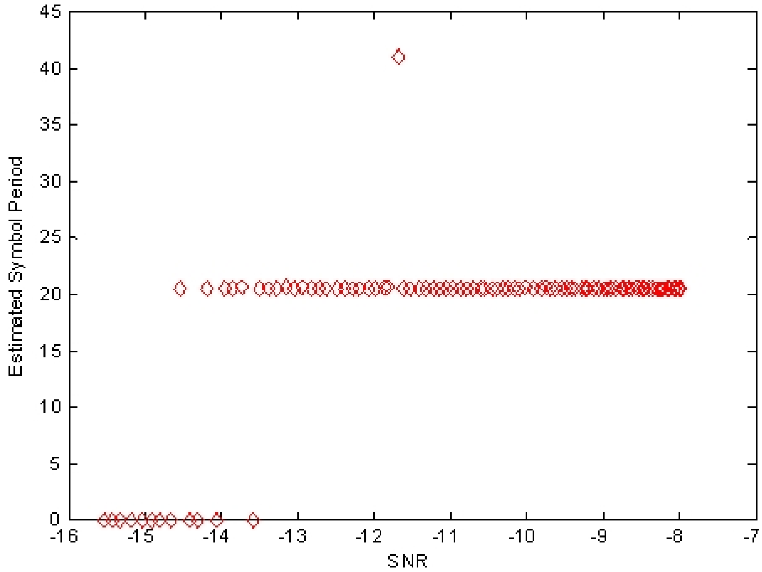

Figure 5.27 Symbol Period Estimation due to SNR (Typical DSSS signal, with interference -1)

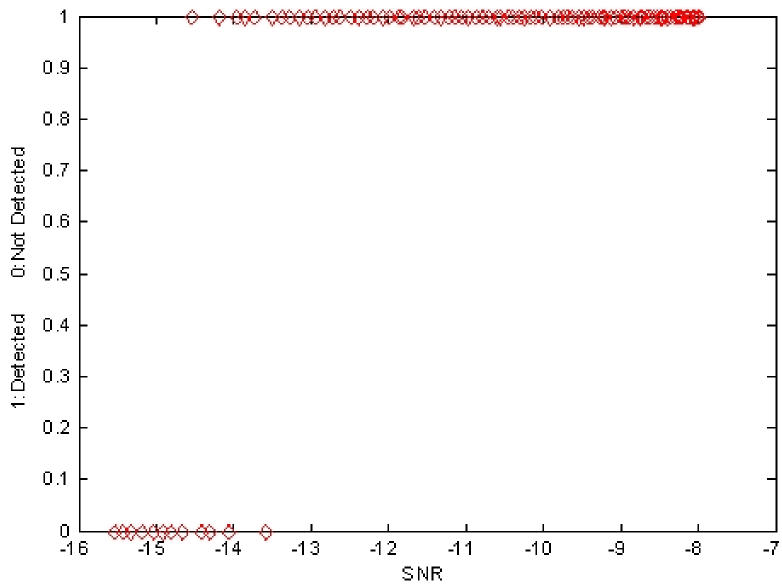

Figure 5.28 Detection Success due to SNR (Typical DSSS signal, with interference -1)

In the following part results are obtained for specific SNR's; -5dB, -10dB, -13dB and -15dB are given. The SNR values of each channel are given before the performance results. The same signal and receiver parameters are used in order to make comparisons. The channel parameters and performance analysis for SNR = -5dB is given below.

Table 5.13 Interference Channel Parameters SNR= –5dB (1)

Channel Type	Values
Gaussian Noise	(noise only) SNR at Output of Receiver Filter = –5dB
Interference signal	(noise + interference) SNR at Output of Receiver Filter = –9.8dB

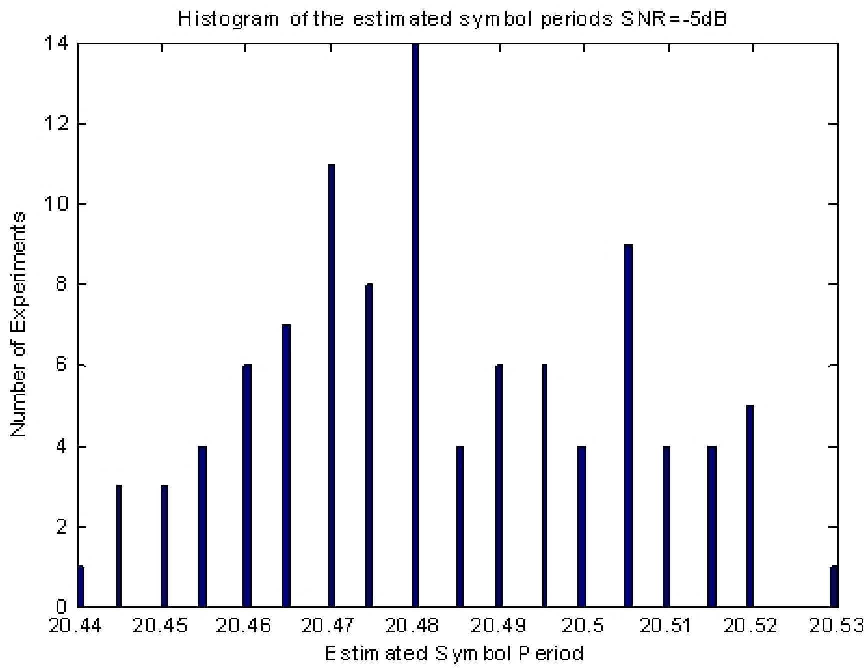

Figure 5.29 Symbol Period Estimation at SNR= -5dB (Typical DSSS signal, Gaussian noise with interference-1)

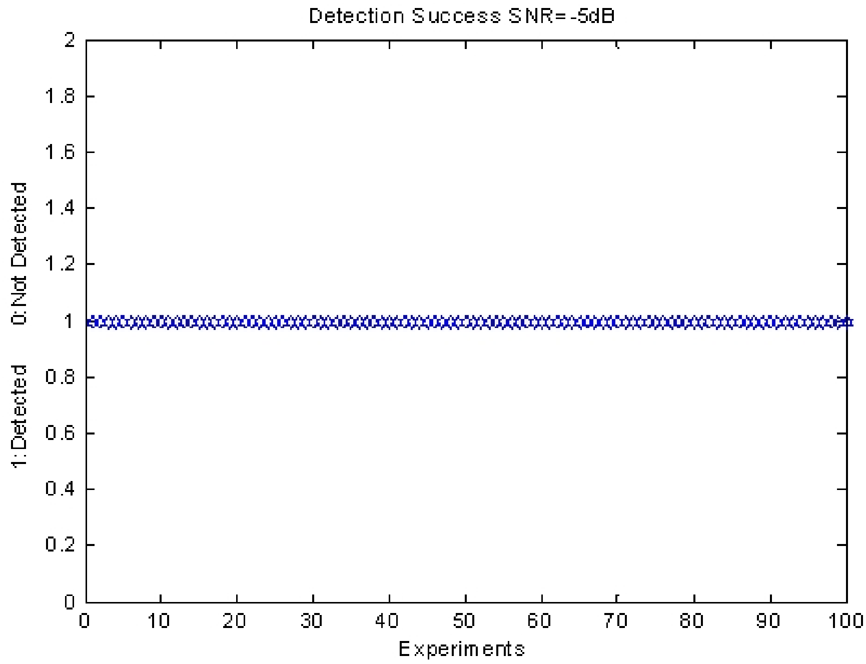

Figure 5.30 Detection Success at SNR = –5dB (Typical DSSS signal, Gaussian noise with interference-1)

The evaluations of the results at SNR=-5dB is summarized below.

Table 5.14 The evaluations of the results at SNR=-5dB (Typical DSSS signal, Gaussian noise with interference-1)

P(Detected)	1
P(Not Detected)	0
P(Correct Symbol period estimation | Detected)	1
P(Wrong Symbol period estimation | Detected)	0
Mean of Correct Estimated Symbol Periods	20.4827μs
Mean of Wrong Estimated Symbol Periods	-
Standard Deviation of Correct Estimated Symbol Periods	0.0209μs
Max Deviation of Correct Estimated Symbol Periods	0.0473μs

The channel parameters and performance analysis for SNR = -10dB is given below.

Table 5.15 Interference Channel Parameters SNR= –10dB (1)

Channel Type	Values
Gaussian Noise	(noise only) SNR at Output of Receiver Filter = –10dB
Interference signal	(noise + interference) SNR at Output of Receiver Filter = –11.8dB

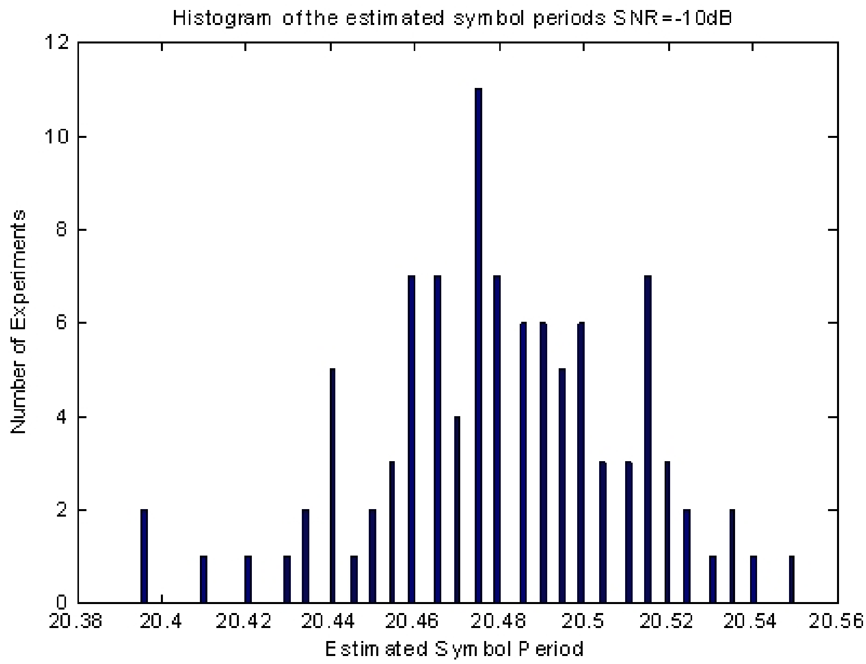

Figure 5.31 Symbol Period Estimation at SNR= -10dB (Typical DSSS signal, Gaussian noise with interference-1)

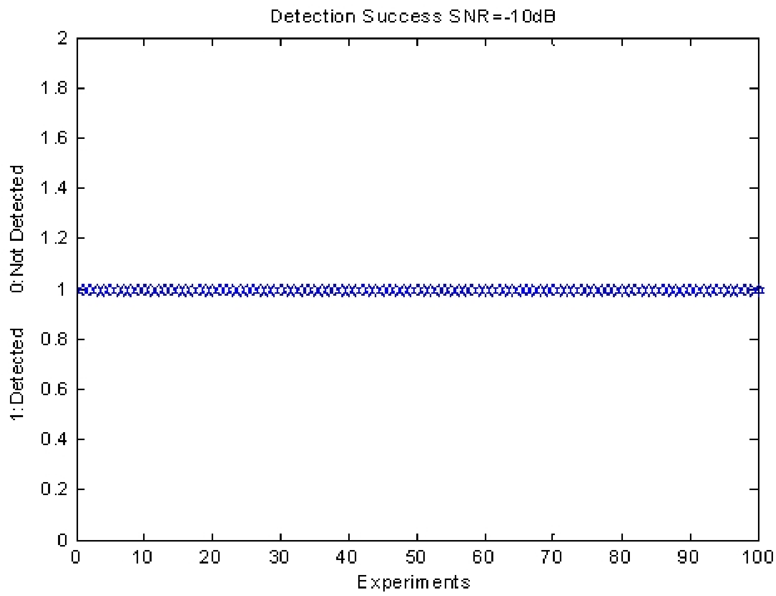

Figure 5.32 Detection Success at SNR = –10dB (Typical DSSS signal, Gaussian noise with interference-1)

The evaluations of the results at SNR=-10dB is summarized below.

Table 5.16 The evaluations of the results at SNR=-10dB (Typical DSSS signal, Gaussian noise with interference-1)

P(Detected)	1
P(Not Detected)	0
P(Correct Symbol period estimation | Detected)	1
P(Wrong Symbol period estimation | Detected)	0
Mean of Correct Estimated Symbol Periods	20.4827µs
Mean of Wrong Estimated Symbol Periods	-
Standard Deviation of Correct Estimated Symbol Periods	0.0209µs
Max Deviation of Correct Estimated Symbol Periods	0.0473µs

The channel parameters and performance analysis for SNR = -13dB is given below.

Table 5.17 Interference Channel Parameters SNR= –13dB (1)

Channel Type	Values
Gaussian Noise	(noise only) SNR at Output of Receiver Filter = –13dB
Interference signal	(noise + interference) SNR at Output of Receiver Filter = –14.02dB

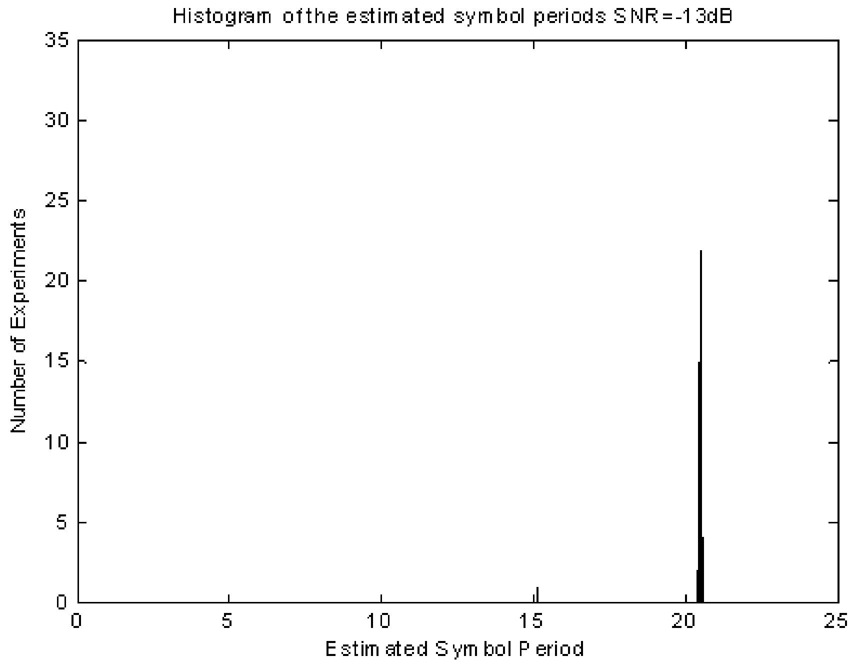

Figure 5.33 Symbol Period Estimation at SNR= -13dB (Typical DSSS signal, Gaussian noise with interference-1)

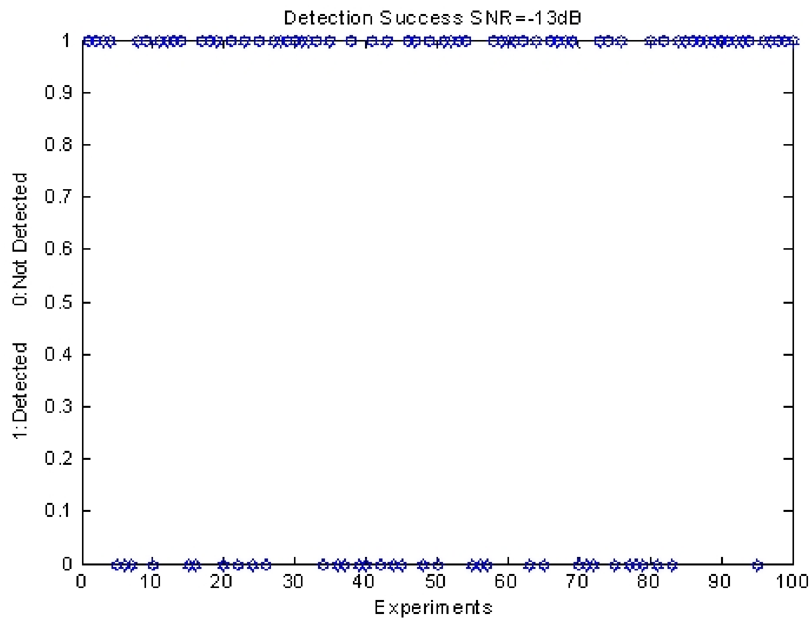

Figure 5.34 Detection Success at SNR = –13dB (Typical DSSS signal, Gaussian noise with interference-1)

The evaluations of the results at SNR=-13dB is summarized below.

Table 5.18 The evaluations of the results at SNR=-13dB (Typical DSSS signal, Gaussian noise with interference-1)

P(Detected)	0.65
P(Not Detected)	0.35
P(Correct Symbol period estimation | Detected)	1
P(Wrong Symbol period estimation | Detected)	0
Mean of Correct Estimated Symbol Periods	20.4028μs
Mean of Wrong Estimated Symbol Periods	-
Standard Deviation of Correct Estimated Symbol Periods	0.6665μs
Max Deviation of Correct Estimated Symbol Periods	0.2022μs

The channel parameters and performance analysis for SNR = -15dB is given below.

Table 5.19 Interference Channel Parameters SNR= –15dB (1)

Channel Type	Values
Gaussian Noise	(noise only) SNR at Output of Receiver Filter = –15dB
Interference signal	(noise + interference) SNR at Output of Receiver Filter = –15.67dB

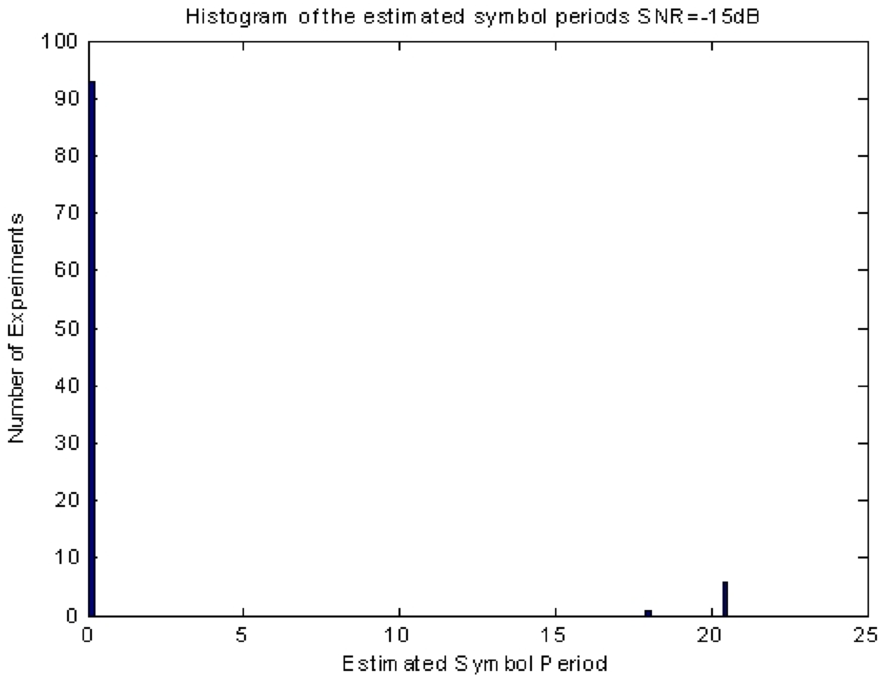

Figure 5.35 Symbol Period Estimation at SNR= -15dB (Typical DSSS signal, Gaussian noise with interference-1)

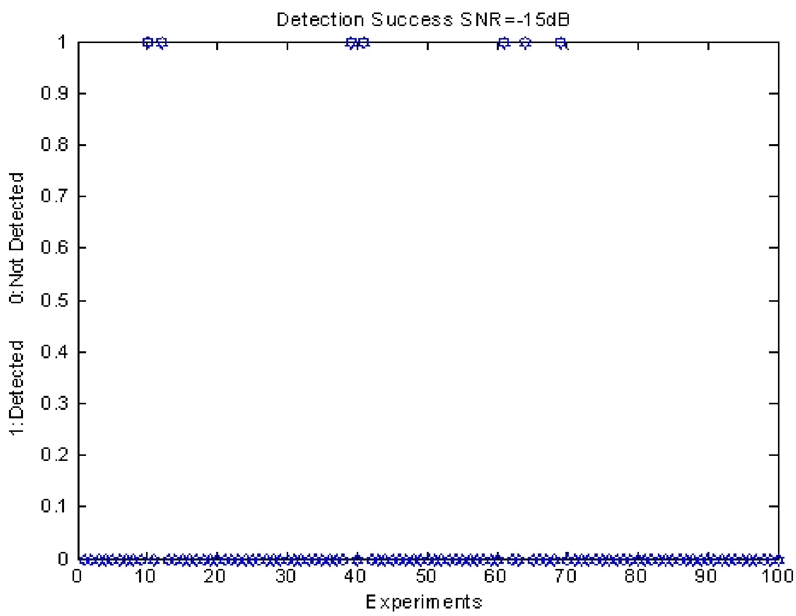

Figure 5.36 Detection Success at SNR = –15dB (Typical DSSS signal, Gaussian noise with interference-1)

The evaluations of the results at SNR=-15dB is summarized below.

Table 5.20 The evaluations of the results at SNR=-15B (Typical DSSS signal, Gaussian noise with interference-1)

P(Detected)	0.07
P(Not Detected)	0.93
P(Correct Symbol period estimation | Detected)	6/7
P(Wrong Symbol period estimation | Detected)	1/7
Mean of Correct Estimated Symbol Periods	20.1214μs
Mean of Wrong Estimated Symbol Periods	18.254μs
Standard Deviation of Correct Estimated Symbol Periods	0.9082μs
Max Deviation of Correct Estimated Symbol Periods	0.4336μs

In the following part the same analysis is done and results are obtained for channel with a different interference effect. This time frequency of interference is in the band of DSSS signal. First detection performance due to SNR is given then results are obtained for specific SNR's; -5dB, -10dB, and -13dB and -15dB. The frequency content of the interference signal and signal at the output of receiver filter is given in Figure 5.37 and Figure 5.38.

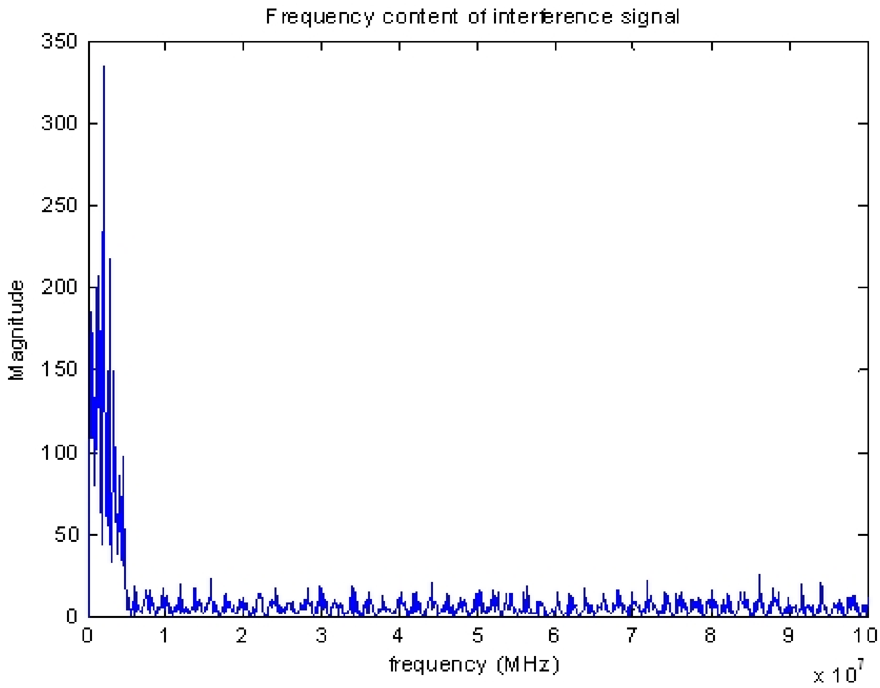

Figure 5.37 The frequency content of the interference signal

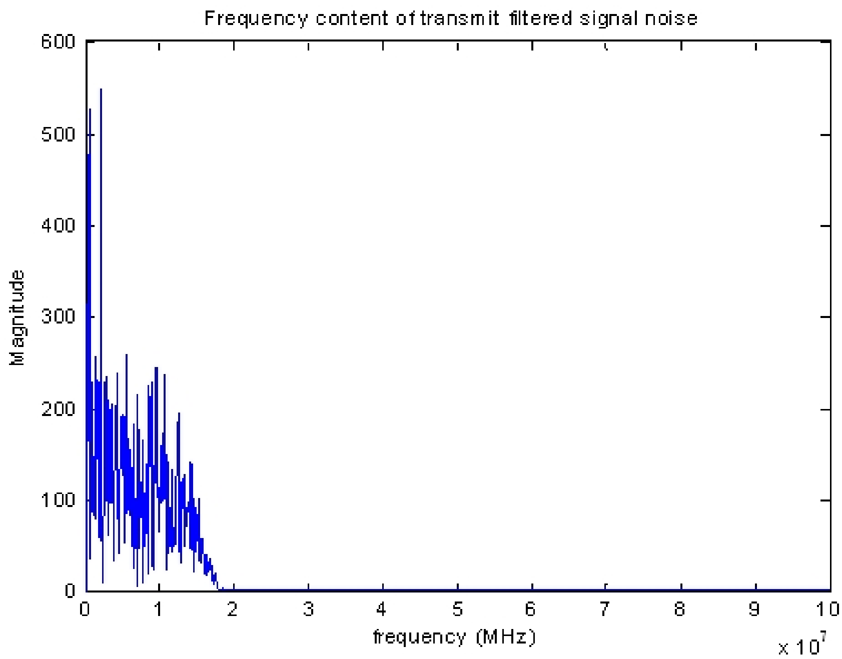

Figure 5.38 Frequency content of output of receiver filter

Estimated symbol periods and detection performance due to SNR is given in Figure 5.39 and Figure 5.40.

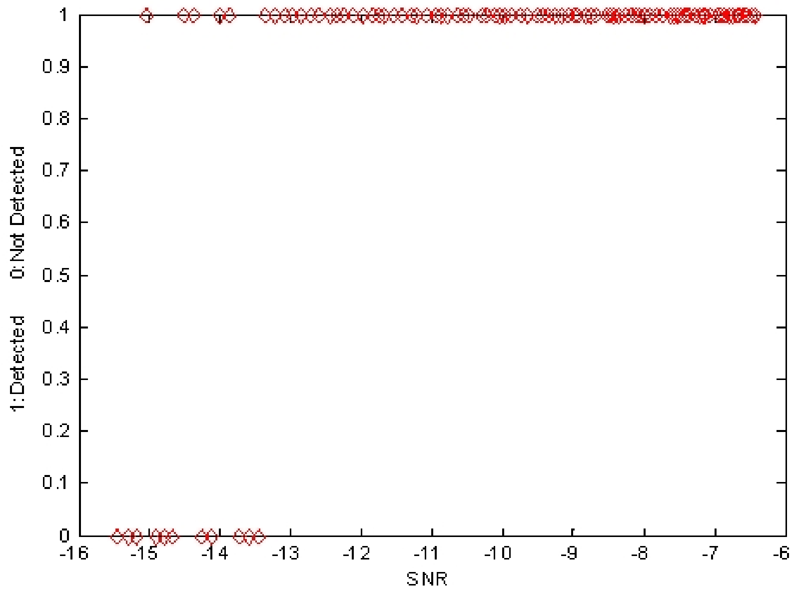

Figure 5.39 Detection Success due to SNR (Typical DSSS signal, with interference -2)

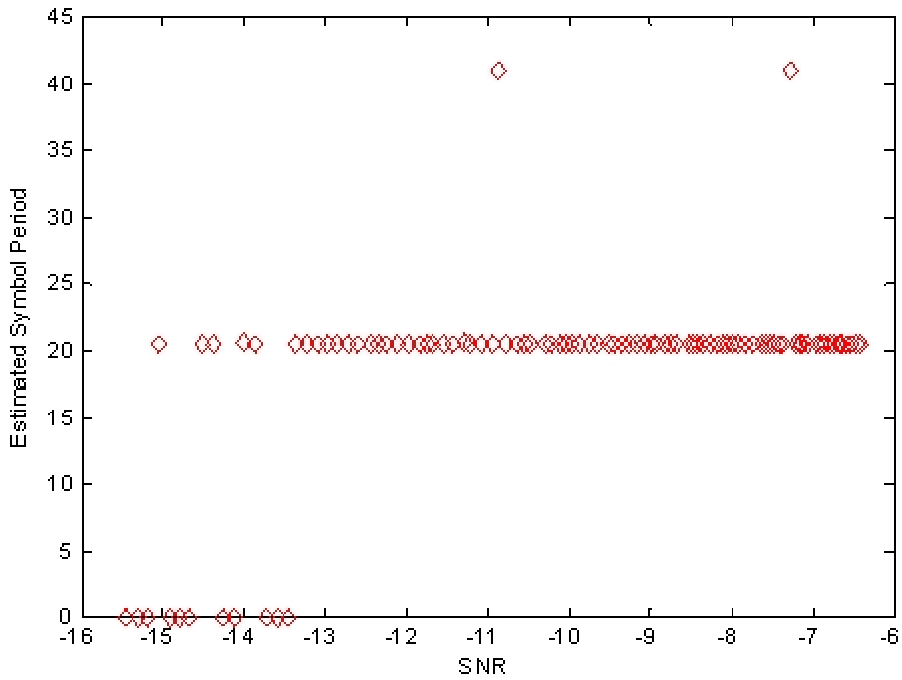

Figure 5.40 Symbol Period Estimation due to SNR (Typical DSSS signal, with interference -2)

In the following part results are obtained for specific SNR's; -5dB, -10dB, -13dB and -15dB are given. The SNR values of each channel are given before the performance results. The same signal and receiver parameters are used in order to make comparisons. The channel parameters and performance analysis for SNR = -5dB is given below.

Table 5.21 Interference Channel Parameters SNR= –5dB (2)

Channel Type	Values
Gaussian Noise	(noise only) SNR at Output of Receiver Filter = –5dB
Interference signal	(noise + interference) SNR at Output of Receiver Filter = –8.15dB

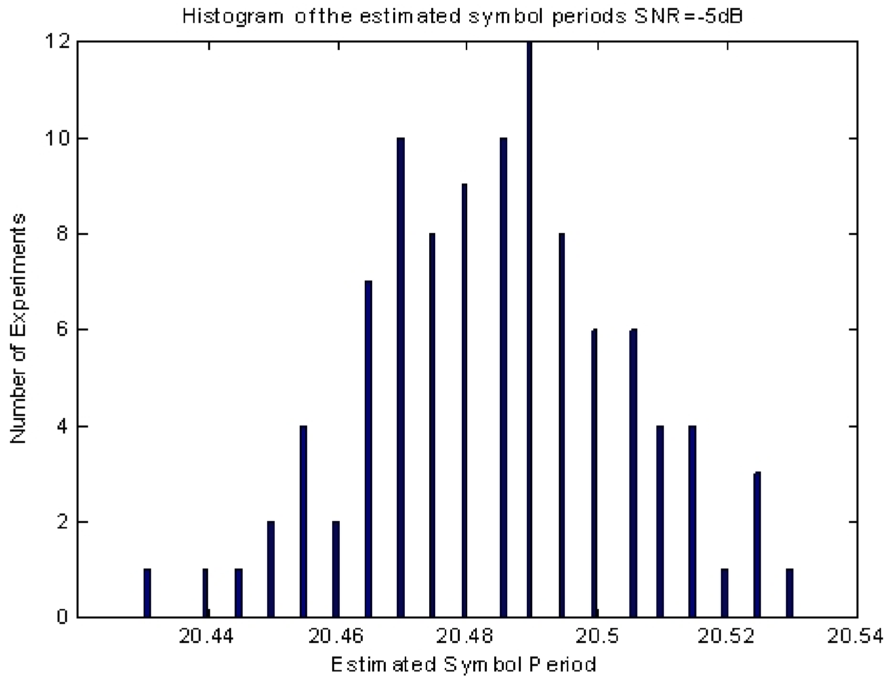

Figure 5.41 Symbol Period Estimation at SNR= -5dB (Typical DSSS signal, Gaussian noise with interference-2)

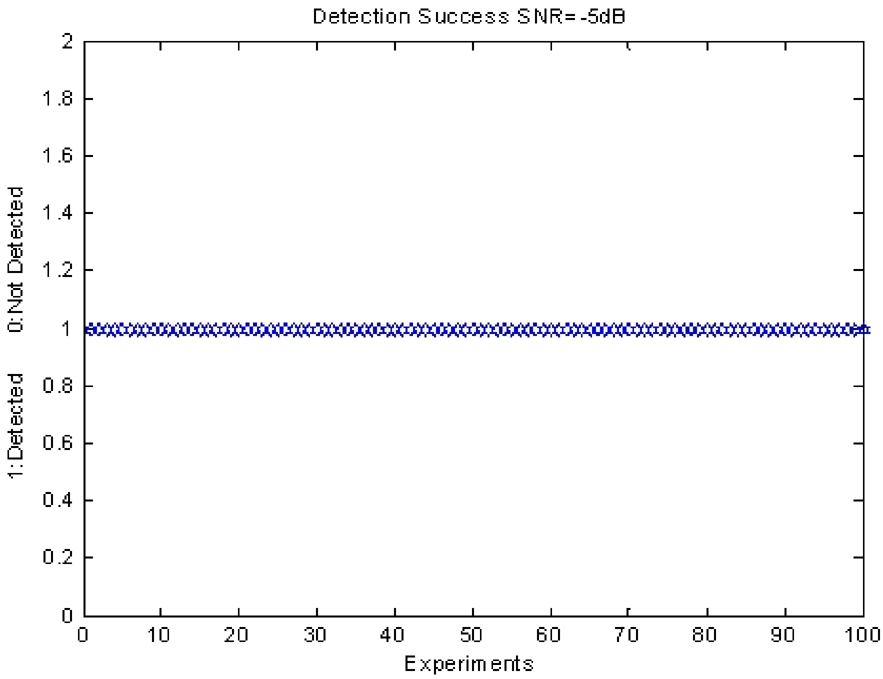

Figure 5.42 Detection Success at SNR = –5dB (Typical DSSS signal, Gaussian noise with interference-2)

The evaluations of the results at SNR=-5dB is summarized below.

Table 5.22 The evaluations of the results at SNR= –5dB (Typical DSSS signal, Gaussian noise with interference-2)

P(Detected)	1
P(Not Detected)	0
P(Correct Symbol period estimation | Detected)	1
P(Wrong Symbol period estimation | Detected)	0
Mean of Correct Estimated Symbol Periods	20.4847μs
Mean of Wrong Estimated Symbol Periods	-
Standard Deviation of Correct Estimated Symbol Periods	0.0199μs
Max Deviation of Correct Estimated Symbol Periods	0.0547μs

The channel parameters and performance analysis for SNR = -10dB is given below.

Table 5.23 Interference Channel Parameters SNR= –10dB (2)

Channel Type	Values
Gaussian Noise	(noise only) SNR at Output of Receiver Filter = –10dB
Interference signal	(noise + interference) SNR at Output of Receiver Filter = –11.27dB

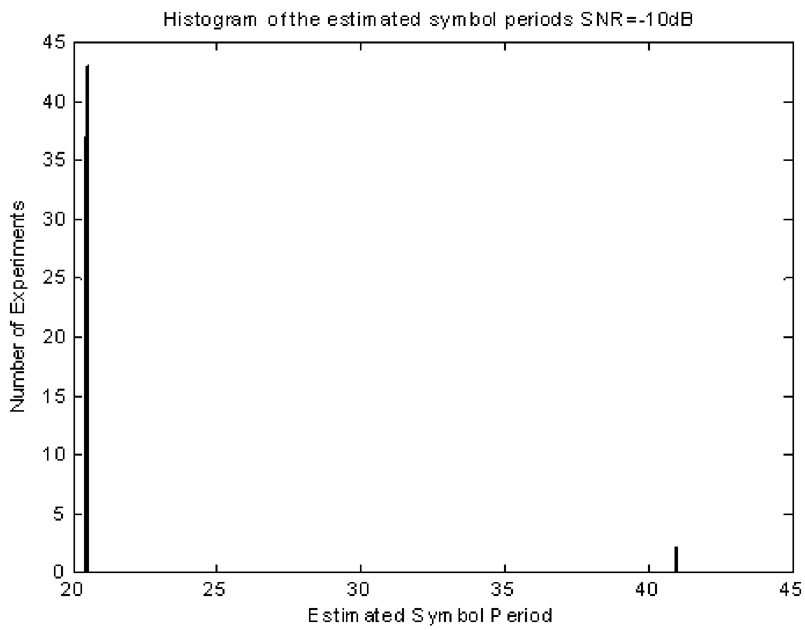

Figure 5.43 Symbol Period Estimation at SNR= -10dB (Typical DSSS signal, Gaussian noise with interference-2)

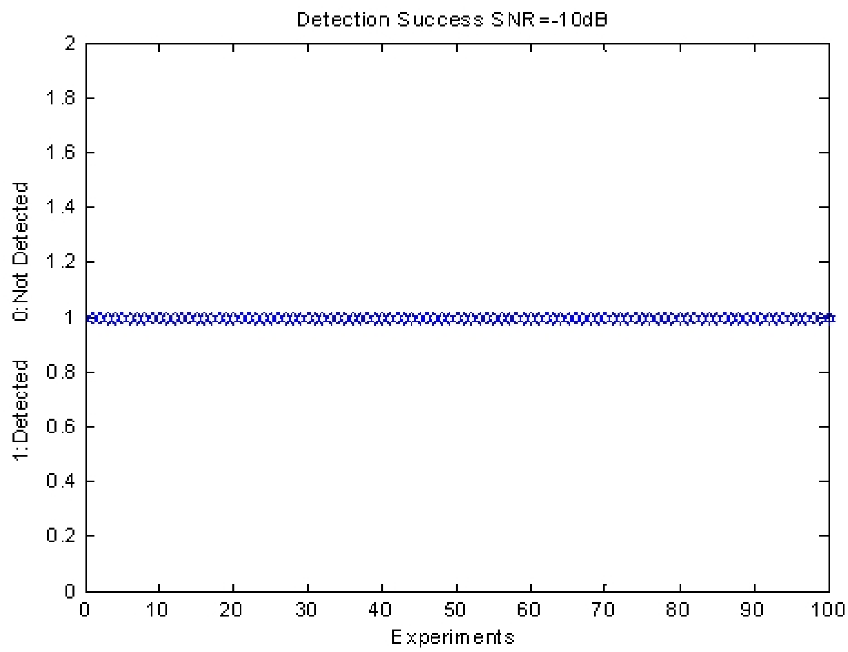

Figure 5.44 Detection Success at SNR = –10dB (Typical DSSS signal, Gaussian noise with interference-2)

The evaluations of the results at SNR=-10dB is summarized below.

Table 5.24 The evaluations of the results at SNR= –10dB (Typical DSSS signal, Gaussian noise with interference-2)

P(Detected)	1
P(Not Detected)	0
P(Correct Symbol period estimation | Detected)	0.98
P(Wrong Symbol period estimation | Detected)	0.02
Mean of Correct Estimated Symbol Periods	20.4801μs
Mean of Wrong Estimated Symbol Periods	41.0256μs
Standard Deviation of Correct Estimated Symbol Periods	0.0299μs
Max Deviation of Correct Estimated Symbol Periods	0.0751μs

The channel parameters and performance analysis for SNR = -13dB is given below.

Table 5.25 Interference Channel Parameters SNR= –13dB (2)

Channel Type	Values
Gaussian Noise	(noise only) SNR at Output of Receiver Filter = –13dB
Interference signal	(noise + interference) SNR at Output of Receiver Filter = –13.71dB

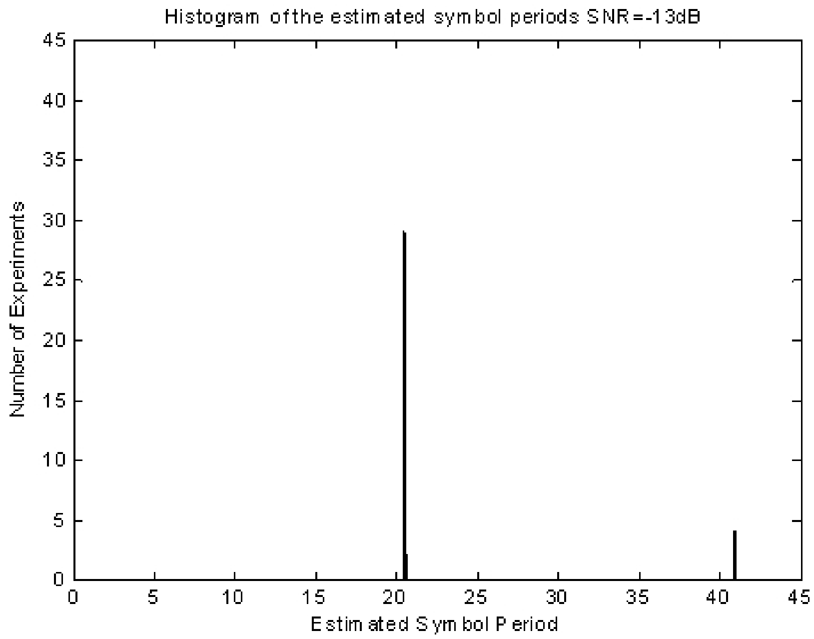

Figure 5.45 Symbol Period Estimation at SNR= -13dB (Typical DSSS signal, Gaussian noise with interference-2)

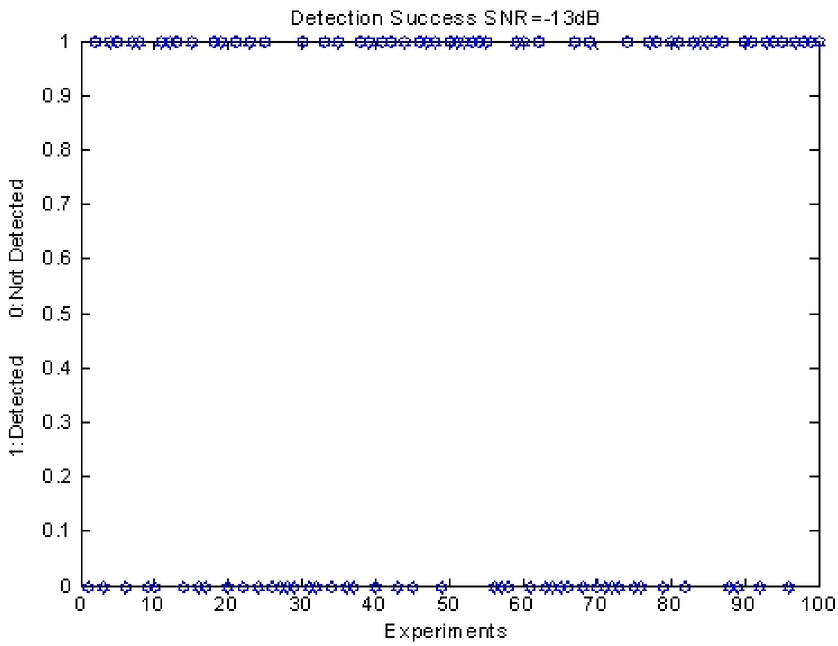

Figure 5.46 Detection Success at SNR = –13dB (Typical DSSS signal, Gaussian noise with interference-2)

The evaluations of the results at SNR=-13dB is summarized below.

Table 5.26 The evaluations of the results at SNR= –13dB (Typical DSSS signal, Gaussian noise with interference-2)

P(Detected)	0.55
P(Not Detected)	0.45
P(Correct Symbol period estimation | Detected)	51/55
P(Wrong Symbol period estimation | Detected)	4/55
Mean of Correct Estimated Symbol Periods	20.4826μs
Mean of Wrong Estimated Symbol Periods	40.965μs
Standard Deviation of Correct Estimated Symbol Periods	0.0406μs
Max Deviation of Correct Estimated Symbol Periods	0.0974μs

The channel parameters and performance analysis for SNR = -15dB is given below.

Table 5.27 Interference Channel Parameters SNR= –15dB (2)

Channel Type	Values
Gaussian Noise	(noise only) SNR at Output of Receiver Filter = –15dB
Interference signal	(noise + interference) SNR at Output of Receiver Filter = –15.45dB

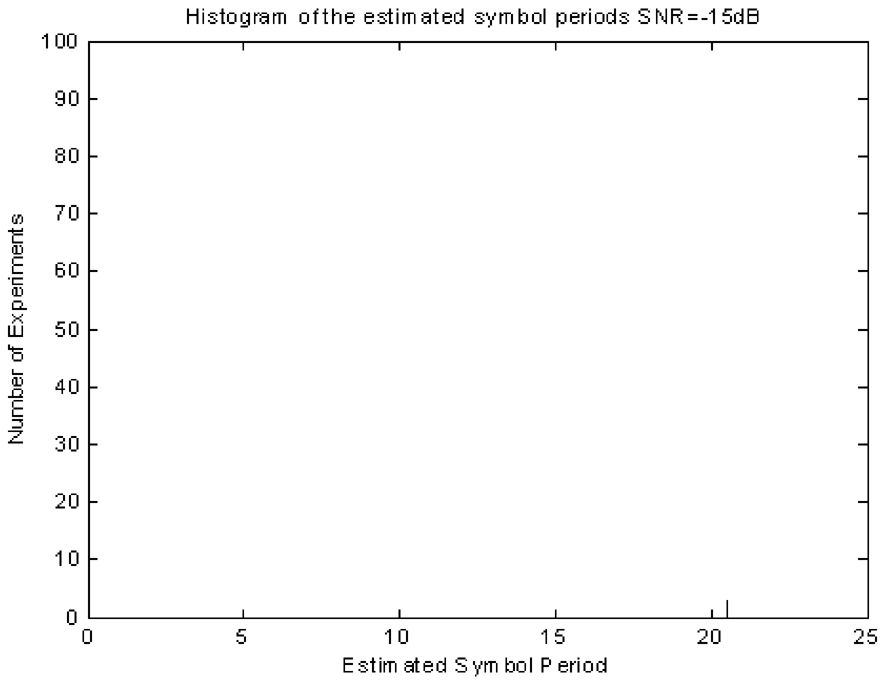

Figure 5.47 Symbol Period Estimation at SNR= -15dB (Typical DSSS signal, Gaussian noise with interference-2)

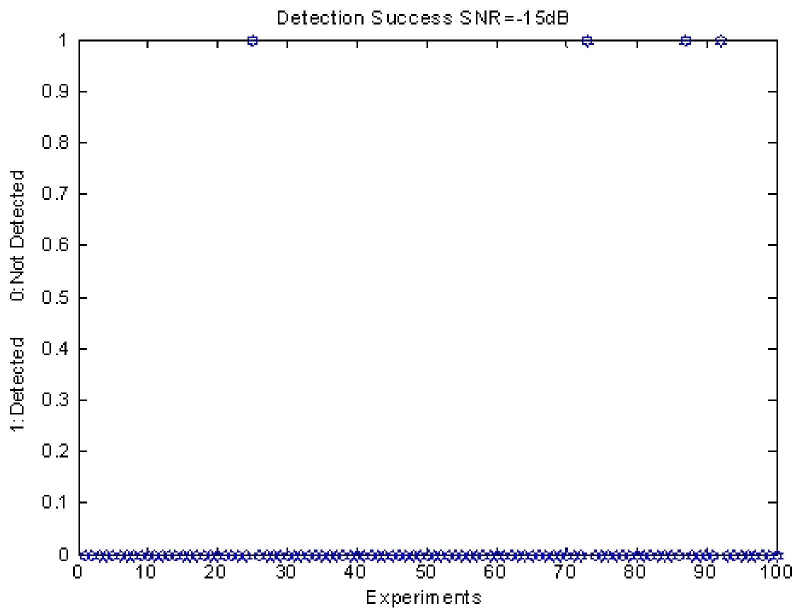

Figure 5.48 Detection Success at SNR = –15dB (Typical DSSS signal, Gaussian noise with interference-2)

The evaluations of the results at SNR=-15dB is summarized below.

Table 5.28 The evaluations of the results at SNR= –15dB (Typical DSSS signal, Gaussian noise with interference-2)

P(Detected)	0.04
P(Not Detected)	0.96
P(Correct Symbol period estimation I Detected)	1
P(Wrong Symbol period estimation I Detected)	0
Mean of Correct Estimated Symbol Periods	20.4963μs
Mean of Wrong Estimated Symbol Periods	--
Standard Deviation of Correct Estimated Symbol Periods	0.0250μs
Max Deviation of Correct Estimated Symbol Periods	0.0337μs

The results obtained for Typical DSSS signal shows that the detection process gives successful results for SNRs above -15dB. The multipath effect decreases performance slightly and preserves estimation of the symbol period. The interference is considered as noise by the system and also decreases the performance of detection process. If the interference is in the band of DSSS signal detection performance decreases more and the probability of correctly estimate the symbol period is also decreased due to this kind of interference.

5.3 Performance Analysis of UMTS Signal

The parameters of UMTS signal type are summarized in Table 5.29 The receiver parameters are given in Table 5.30. The channel type and necessary channel parameters are given for result of each experimental trial set. The object of this first analysis is to obtain the performance of the detection technique due to low SNR conditions so the channel is implementing simple Gaussian noise. Also the symbol period that is estimated is given for each SNR. The detection of the peaks is accomplished by using a fixed threshold because of the non-periodic structure of the peaks.

Table 5.29 UMTS signal parameters

Parameters	**Values**
Modulation Type	Dual channel QPSK
Scrambler	Short
Channels	DPDCH,DPCCH
Chip Rate	256chips/symbol
Total number of symbols	50
Bandwidth	5MHz
Symbol Period	25.6μs

Table 5.30 Receiver parameters (5)

Parameters	**Values**
Receiver filter bandwidth	10MHz
Window Number	20

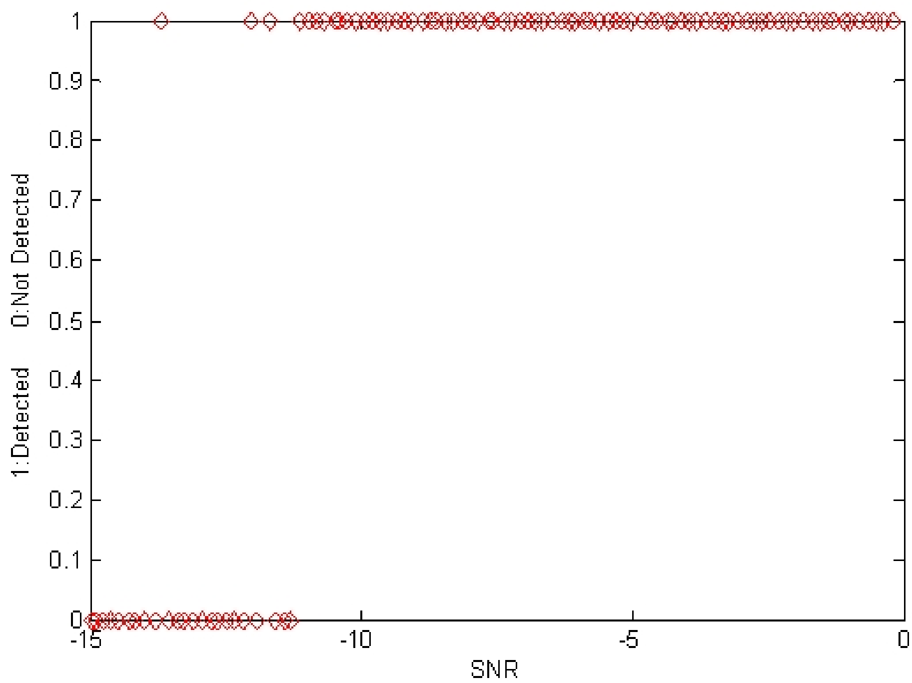

Figure 5.49 Detection Success due to SNR

In Figure 5.49 Detection Success due to SNR is given. This shows the response of receiver to UMTS signal to decreasing SNR in a continuous like manner. Gaussian Noise Channel is used in these simulations. The last SNR that the signal is detected is -13.7dB.

In the following part the results are obtained for specific SNR's; -5dB, -10dB, and - 12 dB in order to clarify the detection performance of the receiver.

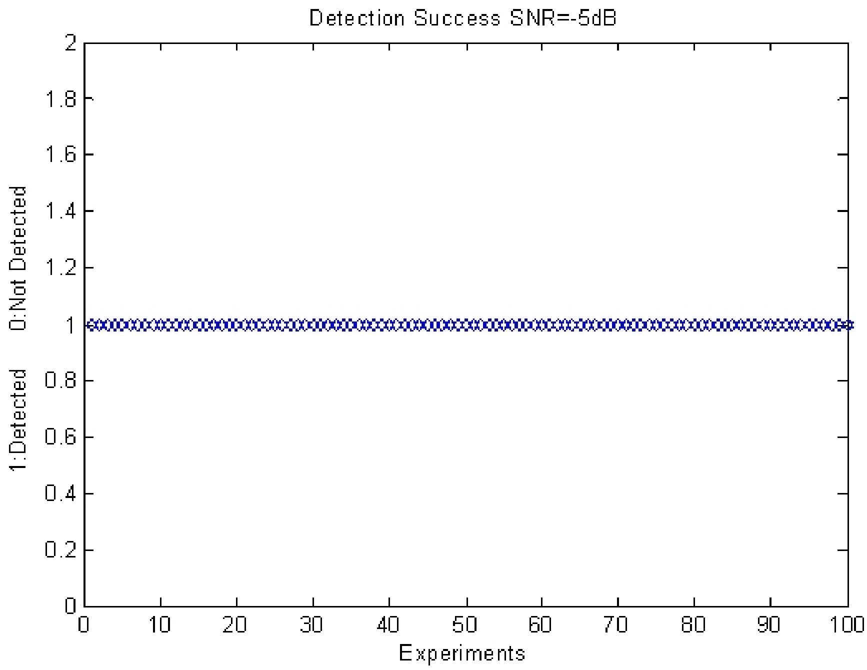

Figure 5.50 Detection Success at -5dB SNR (UMTS)

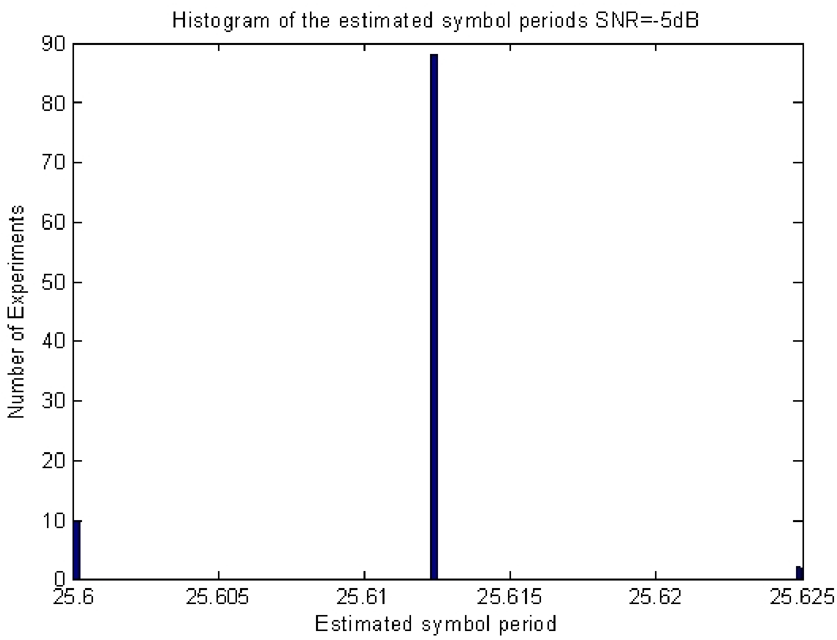

Figure 5.51 Symbol Period Estimation at SNR= -5dB (UMTS)

The evaluations of the results at SNR=-5dB is summarized below.

Table 5.31 The evaluations of the results at SNR= –5dB (UMTS)

P(Detected)	1
P(Not Detected)	0
P(Correct Symbol period estimation I Detected)	1
P(Wrong Symbol period estimation I Detected)	0
Mean of Correct Estimated Symbol Periods	25.6115µs
Mean of Wrong Estimated Symbol Periods	--
Standard Deviation of Correct Estimated Symbol Periods	0.0042µs
Max Deviation of Correct Estimated Symbol Periods	0.0135µs

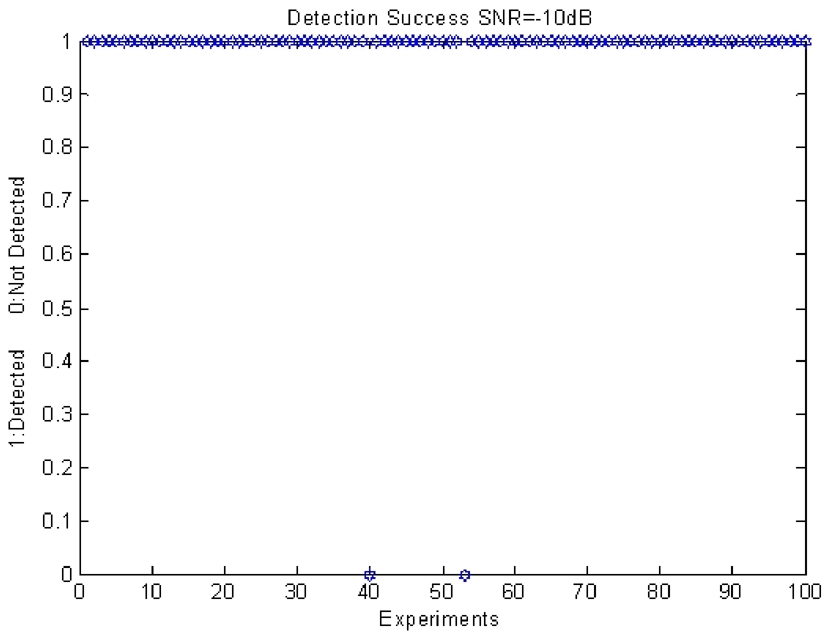

Figure 5.52 Detection Success at -10dB SNR (UMTS)

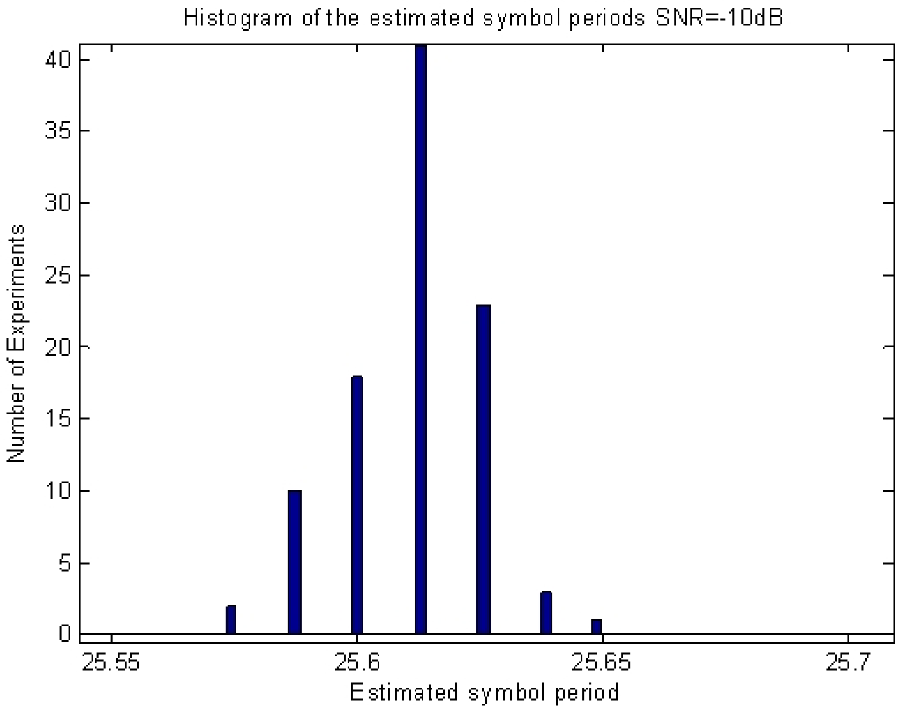

Figure 5.53 Symbol Period Estimation at SNR= -10dB (UMTS)

Table 5.32 The evaluations of the results at SNR= –10dB (UMTS)

P(Detected)	0.98
P(Not Detected)	0.02
P(Correct Symbol period estimation I Detected)	1
P(Wrong Symbol period estimation I Detected)	0
Mean of Correct Estimated Symbol Periods	25.6110µs
Mean of Wrong Estimated Symbol Periods	--
Standard Deviation of Correct Estimated Symbol Periods	0.0138µs
Max Deviation of Correct Estimated Symbol Periods	0.0390µs

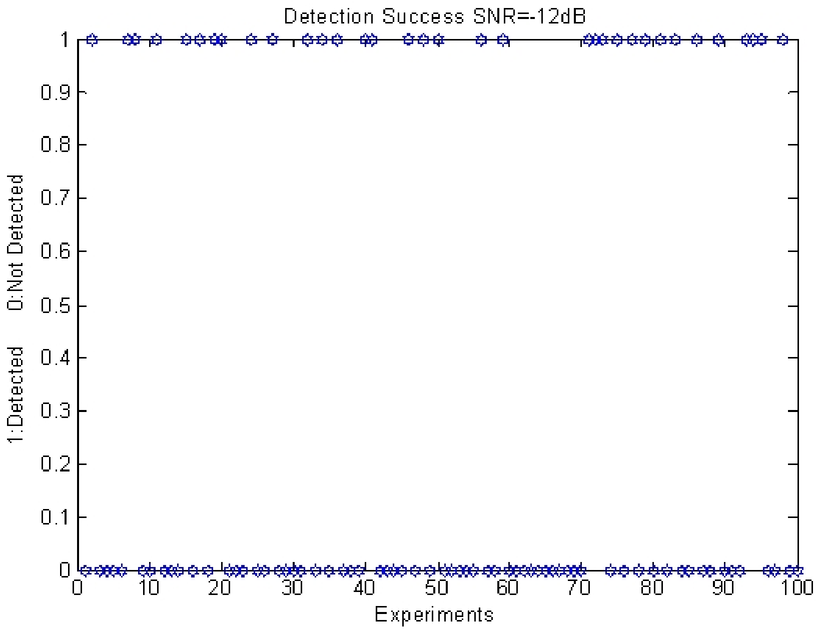

Figure 5.54 Detection Success at -12dB SNR (UMTS)

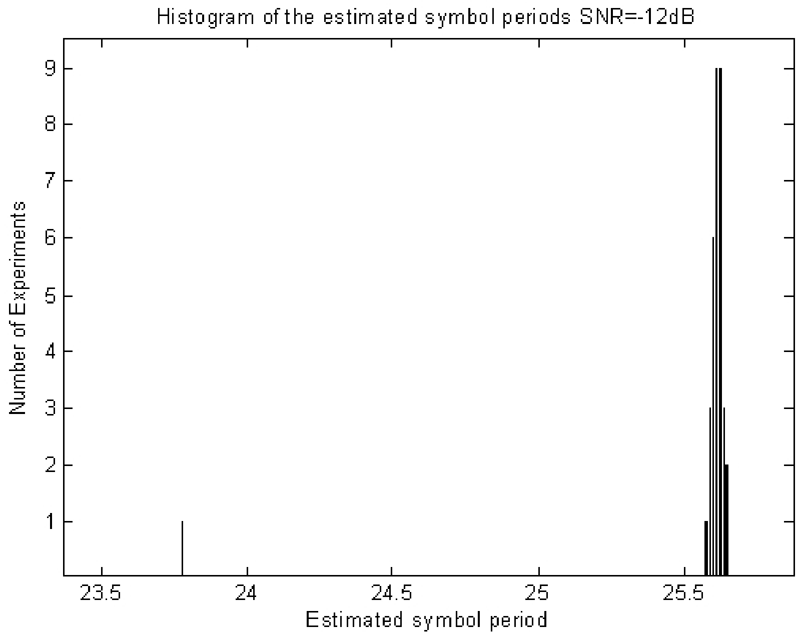

Figure 5.55 Symbol Period Estimation at SNR= -10dB (UMTS)

Table 5.33 The evaluations of the results at SNR= –12dB (UMTS)

P(Detected)	0.34
P(Not Detected)	0.66
P(Correct Symbol period estimation | Detected)	33/34
P(Wrong Symbol period estimation | Detected)	1/34
Mean of Correct Estimated Symbol Periods	25.6148μs
Mean of Wrong Estimated Symbol Periods	23.7750μs
Standard Deviation of Correct Estimated Symbol Periods	0.0178μs
Max Deviation of Correct Estimated Symbol Periods	0.0398μs

Performance analysis shows that the detection of the UMTS signal is performed successfully for SNRs below -12dB. This is less than the performance obtained for Typical DSSS signal. This is because of the multichannel and more complicated structure of the DSSS signal also number of symbols processed and windows used is effective on this result.

5.4 Performance Analysis of LPI Radar Signals

In this section the performance analysis is obtained for typical LPI radar signals. The parameters of the radar signal are summarized in Table 5.34.

Table 5.34 DSSS Radar Signal Parameters

Parameters	Values
Modulation Type	BPSK
Sampling Freq.	200MHz
Total sample number	80000
Bandwidth	50MHz
Total number of analyzed pulses	10
Pulse width	10µs
PRI	40µs

Table 5.35 Receiver parameters

Parameters	**Values**
Receiver filter bandwidth	70MHz
Window Number	2

In the Figure 5.56 the result of first analysis is given. This figure shows that the PRI estimation error is increased after -12dB SNR. The best performance is achieved between 0dB and –12BdB SNR’s. In this interval the PRI is estimated correctly as 40µs as given in Table 5.34. The other necessary statistical results are given in the following parts.

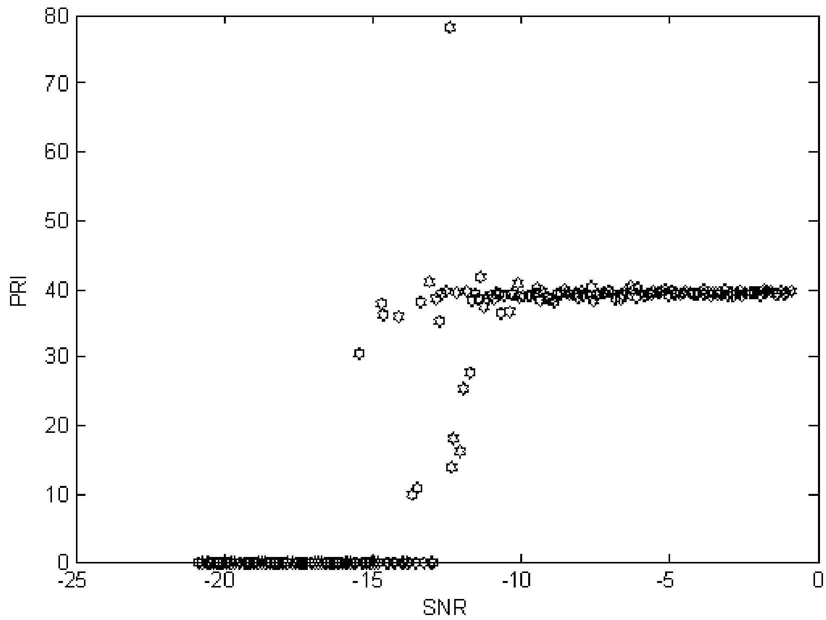

Figure 5.56 PRI Estimation due to SNR

The result of the next analysis shows the performance of the receiver at different specific SNR’s; -5dB, -10dB, -13dB and -15dB.

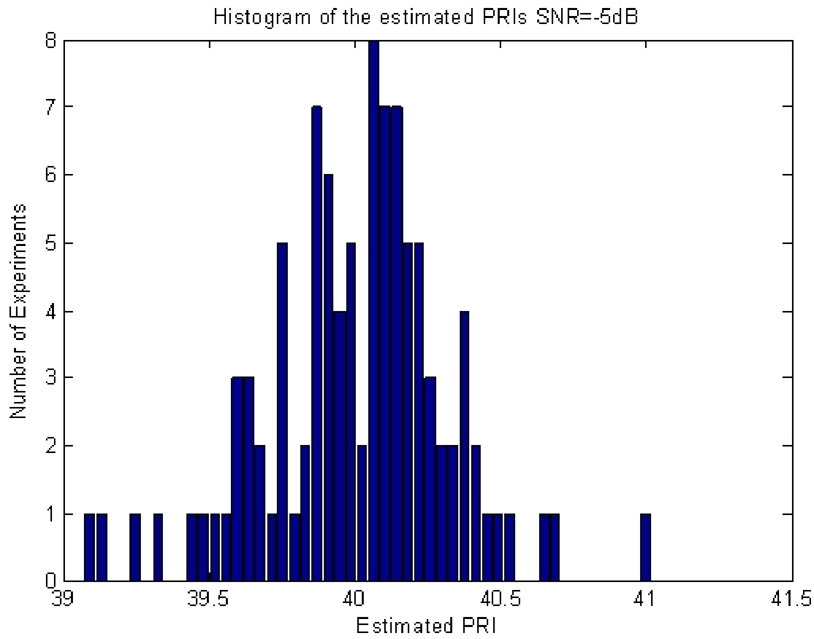

Figure 5.57 PRI Estimation at SNR= -5dB

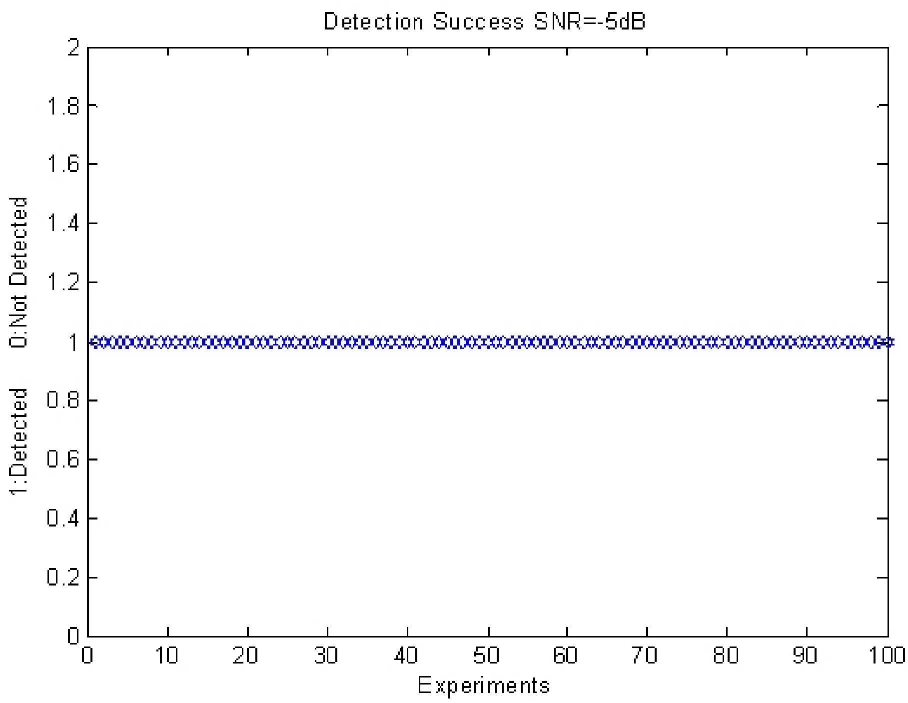

Figure 5.58 Detection Success at -5dB SNR

The evaluations of the results at SNR = -5dB is summarized below

Table 5.36 The evaluations of the results at SNR= –5dB (LPI radar)

P(Detected)	1
P(Not Detected)	0
P(Correct PRI estimation I Detected)	1
P(Wrong PRI estimation I Detected)	0
Mean of Correct Estimated PRIs	40.0053μs
Mean of Wrong Estimated Symbol PRIs	--
Standard Deviation of Correct Estimated PRIs	0.3207μs
Max Deviation of Correct Estimated PRIs	1.0147μs

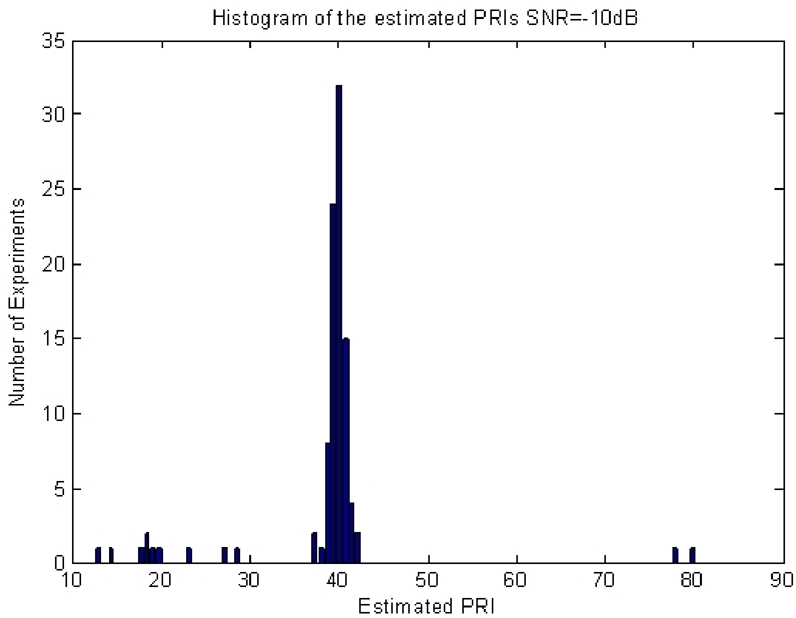

Figure 5.59 PRI Estimation at SNR= -10dB

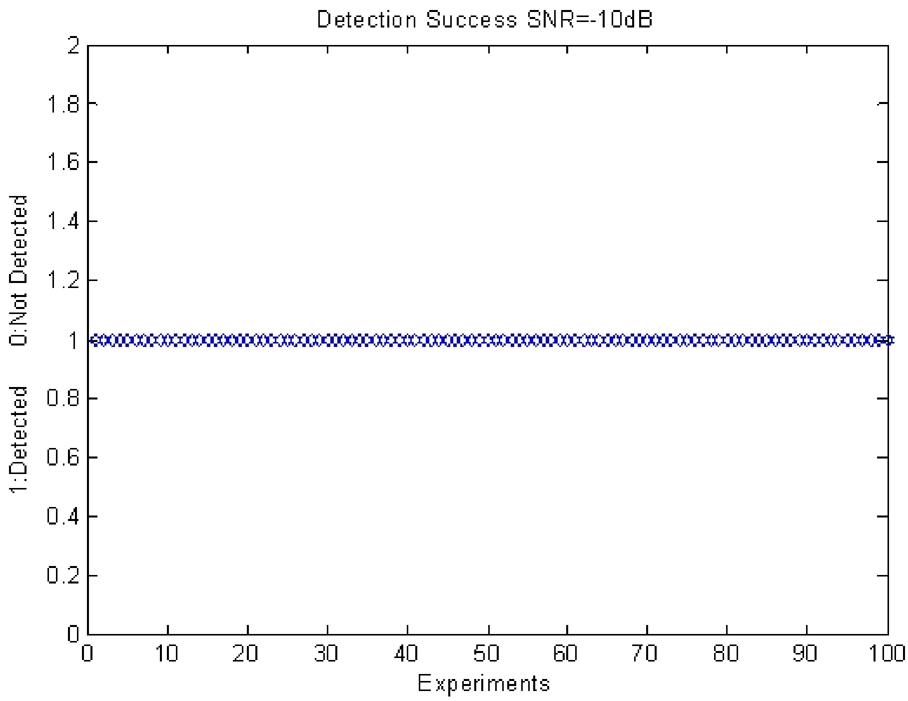

Figure 5.60 Detection Success at -10dB SNR

The evaluations of the results at SNR = -10dB is summarized below

Table 5.37 The evaluations of the results at SNR= –10dB (LPI radar)

P(Detected)	1
P(Not Detected)	0
P(Correct Symbol period estimation I Detected)	0.88
P(Wrong Symbol period estimation I Detected)	0.12
Mean of Correct Estimated PRIs	39.8072μs
Mean of Wrong Estimated PRIs	29.7871μs
Standard Deviation of Correct Estimated PRIs	0.8380μs
Max Deviation of Correct Estimated PRIs	2.3872μs

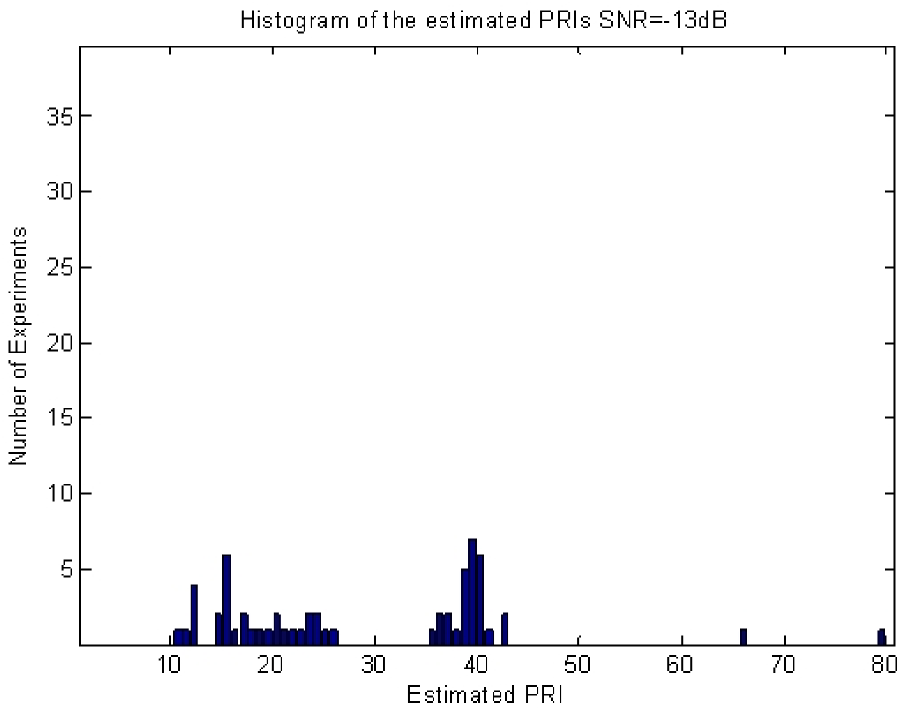

Figure 5.61 PRI Estimation at SNR= -13dB

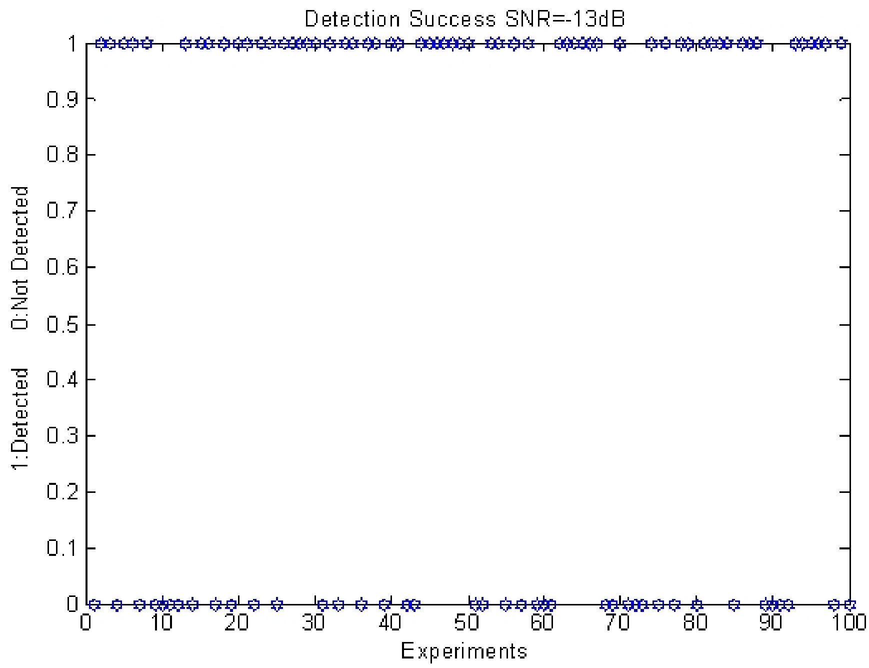

Figure 5.62 Detection Success at -13dB SNR

Table 5.38 The evaluations of the results at SNR= –13dB (LPI radar)

P(Detected)	0.60
P(Not Detected)	0.40
P(Correct Symbol period estimation l Detected)	27/60
P(Wrong Symbol period estimation l Detected)	33/60
Mean of Correct Estimated PRIs	39.2207μs
Mean of Wrong Estimated PRIs	21.2445μs
Standard Deviation of Correct Estimated PRIs	1.7709μs
Max Deviation of Correct Estimated PRIs	3.9457μs

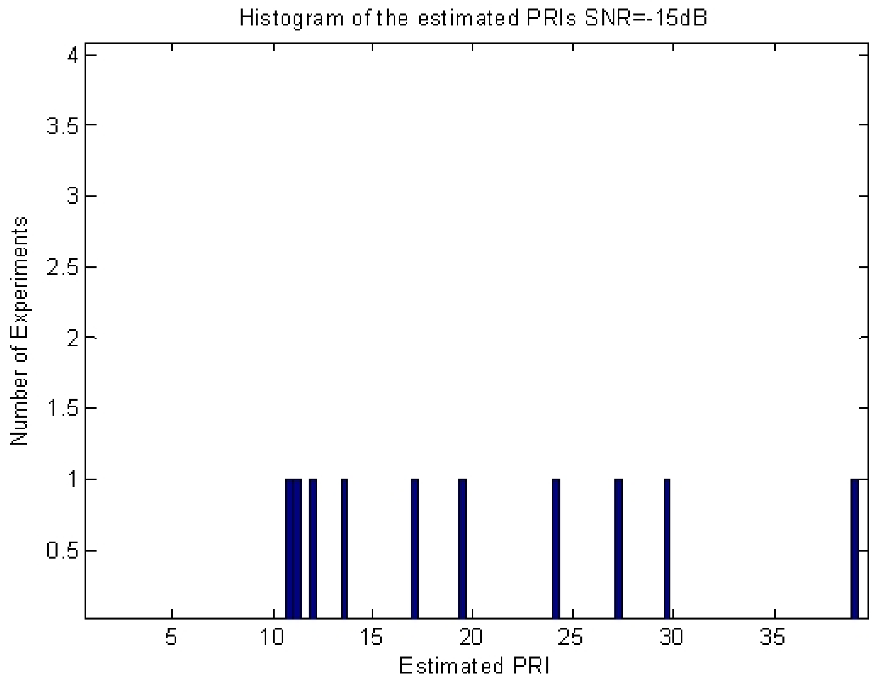

Figure 5.63 PRI Estimation at SNR= -15dB

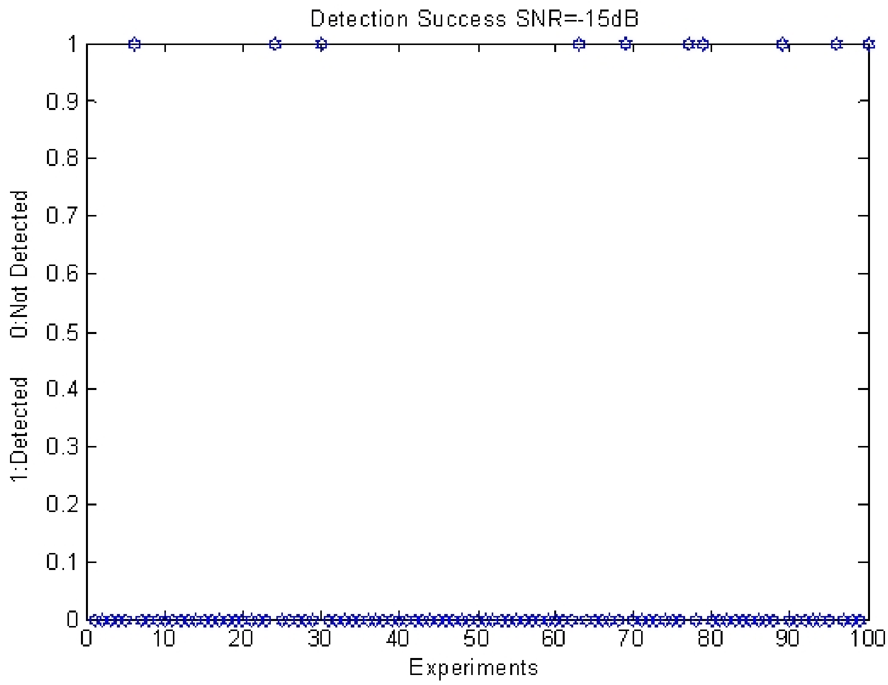

Figure 5.64 Detection Success at -15dB SNR

Table 5.39 The evaluations of the results at SNR= –15dB (LPI radar)

P(Detected)	0.10
P(Not Detected)	0.90
P(Correct Symbol period estimation | Detected)	1/10
P(Wrong Symbol period estimation | Detected)	9/10
Mean of Correct Estimated PRIs	39.2950μs
Mean of Wrong Estimated PRIs	18.3594μs
Standard Deviation of Correct Estimated PRIs	--
Max Deviation of Correct Estimated PRIs	--

The performance analyses results show that, the LPI radar signal can be detected successfully for SNRs above -15dB. Because of the discontinuous pulse characteristics and different autocorrelation fluctuations outputs PRI can be estimated with less performance even if the radar signal is detected.

5.5 Performance Analysis of Spreading Code Estimation

In this part the performance analysis results of Spreading code estimation is given. Typical DSSS signal with a 64 bit spreading code is used as an input to the process and performance results for different SNRs is obtained.

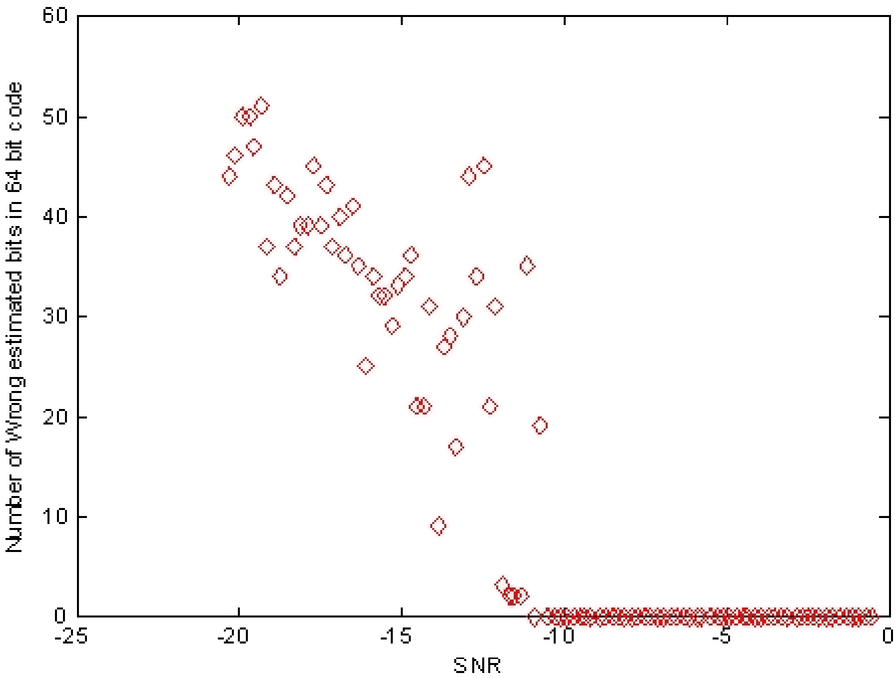

Figure 5.65 Number of wrong estimated bits due to SNR

In Figure 5.65 the number of wrong estimated bits from the 64 bit spreading code due to changes in SNR is given. It is observed that spreading code estimation is successfully performed SNRs higher than -10dB. In the following part results are obtained for specific SNR's; -5dB, -10dB, -13dB and -15dB are given.

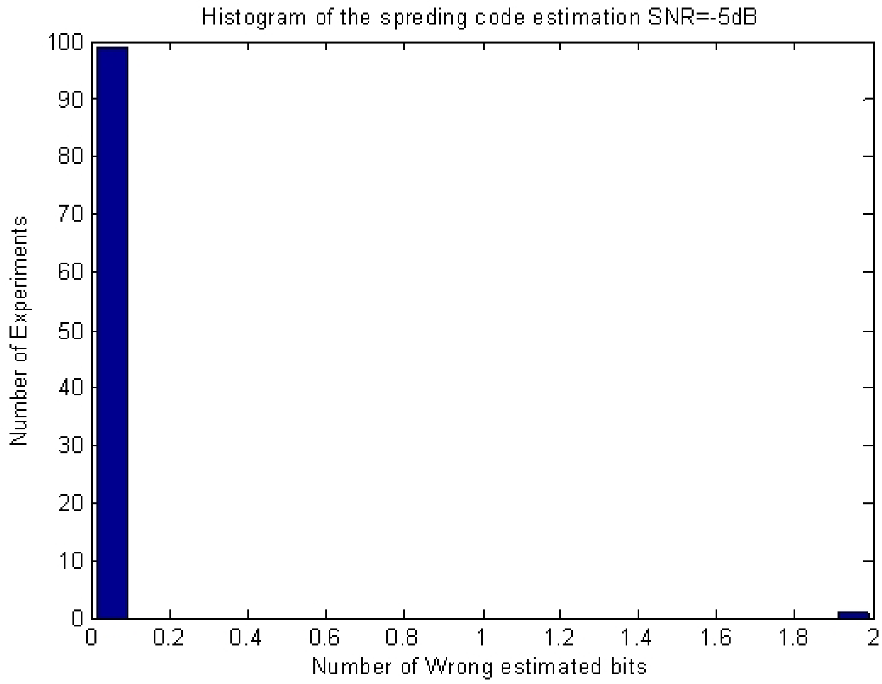

Figure 5.66 Histogram of number of wrong estimated bits SNR= -5dB

Table 5.40 The evaluations of the results at SNR= –5dB

P(Correct Estimated)	0.99
P(Wrong Estimated)	0.01
P(Number of wrong estimated bits<=5 | Wrong Estimated)	1
P(Number of wrong estimated bits<=10 | Wrong Estimated)	0
P(Number of wrong estimated bits>10 | Wrong Estimated)	0

In Figure 5.66 the spreading code estimation bit error histogram is given. Also evaluation of the result is given in Table 5.40.

In the following performance analysis the SNR is decreased to -10dB. The spreading code estimation bit error histogram is given Figure 5.67 and evaluation of the result is given in Table 5.41.

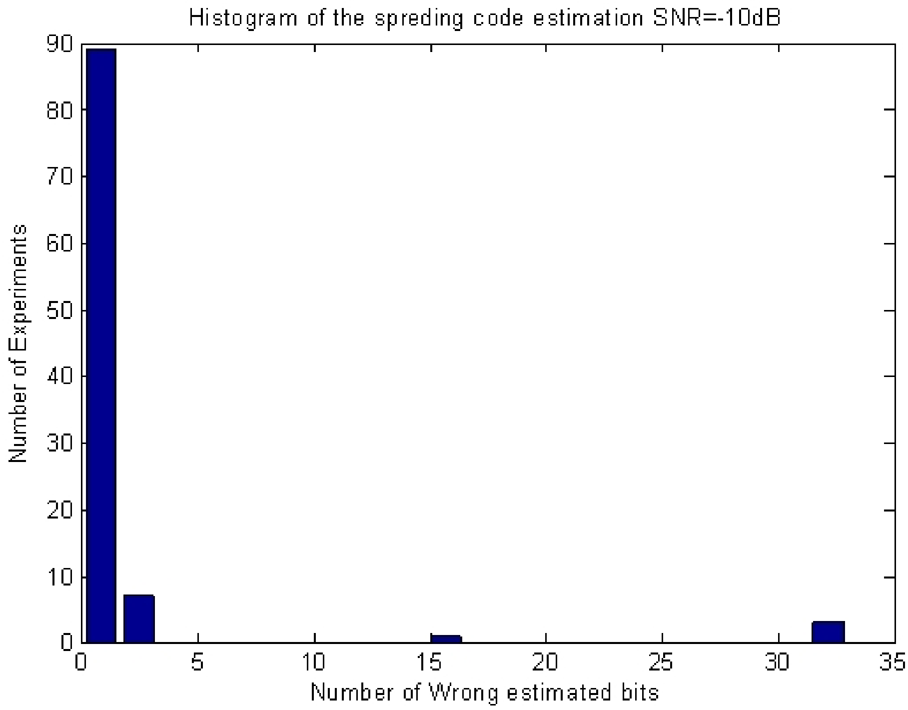

Figure 5.67 Histogram of number of wrong estimated bits SNR= -10dB

Table 5.41 The evaluations of the results at SNR= –10dB

P(Correct Estimated)	0.89
P(Wrong Estimated)	0.11
P(Number of wrong estimated bits<=5 l Wrong Estimated)	7/11
P(Number of wrong estimated bits<=10 l Wrong Estimated)	7/11
P(Number of wrong estimated bits>10 l Wrong Estimated)	4/11

In the following performance analysis the SNR is decreased to -13dB. The spreading code estimation bit error histogram is given Figure 5.68 and evaluation of the result is given in Table 5.42.

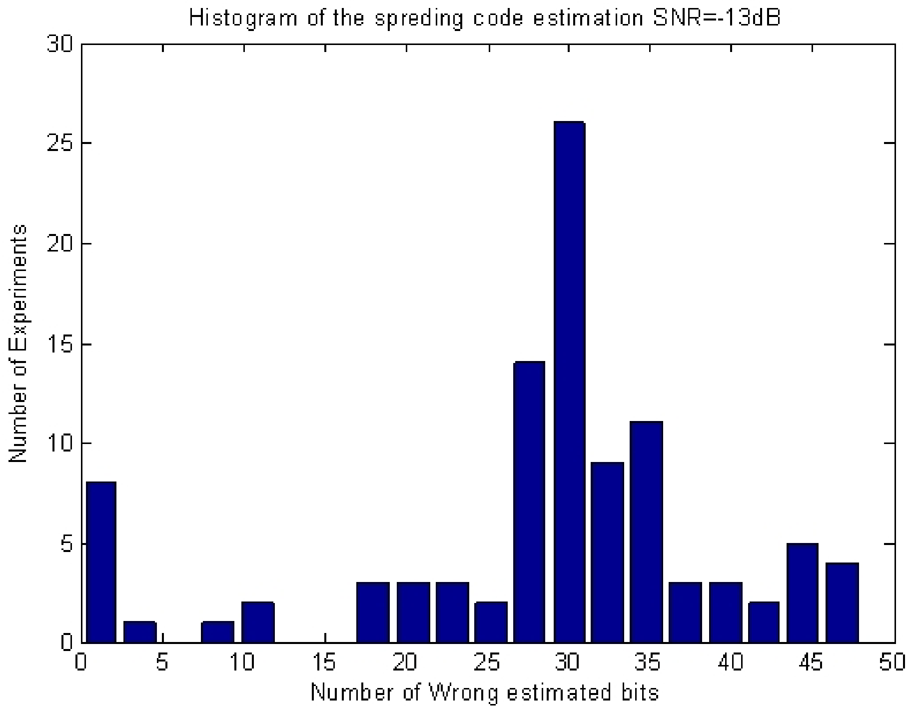

Figure 5.68 Histogram of number of wrong estimated bits SNR= -13dB

Table 5.42 The evaluations of the results at SNR= –13dB

P(Correct Estimated)	0.04
P(Wrong Estimated)	0.96
P(Number of wrong estimated bits<=5 l Wrong Estimated)	5/96
P(Number of wrong estimated bits<=10 l Wrong Estimated)	7/96
P(Number of wrong estimated bits>10 l Wrong Estimated)	89/96

In the following performance analysis the SNR is decreased to -15dB. The spreading code estimation bit error histogram is given Figure 5.68 and evaluation of the result is given in Table 5.42.

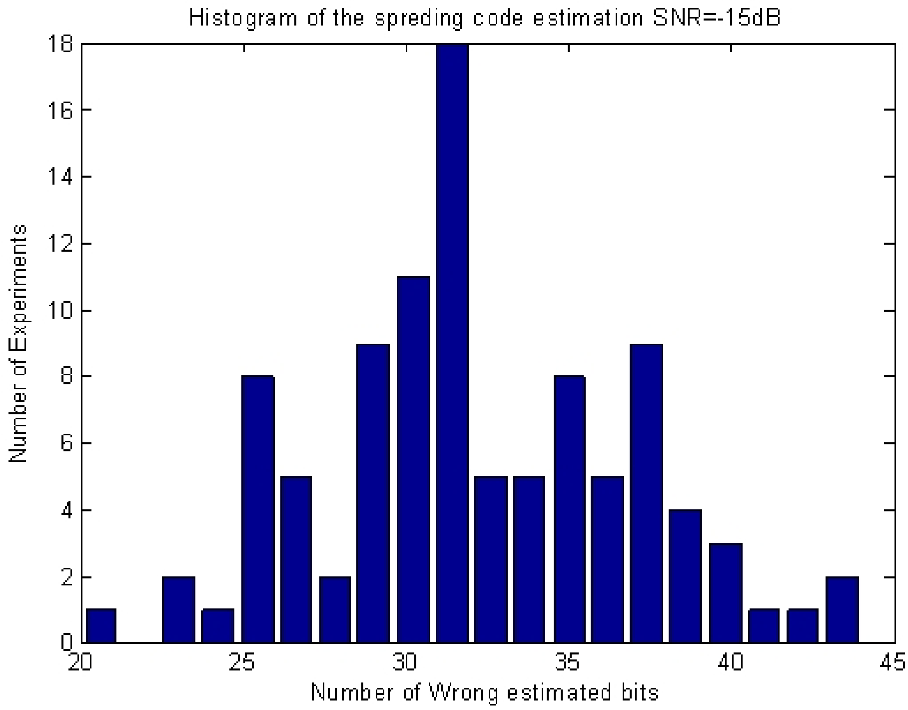

Figure 5.69 Histogram of number of wrong estimated bits SNR= -15dB

Table 5.43 The evaluations of the results at SNR= –15dB

P(Correct Estimated)	0
P(Wrong Estimated)	1
P(Number of wrong estimated bits<=5 I Wrong Estimated)	0
P(Number of wrong estimated bits<=10 I Wrong Estimated)	0
P(Number of wrong estimated bits>10 I Wrong Estimated)	1

In the following analysis the multipath effect is added to channel and it is simulated that the receiver is not in the LOS of the transmitter.

Table 5.44 Channel Parameters (multipath-1)

Channel Type	Values
Multipath Effect	1.Path→ delay: 0.5µs Attenuation: %60 2.Path→ delay: 5µs Attenuation: %70 3.Path→ delay: 25µs Attenuation: %80 4.Path→ delay: 250µs Attenuation: %90

The performance analysis result shows that (Figure 5.70 and Table 5.45) multipath effect prevents the spreading code estimation process. Although detection is successfully performed at SNR=-5dB the spreading code estimation is impossible. The sum of two periodic signals with same periodicity will be again periodic with the same period so multipath effect preserves the symbol period and also the performance of the detection does not change as said before. But sum of two periodic signals with same periodicity will produce a different sequence with same period so the spreading code will be completely changed. In order to eliminate the multipath effect some how channel estimation process must be performed.

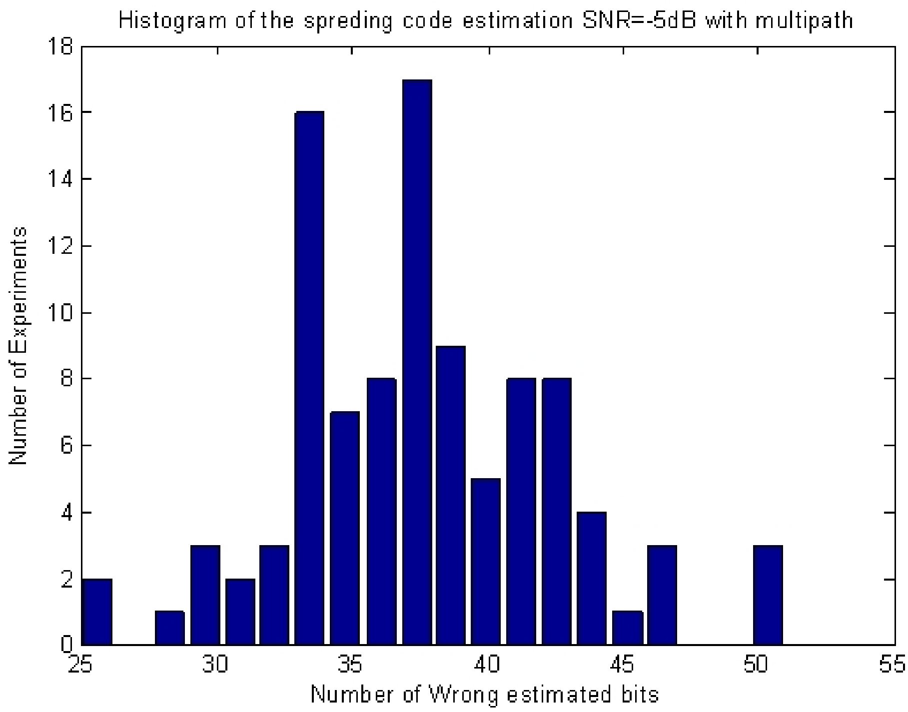

Figure 5.70 Histogram of number of wrong estimated bits SNR= -5dB with multipath

Table 5.45 The evaluations of the results at SNR= –5dB with multipath

P(Correct Estimated)	0
P(Wrong Estimated)	1
P(Number of wrong estimated bits<=5 l Wrong Estimated)	0
P(Number of wrong estimated bits<=10 l Wrong Estimated)	0
P(Number of wrong estimated bits>10 l Wrong Estimated)	1

5.6 Comparisons with Alternative Techniques

In this part alternative techniques proposed for interception of DSSS signal is discussed and necessary comparisons are done.

The first approach discussed here is the Amplitude Distribution Function (ADF) based technique. ADF is simply the time fraction that the input signal is below a given threshold. [17].

$$F_x(\alpha) = \lim_{T \to \infty} \frac{1}{T} E\left(L \mid t : X(t) \le \alpha, 0 \le t \le T\right) \qquad \text{E- 5.1}$$

Under general conditions the ADF of signal plus noise is the convolution of the signal ADF and the noise ADF individually. The application of the ADF to signal detection is enabled by the idea of transforming ADF to $F_x(w)$ [17].

$$F_x(w) = \frac{1}{T} \int_0^T e^{j\omega X(t)} dt \qquad \text{E- 5.2}$$

For large T this function converges directly to the moment generating function of ADF. For this reason this function is called the "Amplitude Moment Statistics" (AMS) and composes "Amplitude Moment Function" (AMF) which is used in detection [17].

In the Figure 5.71 performance of the AMF detector and classic radiometer with respect to SNR is given. The performances of both AMF detector and classic radiometer are poor compared to the autocorrelation based approach discussed in this thesis.

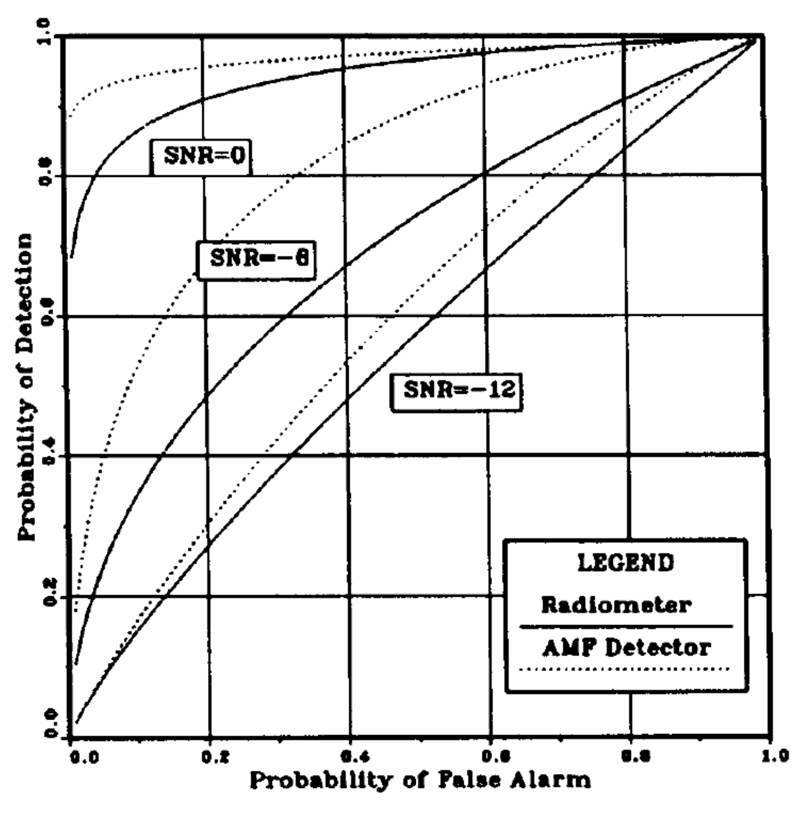

Figure 5.71 Comparisons between AMF detector and Radiometer. [17].

The second approach is correlation based. Outputs of two spatially separated receivers is used [15]. Cross-correlation function (CCF) and the cross-spectral density (CSD) are estimated from the two received sequences. Detection is performed in the frequency domain by analysis of phase and amplitude of the CSD. Time difference of arrival (TDOA) based direction-finding is also performed in frequency domain by estimating the phase-slope of the CSD. Narrowband rejection is implemented using digital notch filters. The structure of the interception system is given in Figure 5.72.

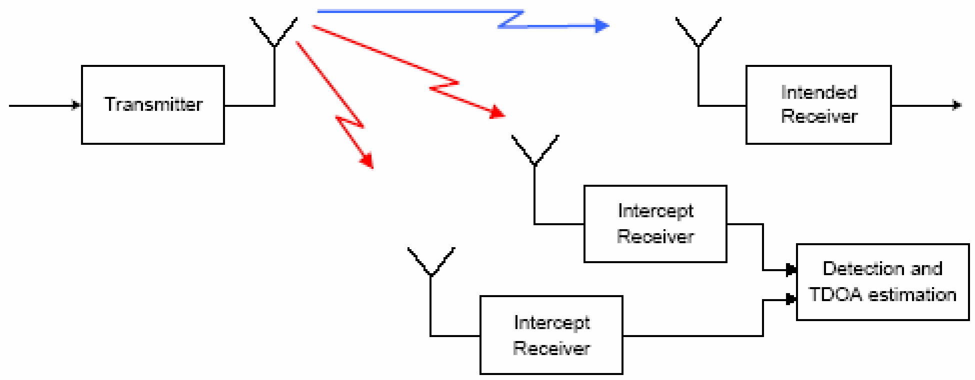

Figure 5.72 Structure of the alternative interception system [15].

The essence of this approach is receiving the same signal by two spatially separated antennas (750m for siulation) with uncorrelated noise. This leads to a high correlation between the received sequences. But when the received signal contains narrowband interferes, they result with high correlation similar to the DSSS signal. This can be considered as the main problem of this approach. In Figure 5.73 the PSD and CCF of the DSSS signal added to noise sequences recorded form HF band is given. From these results it is impossible to distinguish the correlation caused by the DSSS signal [15].

With the application of the interference rejection by digital notch filters, the results become clear for detection of DSSS signal (Figure 5.74). The frequency domain notch filter used here is suppresses all high power narrowband signals [15].

In the autocorrelation based approach discussed in this thesis the effect of narrowband interference is less as seen in the performance analysis because of the single antenna usage and multiple windowed approach. Furthermore the detection process in not accomplished in frequency domain so the narrowband interference signals are considered as noise unless they form a correlation similar to DSSS signal at the output of autocorrelation fluctuation calculation.

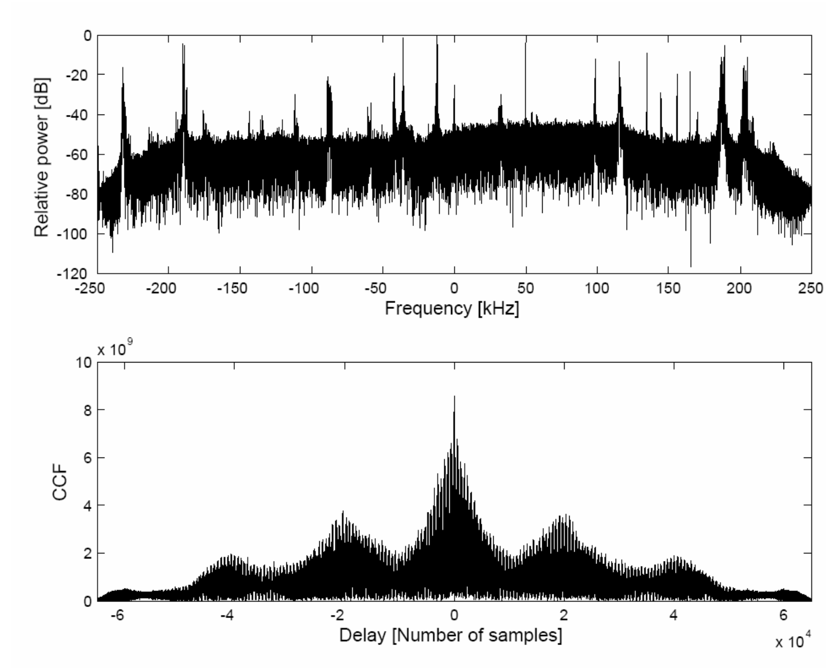

Figure 5.73 PSD and CCF obtained from DSSS signal added to noise [15].

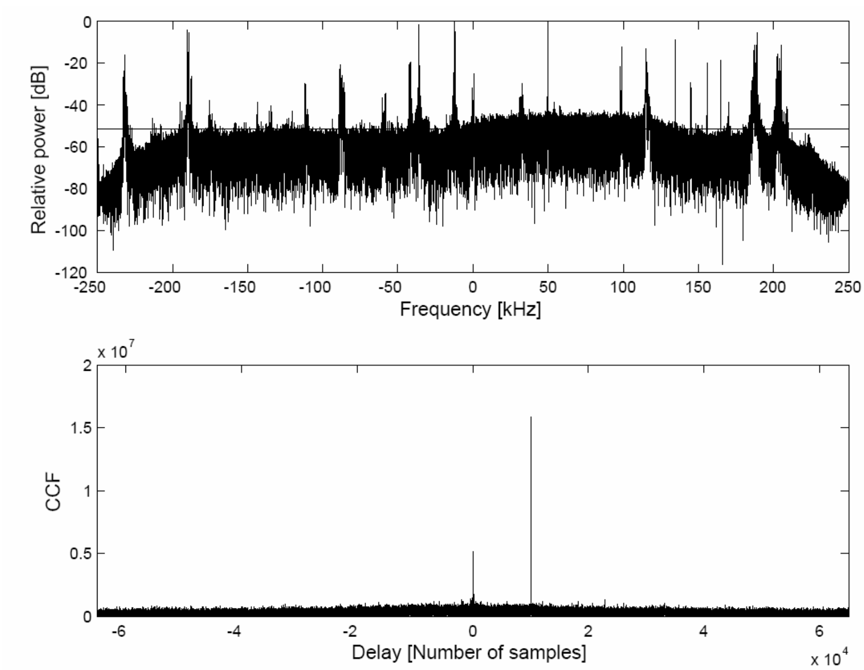

Figure 5.74 PSD and CCF obtained from DSSS signal added to noise after interference rejection [15].

The performance at the output of this interception system (without interference) is given in Figure 5.75 as the change in probability of detection due to different SNRs. In these performance analysis two different kinds of DSSS signals is used. One of them is a DSSS signal and the other one is a military stealth signal denoted LPI [15]

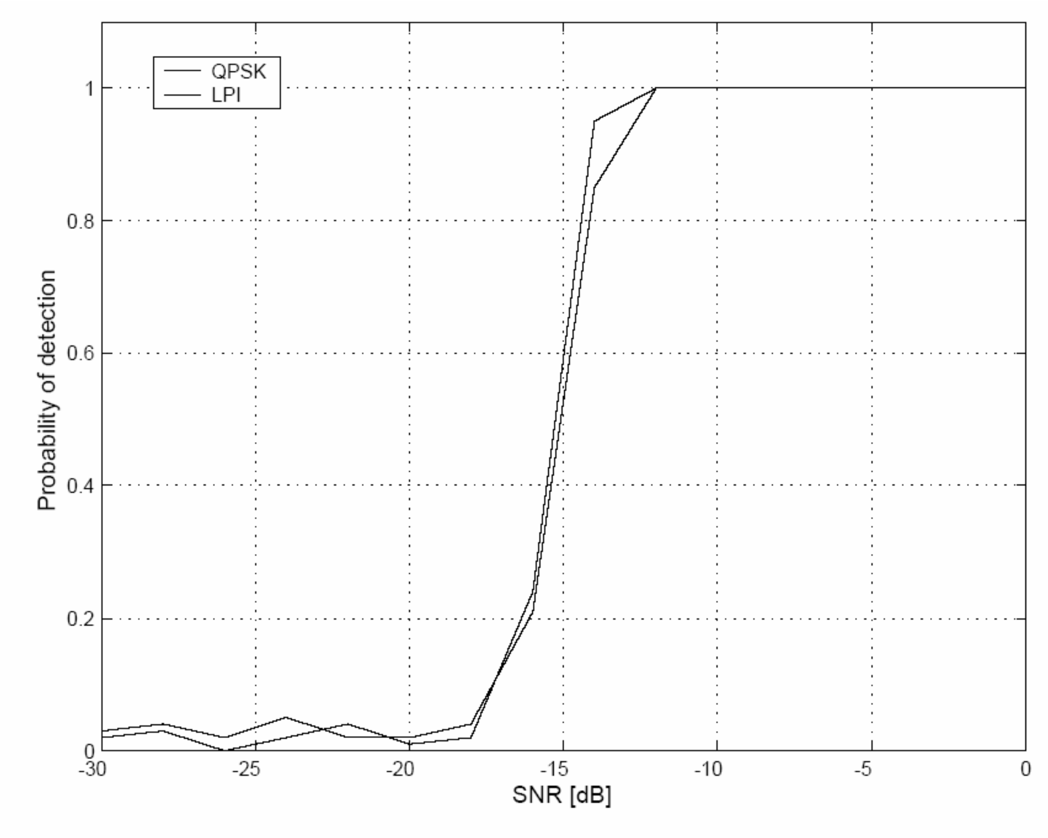

Figure 5.75 PSD Probability of detection for different SNRs [15].

In Figure 5.76 the performance analysis is given for probability of detection for different signal to interference ratios. In this result the decrease in probability of detection due to interference effect is investigated.

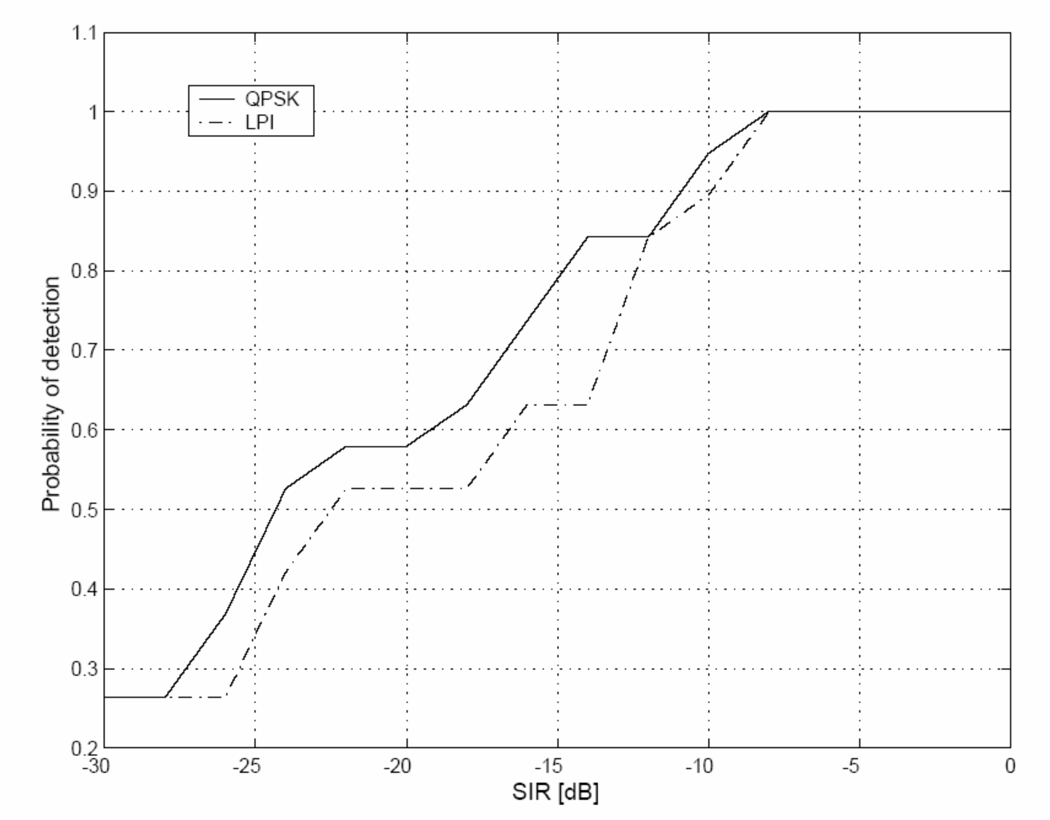

Figure 5.76 PSD Probability of detection for different SIRs [15].

The Third alternative technique is cyclostationary analysis. Cyclostationary spectral analysis concentrates on statistical behavior in the frequency domain of cyclostationary signals. The statistical properties of these signals are considered to be periodically changed due to time. This analysis is depends on cyclic autocorrelation and cyclic spectrum functions. The two primary methods of cyclic spectral analysis are cyclic auto correlation and cyclic periodogram. But with the application of these methods, problems of excessive computational complexity and need of large storage capacity is occur. To overcome these problems, Time Smoothing (TS), Frequency Accumulation Method (FAM), Autocorrelated Cyclic Autocorrelation and Autocorrelated Cyclic Periodogram techniques is stated [16].

In the output of cyclic spectral analysis for SNR>0 is given. One of the differences between cyclostationary analysis and autocorrelation based approach discussed in this thesis, is the complexity of cyclostationary analysis and frequency domain signal the detection approach.

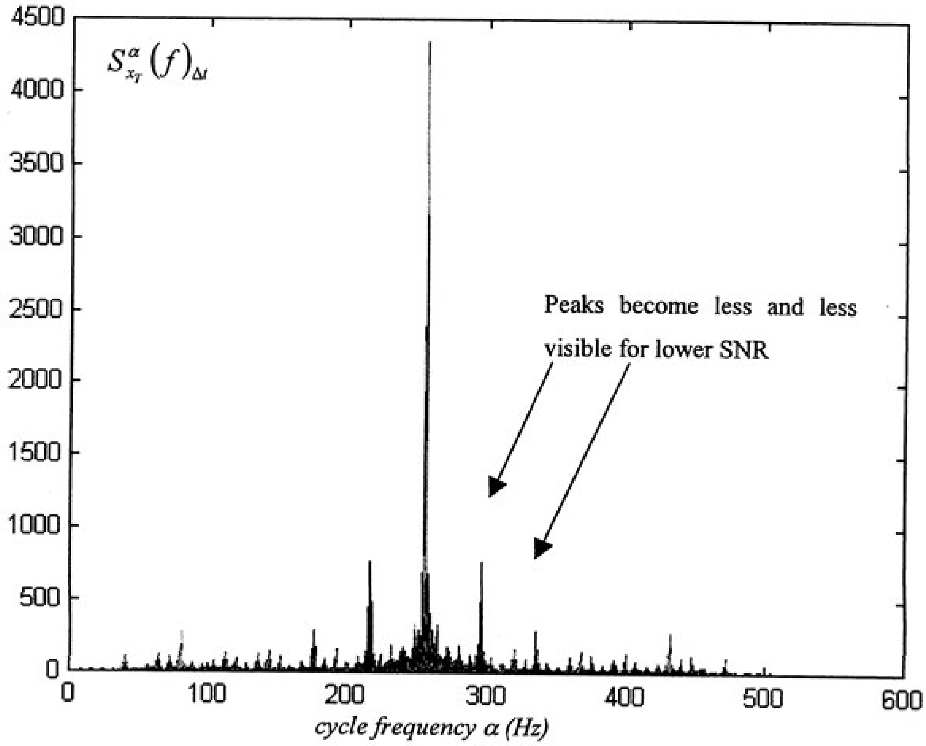

Figure 5.77 of Cyclic spectral analysis for SNR>0 [16].

CHAPTER 6

CONCLUSIONS

This thesis discusses interception concept and concentrates on a special interception and spreading code estimation technique for DSSS signals. This technique is tested on different type of DSSS signals by using different channel effects. The performance analyses are obtained for typical DSSS signals, Universal Mobile Telecommunications System (UMTS) waveform created depending on technical specification of European Telecommunications Standards Institute (ETSI) and typical LPI radar signals. The channel characteristics used for performance analysis are simple Gaussian noise channel, multipath and interference. Also necessary comparisons with performances of alternative interception techniques are accomplished.

The results of performance analysis of typical DSSS signals show that this technique can be used in practical online and offline analysis systems after necessary optimizations are made and utilizing faster dedicated signal processors.

The automatic detection capability is gained by using the peak detection algorithm which extracts the signal peaks hidden in noise peaks by using the property of periodicity. In the design of this algorithm inspired by radar deinterleaving methods which are also uses histogram based techniques.

It is seen that the multipath effect with no LOS signal is available slightly decreases the detection performance and if any LOS signal available and multipath causes an increase in the input power than it is observed that the detection performance increased.

The effect of an interference caused by another signal considered as noise by the detection algorithm so decreases the SNR and performance. The performance decreases more if the interference is in the band of DSSS signal. It is investigated that robustness of the applied interception technique to the interference is good compared with alternative interception approaches.

Based on the results of performance analysis of UMTS signal it is possible to detect the signal at very Low SNR's. The spreading code can not be estimated because of the complex scrambling. This approach can also be used on UMTS like signals. Considering the UMTS signal standard being open the interception and monitoring UMTS like communications can start with a this kind of interception approach and than completed by using standard defined data like the complex scrambler.

For the LPI radar signal, same fixed threshold technique is applied and satisfying results are obtained at low SNRs. Detailed performance analysis shows that also PRI estimation can be performed at very low SNRs and this technique can be used in order to detect and identify LPI radars which utilizes the spreading codes in the pulses.

Spreading code estimation is performed at different SNRs and the results show that it is possible to estimate the spreading sequence even if the SNR is very low. It is determined that the multipath effect prevents to estimate the spreading sequence and also it is not possible to estimate the spreading sequence of UMTS signal due to complex scrambling. Also spreading sequence estimation can not be applied to LPI radar signals because of the discontinuous structure of the pulses.

For all types of signals discussed in this thesis with more computational power some improvements can be obtained by using comparisons at different times. More windows improve performance based on theoretical results. This can be done either using fast real time processors or off line analysis.

Considering the comparisons with alternative approaches; as a result; this approach must be considered as a powerful candidate for being one of the techniques that is to be used in modern signal intelligence and EW systems. Also development of this kind of successful methods will give a rise to development of alternative techniques like chaotic direct sequence spread spectrum, in order to meet the needs for secure transmissions.

REFERENCES

[1] C. Bouder, S Azoul, G. Burel, "Performance analysis of a spreading sequence estimator for spread spectrum transmissions", *Journal of The Franklin Institut, Science Direct*.

[2] Gilles Burel, Andre Quinquis, Stephane Azoul "Interception and Furtivity of Digital Transmissions", *IEEE- Communications'2002* Bucharest, Dec.5-7,2002

[3] Gilles Burel, "Detection of spread spectrum transmissions using fluctuations of correlation estimators" *IEEE-ISPACS*, Nov, 5-8,2000 Honolulu, Hawai, USA

[4] F.Taboada, A.Lima, J. Gau, P. Jarpa, P.E. Pace, "Intercept Receiver Signal Processing Techniques to detect LPI radar signals", *Center For joint Services EW*, Naval Postgraduate School.

[5] Celine Bounder, Gilles Bruel "Blind estimation of the pseudo-random sequence of a direct sequence spread spectrum signal", *IEEE-MILCOM*, Oct, 22-25,2000 Los Angles, USA

[6] Slobodan Simic, Miljko Eric , Miroslav Dukic "Blind Detection Complex Radar Pulses In The Eigen-Space Of Correlation Matrix" *XII Telecomunication forum*, telfor 2003, Beograd, Sava Centar

[7] ETSI TS 125 213 v6.2.0 (2005-03) "Universal Mobile Telecommunications System (UMTS) Spreading modulation" *Technical Specification*

[8] Fakhrul Alam ,"Simulation of third generation CDMA systems" *M.S Thesis* Virginia Polytechnic Institute & State University.

[9] Bassem R. Mahafza, “Radar signal analysis and design using matlab” *Chapman* 2000.

[10] D.J. van Wyk and L.P. Linde, “A discrete pseudo wigner distribution spread spctrum detection procedure emplying complex spreading sequences” *IEEE COMSIG’94*

[11] Thakur Gyamali and Hyuck M. Kwon “An inverse Problem Based Approach to detection in LPI Systems” *IEEE ISSSTA 2004 Australia*

[12] George W. Stimsom, “Introduction to air born radar” *scitech publishing*

[13] Dean Gagnon, “Handheld Battlefield Surveillance Radar Warner” School of Electrical Engineering, University of New South Wales, Australian Defense Force Academy, *Thesis for B.S.*

[14] Dallas Maxim *Application Note* 1890: Feb 18, 2003

[15] Ulrika Ahnström, Johan Falk, Peter Handel, Maria Wikström, ”Detection and direction-finding of spread spectrum signals using correlation and narrowband interference rejection” *Department of Electronic Warfare Systyems, Swedish Defense Research Agency*, Linköping, Sweeden

[16] Işıl Yazgan, “Cyclostationarity Based Signal Detection and Direction Finding Using Time Difference of Arrival Method” *M.Sc Thesis in the Middle East Technical University, Department of Electrical and Electronics Engineering*.

[17] William E.Snelling, Evaggelos A. Geraniotis, “The interception of Spread Spcetrum Waveforms via the Amplitude Distribution Function.” *MILCOM’91*

[18] Richard G. Willey “The future of EW and modern radar signals”, *IEEE AESS* November 2004 presentation

APPENDIX: DERIVATION OF THE DETECTION APPROACH

In this section the detailed theoretical analysis of the detection approach in [1], [2], [3], [5] is given in order to clarify; why this approach works.

The DSSS signal and noise is uncorrelated so we can write;

$$\hat{R}_{yy}(\tau) \cong \hat{R}_{ss}(\tau) + \hat{R}_{nn}(\tau) \qquad \text{E- 6.1}$$

Lets consider estimation of correlation between u(t) and v(t);

$$\hat{R}_{uv}(\tau) = \frac{1}{T}\int_{0}^{T} u(t)v^{*}(t-\tau)dt \qquad \text{E- 6.2}$$

if we use;

- $d(t) = u(t)/T$ for $0 \le t \le T$ and $d(t) = 0$ elsewhere
- $e(t) = v^{*}(-t)$ so; $v^{*}(t-\tau) = e(\tau - t)$

we can write;

$$\hat{R}_{uv}(\tau) = \frac{1}{T}\int_{0}^{T} u(t)v^{*}(t-\tau)dt = \int_{-\infty}^{+\infty} d(t)e(\tau - t)dt \qquad \text{E- 6.3}$$

We can consider correlation estimation as the output of e(t) filtered by d(t) (Figure 6.1).

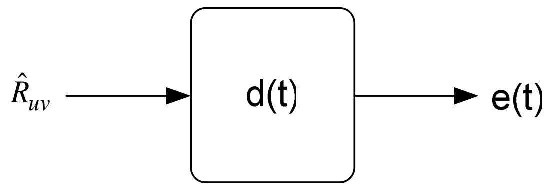

Figure 6.1 e(t) filtered by d(t)

If we use discrete space analysis;

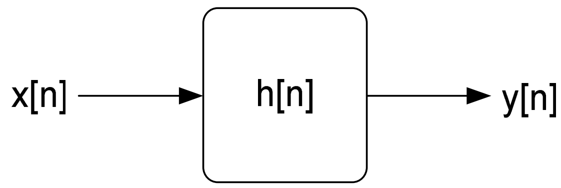

Figure 6.2 Discrete space analysis

$$y[n] = \sum_{k=-\infty}^{+\infty} h[n-k]x[k] \qquad \text{E- 6.4}$$

$$R_{yx}[k] = E\{y[n]x^*[n-k]\} \qquad \text{E- 6.5}$$

$$R_{yx}[k] = E\left\{\sum_{m=-\infty}^{+\infty} h[n-m]x[m]x^*[n-k]\right\} \qquad \text{E- 6.6}$$

h[n] can be considered deterministic so;

$$R_{yx}[k]=\sum_{m=-\infty}^{+\infty}h[n-m]E\{x[m]x^*[n-k]\}$$ E- 6.7

if we use n-m=l

$$R_{yx}[k]=\sum_{l=-\infty}^{+\infty}h[l]E\{x[n-l]x^*[l-k]\}$$ E- 6.8

$$R_{yx}[k]=\sum_{l=-\infty}^{+\infty}h[l]R_{xx}[l-k]$$ E- 6.9

$$R_{yx}[k]=h[k]*R_{xx}[k]$$ E- 6.10

Now lets consider autocorrelation of y[t]

$$R_{yy}[k]=E\{y[n]y^*[n-k]\}$$ E- 6.11

where;

$$y^*[n-k]=\sum_{m=-\infty}^{+\infty}h^*[m]x^*[n-k-m]$$ E- 6.12

so;

$$R_{yy}[k]=E\left\{y[n]\sum_{m=-\infty}^{+\infty}h^*[m]x^*[n-k-m]\right\}$$ E- 6.13

h[n] can be considered deterministic so;

$$R_{yy}[k] = \sum_{m=-\infty}^{+\infty} h^*[m] E\{y[n]x^*[n-m-k]\} \qquad \text{E- 6.14}$$

$$R_{yy}[k] = \sum_{m=-\infty}^{+\infty} h^*[m] R_{yx}[k+m] \qquad \text{E- 6.15}$$

$$R_{yy}[k] = R_{yx}[k] * h^*[-k] \qquad \text{E- 6.16}$$

if we write R_{yx} ;

$$R_{yy}[k] = h[k] * h^*[-k] * R_{xx}[k] \qquad \text{E- 6.17}$$

Taking the Fourier transform we get;

$$S_y(\omega) = \left|H(e^{j\omega})\right|^2 S_x(\omega) \qquad \text{E- 6.18}$$

so by using the approach above we can write;

$$\hat{R}_{uv}(\tau) = \frac{1}{T}\int_0^T u(t)v^*(t-\tau)dt = \int_{-\infty}^{+\infty} d(t)e(\tau-t)dt$$
$$\Rightarrow S_{uv}(\omega) = \left|D(e^{j\omega})\right|^2 S_e(\omega) \qquad \text{E- 6.19}$$

if we consider;

$$R_d(\tau) = \int_{-\infty}^{+\infty} d(t) d^*(t-\tau) dt \qquad \text{E- 6.20}$$

$$R_d(\tau) = d(t) * d(-t) \qquad \text{E- 6.21}$$

if T is large enough;

$$S_d(\omega) = |D(t)|^2 \qquad \text{E- 6.22}$$

if we use u(t) for d(t) where $d(t) = u(t)/T$;

$$\frac{1}{T} S_u(\omega) = |D(t)|^2 \qquad \text{E- 6.23}$$

and

$$S_e(\omega) = S_v(\omega) \qquad \text{E- 6.24}$$

so we can write;

$$S_{uv}(\omega) = \frac{1}{T} S_u(\omega) S_v(\omega) \qquad \text{E- 6.25}$$

Since $E\left\{\left|\hat{R}_{uv}(\tau)\right|^2\right\}$ is the average power (P_{av}) of R_{uv} ; and PSD measures the distribution of signal power;

$$E\left\{\left|\hat{R}_{uv}(\tau)\right|^2\right\} = P_{av} = \frac{1}{2T}\int_{+T}^{-T}\left|R_{uv}\right|^2 dt \qquad \text{E- 6.26}$$

T is large enough;

$$P_{av} = \lim_{T\to\infty}\frac{1}{2T}\int_{+T}^{-T}\left|R_{uv}\right|^2 dt = \int_{-\infty}^{+\infty} S_{uv}(\omega)d\omega \qquad \text{E- 6.27}$$

so finally;

$$E\left\{\left|\hat{R}_{uv}(\tau)\right|^2\right\} = \frac{1}{T}\int_{-\infty}^{+\infty} S_u(\omega)S_v(\omega)d\omega \qquad \text{E- 6.28}$$

After this point we will define fluctuations of autocorrelation estimator in cases; noise alone and signal alone. The comparison between these two cases will be the proof of detection by using fluctuations of autocorrelation estimator.

Noise Alone Case

Since noise is random, fluctuations of autocorrelation estimator is random too. So mean and standard deviation will be used in order to define fluctuations of autocorrelation estimator when only noise is present at the receiver.

If we use E- 6.28 for noise alone;

$$E\left\{\left|\hat{R}_{nn}(\tau)\right|^2\right\} = \frac{1}{T}\int_{-\infty}^{+\infty}\left|S_n(\omega)\right|^2 d\omega \qquad \text{E- 6.29}$$

as n'(t) is filtered by receiver filter g(t) (Figure 6.3);

$$S_n(\omega) = \left|G(e^{j\omega})\right|^2 S'_n(\omega) \qquad \text{E- 6.30}$$

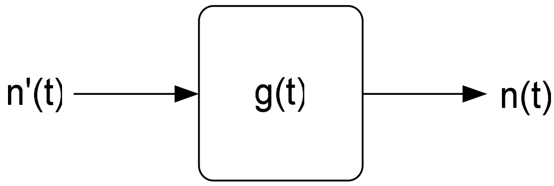

Figure 6.3 Noise is filtered by receiver filter

$$S'_n(\omega) = \frac{N_0}{2} \qquad \text{E- 6.31}$$

so

$$S_n(\omega) = \left|G(e^{j\omega})\right|^2 \frac{N_0}{2} \qquad \text{E- 6.32}$$

if we re-write E- 6.28 for noise alone

$$E\left\{\left|\hat{R}_{nn}(\tau)\right|^2\right\} = \frac{1}{T}\int_{-\infty}^{+\infty}\left|\left|G(e^{j\omega})\right|^2 \frac{N_0}{2}\right|^2 d\omega \qquad \text{E- 6.33}$$

since $G(e^{jw})$ is simple band pass filter as shown in Figure 6.4;

$$\left|G(e^{j\omega})\right|^2 = G(e^{j\omega}) \qquad \text{E- 6.34}$$

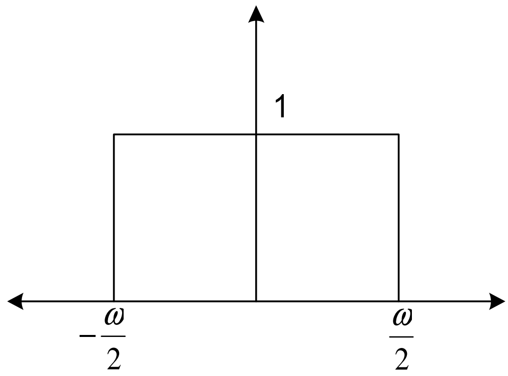

Figure 6.4 Receiver Filter

$$E\left\{\left|\hat{R}_{nn}(\tau)\right|^2\right\} = \frac{1}{T}\int_{-\infty}^{+\infty}\left|G(e^{j\omega})\frac{N_0}{2}\right|^2 d\omega \qquad \text{E- 6.35}$$

$$E\left\{\left|\hat{R}_{nn}(\tau)\right|^2\right\} = \frac{1}{T}\int_{-\omega/2}^{+\omega/2}\left|\frac{N_0}{2}\right|^2 d\omega \qquad \text{E- 6.36}$$

$$E\left\{\left|\hat{R}_{nn}(\tau)\right|^2\right\} = \frac{1}{T}\frac{N_0{}^2}{4}\omega \qquad \text{E- 6.37}$$

if we consider filtered noise characteristic as Figure 6.5

$$\sigma_n{}^2 = \frac{N_0}{2}\omega \qquad \text{E- 6.38}$$

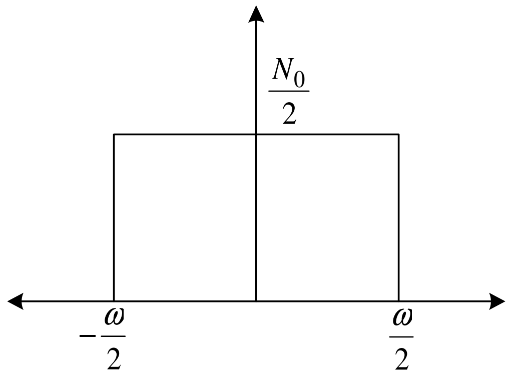

Figure 6.5 Filtered noise characteristic

as a result;

$$E\left\{\left|\hat{R}_{nn}(\tau)\right|^2\right\} = \frac{1}{T\omega}\sigma_n{}^4 \qquad \text{E- 6.39}$$

so average value of fluctuations m_p^n;

$$m_p^n = \frac{1}{T\omega}\sigma_n{}^4 \qquad \text{E- 6.40}$$

Now consider standard deviation of fluctuations;

$$\sigma_p^n = \sqrt{\operatorname{var}\left(E\left\{\left|\hat{R}_{nn}(\tau)\right|^2\right\}\right)} \qquad \text{E- 6.41}$$

where;

$$\mathrm{var}\left(E\left\{\left|\hat{R}_{nn}(\tau)\right|^2\right\}\right)=\mathrm{var}\left(\frac{1}{M}\sum_{n'=0}^{M-1}\left|\hat{R}_{nn}^{n'}(\tau)\right|^2\right) \qquad \text{E- 6.42}$$

we use variance property var(ax)=a^2var(x);

$$\mathrm{var}\left(E\left\{\left|\hat{R}_{nn}(\tau)\right|^2\right\}\right)=\frac{1}{M^2}\mathrm{var}\left(\sum_{n'=0}^{M-1}\left|\hat{R}_{nn}^{n'}(\tau)\right|^2\right) \qquad \text{E- 6.43}$$

$$\mathrm{var}\left(E\left\{\left|\hat{R}_{nn}(\tau)\right|^2\right\}\right)=\frac{1}{M^2}\sum_{n'=0}^{M-1}\mathrm{var}\left(\left|\hat{R}_{nn}^{n'}(\tau)\right|^2\right) \qquad \text{E- 6.44}$$

$$\mathrm{var}\left(E\left\{\left|\hat{R}_{nn}(\tau)\right|^2\right\}\right)=\frac{1}{M}\mathrm{var}\left(\left|\hat{R}_{nn}^{n'}(\tau)\right|^2\right) \qquad \text{E- 6.45}$$

where;

$$\mathrm{var}\left(\left|\hat{R}_{nn}^{n'}(\tau)\right|^2\right)=E\left\{\left|\hat{R}_{nn}^{n'}(\tau)\right|^4\right\}-\left(m_p^n\right)^2 \qquad \text{E- 6.46}$$

Statistical behavior of R_{nn} is close to Gaussian as it is the average of a large number of random variables. Also except for small τ its average is null. So we can write

$$E\left\{\left|\hat{R}_{nn}(\tau)\right|^4\right\}\cong 3\left(\left(m_p^n\right)^2\right) \qquad \text{E- 6.47}$$

so;

$$E\left\{\left|\hat{R}_{nn}(\tau)\right|^2\right\} \cong 2\left(\left(m_p^n\right)^2\right) \qquad \text{E- 6.48}$$

and that concludes;

$$\sigma_p^n \cong \sqrt{\frac{2}{M}}\left(m_p^n\right) \qquad \text{E- 6.49}$$

Signal Alone Case

When only signal is present at the receiver, the fluctuations are obtained at the multiples of symbol period ($\tau = kT_s$). So for simplicity we will consider the case $\tau = T_s$.

The autocorrelation estimation of the received signal for $\tau = T_s$ is;

$$\hat{R}_{ss}(T_s) = \frac{1}{T}\int_0^T s(t)s^*(t - T_s)dt \qquad \text{E- 6.50}$$

s(t) is the filtered received DSSS signal. Where;

$$s'(t) = \sum_{k=-\infty}^{+\infty} a_k h(t - kT_s) \qquad \text{E- 6.51}$$

and

$$r(t) = h(t) * g(t) \qquad \text{E- 6.52}$$

as shown in Figure 6.6.

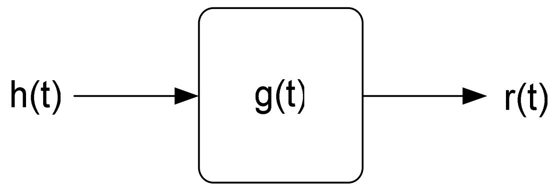

Figure 6.6 h(t) is filtered by receiver filter g(t)

then we can write;

$$\begin{aligned} s(t) &= \sum_{k=-\infty}^{+\infty} a_k r(t - kT_s) \\ s^*(t - T_s) &= \sum_{m=-\infty}^{+\infty} a_m{}^* r^*(t - (m+1)T_s) \end{aligned} \qquad \text{E- 6.53}$$

so;

$$\hat{R}_{ss}(T_s) = \frac{1}{T} \sum_{k=-\infty}^{+\infty} \sum_{m=-\infty}^{+\infty} a_k a_m{}^* \int_0^T r(t - kT_s) r^*(t - (m+1)T_s) dt \qquad \text{E- 6.54}$$

we consider $\tau = T_s$ case so m=k-1, because only the two successive symbols are included.

So:

$$\hat{R}_{ss}(T_s) = \frac{1}{T}\sum_{k=-\infty}^{+\infty} a_k a_{k-1}^* \int_0^T \left|r(t-kT_s)\right|^2 dt \qquad \text{E- 6.55}$$

Then the fluctuations of autocorrelation estimator are;

$$E\left\{\left|\hat{R}_{ss}(T_s)\right|^2\right\} = \frac{1}{T^2} E\left\{\sum_{k=-\infty}^{+\infty} a_k^{\,2} a_{k-1}^{*2} \left(\int_0^T \left|r(t-kT_s)\right|^2 dt\right)^2\right\} \qquad \text{E- 6.56}$$

$$E\left\{\left|\hat{R}_{ss}(T_s)\right|^2\right\} = \frac{1}{T^2}\sum_{k=-\infty}^{+\infty} E\left\{a_k^{\,2} a_{k-1}^{*2}\right\}\left(\int_0^T \left|r(t-kT_s)\right|^2 dt\right)^2 \qquad \text{E- 6.57}$$

At this point we can write;

$$\begin{aligned} \sigma_a^{\,2} &= E\left\{\left|a_k\right|^2\right\} \\ \sigma_r^{\,2} &= \frac{1}{T_s}\int_0^{T_s} \left|r(t)\right|^2 dt \end{aligned} \qquad \text{E- 6.58}$$

and by using these standard deviations;

$$E\left\{\left|\hat{R}_{ss}(T_s)\right|^2\right\} = \frac{1}{T^2}\sigma_a^{\,4}\sum_{k=-\infty}^{+\infty}\left(\int_0^T \left|r(t-kT_s)\right|^2 dt\right)^2 \qquad \text{E- 6.59}$$

and;

$$E\left\{\left|\hat{R}_{ss}(T_s)\right|^2\right\}=\frac{1}{T^2}\sigma_a{}^4\frac{T}{T_s}(T_s\sigma_r{}^2)^2 \qquad \text{E- 6.60}$$

because for all k the number of $(T_s\sigma_r{}^2)^2$ is T/T_s . Since the signal power is;

$$\sigma_s{}^2=\sigma_a{}^2{}_s\sigma_r{}^2 \qquad \text{E- 6.61}$$

so,

$$m_p^s=\frac{T_s}{T}\sigma_s{}^4 \qquad \text{E- 6.62}$$